Final Report

on

D.S.S. Contract 01SU.36100-5-0297

"Determination of Winds in

the Lower Ionosphere".

Atmospheric Dynamics Group

Institute of Space & Atmospheric Studies

University of Saskatchewan
Saskatoon, Saskatchewan

Final Report on D.S.S. Contract 01SU.36100-5-0297 "Determination of Winds in the Lower Ionosphere"

Report prepared by

J.B. Gregory, Ph.D.,
Professor of Physics.

C.E. Meek, M.Sc.

Physics Department,
University of Saskatchewan.
30 March 1976.

I N D E X

I N D E X (cont'd)

Chapter 1.

Analysis of Drift Data

1.1 Introduction

Some twenty-five years have elapsed since the introduction of experiments to derive the motion of irregularities of atmospheric electron density from a study of the diffraction pattern, at ground level, of reflected radio waves (Mitra, 1949; Briggs, Philips and Shinn, 1950). In that time, no finality has been reached in respect to a preferred method of analysis of the data sequences. Implicit in this matter are questions as to the physical processes which are involved - e.g. how is an irregularity in electron density created, and does its motion reveal mass translation of the neutral gas or the phase aspect of a wave?

The matters of physics inherent in these questions present their intrinsic challenge, and their solution will undoubtedly require further experiments, probably in situ. However, an additional impetus to the study of data analysis has now arisen. The radiowave "drifts" technique has now been applied to partial radiowave reflections (Fraser, 1965; Gregory and Rees, 1971; Manson, Gregory and Stephenson, 1974), thereby opening up possibilities for sustained, automated observation of atmospheric motion in the difficult altitude range, 60-120 km. In this application, it is the cost of data processing which determines the scale on which observations can be made. This

applies particularly to studies of gravity waves, for which observation at 5-minute intervals is appropriate. Hence it is important to find methods of data processing which are convenient and economical, and thus suited to large scale useage. A means of specifying the uncertainty of values, and preferably of reducing it, is also desirable.

Application of the drifts technique on a large scale raises in turn a question of philosophy of measurement. The technique originated among physicists; and most studies of the technique have been made by those whose basic training is in physics. Inherent in this discipline is a search for precision of measurement, as a counterpart of the development of comprehensive and satisfactory theories and models. However, the study of atmospheric motion has been considered as the domain of meteorology. Meteorologists have learned, in face of great variability in phenomena often difficult of access, that larger bodies of data, of moderate accuracy and preferably uninterrupted, are more useful than smaller quantities of data of higher accuracy. Typically, measurements whose precision is of the order of $\pm$ 20% are acceptable for many purposes, particularly when, on grounds that some part of the data cannot be assimilated, some wastage of effort is inevitable. In this report, the two questions of form of analysis and accuracy of results will be treated from the viewpoint of application of the method to problems of dynamical meteorology.

1.2 Form of measurement

In their classic paper on the bases of measurements of drift velocities, Briggs, et al. (1950) distinguished between the forms of velocity which can be defined by means of observations of the "fading" of reflected radiowave amplitudes at sampling points on the ground (antennas). They define an "apparent" velocity, and a "true" velocity. The former is

$$V' = \xi_o/\tau_o \qquad (1.1)$$

where τ_o is that delay which gives maximum correlation between separate amplitude sequences, R(t), determined at antennas spaced ξ_o apart. The "true" velocity, V, is defined as

$$V = \xi_1/\tau_1 \ , \qquad (1.2)$$

where ξ_1 is that displacement which for a time separation τ, produces slowest possible fading. Briggs, et al. describe methods for determining V, and also a velocity V'_c - a measure of the speed of fading. These are related as

$$V'V = V'^2_c \qquad (1.3)$$

Their methods require assumptions concerning the form of the auto and cross correlograms, $\rho(o,\tau)$ and $\rho(\xi,\tau)$ respectively. Briggs, et al. comment that "it may be more convenient in practice to make measurements leading to the apparent velocity" (rather than the "true" velocity, V).

In applications to date, various research groups have made individual choices in respect to the use of "apparent" and "true" velocities. In the absence of independent confirmation that the "true" velocity is indeed such, the logical arguments in favour of this form have suggested that it should be used.

The assumptions in the method, and the relations between "true", (temporal), "true" (spatial) and "apparent" have been investigated by Dr. Briggs' group at Adelaide.

Golley and Rossiter (1970) have shown that the "apparent" velocity is consistently larger, by 10-30%, than a velocity derived by spatial correlation; while the "true" velocity, derived by temporal correlation, tends to be low by similar factors when the size of the receiving antenna triangle is small, and approaches the spatial value when a sufficiently large triangle is used. It may be noted here that the "apparent" velocity was found not to be affected by triangle size. Directions of drift were equally well determined by both forms of analysis.

The finding that the "true" velocity is dependent on spacing of antennas suggests that the spectral distribution of scales of dimension in the ground diffraction pattern may have influence on the accuracy of this form of analysis. An allied finding is that of Sprenger and Schminder, (1969) who noted a trend towards a larger and more consistent value when low-frequency components of the data sequence were reduced by filtering.

In application of the drifts method to partial reflections, experience at Saskatoon shows that the recorded data often fail to produce the form of lag correlogram required to in order to conduct a full correlation analysis leading to V, the "true" velocity. Examples of correlograms obtained in practice are

given in Figure 1.1. Rather than discard such data sequences, it has been decided to compute the "apparent" velocity, using the method of "numberical correlation", in which the time delay for maximum correlation between data sequences is found.

However, this method does not contain within it any obvious criterion for the "goodness" of the derived velocity; and it does not produce any parameter such as the characteristic velocity defined by Briggs et al., which might service. Two approaches to this problem have been in progress. The first, a selection of criteria for assessing self-consistentency of data, has been adopted by U. of S. workers. The second, an investigation of the use of "samples" of a longer data sequence, to permit a statement of statistical significance, has been in progress at Communications Research Centre by Dr. M.J. Burke.

The work reported here comprises essentially an examination of the variants of the "sample" method (Chapter 3), and of the long sequence method (Chapter 4). The two methods, and their variants, are then applied to raw data from Saskatoon and Ottawa (Chapter 5). The methods are compared in Chapter 6; and the relations between them are discussed in Chapter 7.

It is appropriate to note here that this exercise has revealed distinct differences in the characteristics of data taken at the two locations. This finding, which had been suspected previously, is being followed up. Its existence suggests caution in assuming that a method of analysis which is satisfactory at one location will necessarily be satisfactory elsewhere.

1.3 Comparisons with alternative experimental techniques.

Although it is usually not possible in large scale observations to compare drifts measurements with other measurements, e.g. by means of chemical releases, a number of such comparisons have been made by various groups of workers. It has appeared desirable that the investigation of methods of analysis should be paralleled by a review of the findings from experimental comparisons. This is presented in Chapter 2; and includes a brief study of the nature of the scales of motion, since comparisons are limited the conditions of sampling of these scales.

Figure for Chapter 1

CAPTION

Figure No.

1.1 Sample lag correlograms, selected at random, which demonstrate unsuitability for full correlation analysis.

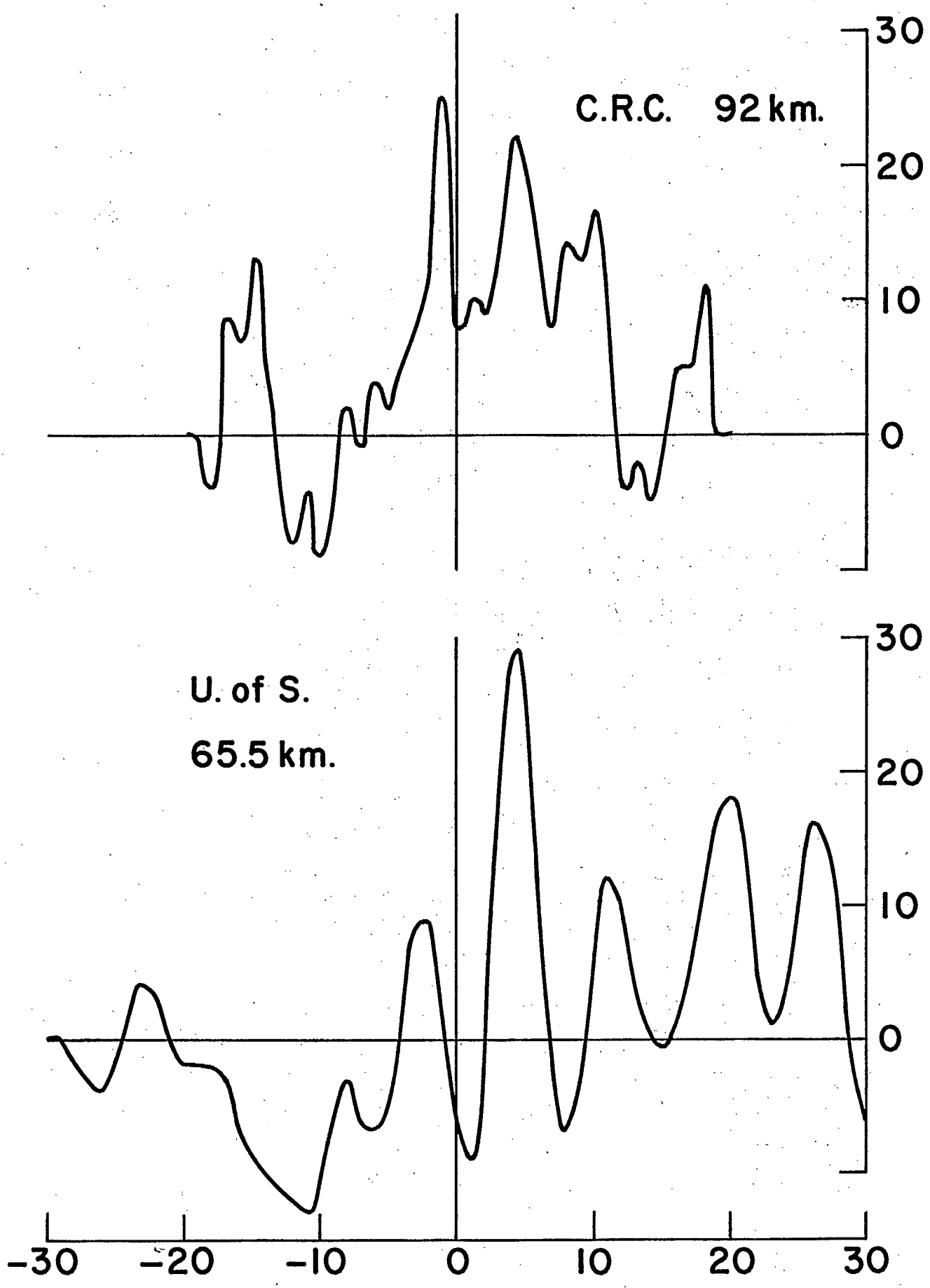

Fig. 1.1

Chapter 2. Comparison Experiments

2.1 The bases of comparisons.

Before examining the results of experimental comparisons between the drifts technique and other techniques of wind measurements, some aspects of the rationale of comparisons will be discussed. Attention will be given to two key matters: viz; the question of the scales of motion which are to be studied, and the matter of the limitations inherent in all wind measuring techniques. Together, those aspects determine the way in which a comparison should desirably be conducted; and also, how it may be interpreted, particularly when there are limitations on the available experimental facilities.

2.2 Scales of Motion

It is desirable to consider scales of motion in the light of the physical processes which are believed to operate. These include the mean circulation and its seasonal changes in response to heating patterns and momentum transfer; the propagation of planetary waves, generated either at lower altitudes or in situ; the occurrence of tidal oscillations; the propagation of gravity waves; and the occurrence of turbulence. However, the measurements currently available which might permit the identification of these processes separately are not extensive. It is usually necessary to attempt to extract the magnitudes of the contributions of different physical processes from a set of data which may or may not have been obtained at appropriate

time and space scales.

The various processes are selected by choice of suitable averaging and differencing times. They may be expressed in terms of time and length scales by means such as the structure function employed by Justus and Woodrum, (1972); or by comparable correlation functions. The investigation by these workers appears to be the most comprehensive one which is relevant to the matter of comparison experiments, and a number of their results will be quoted here. In addition, the results of other workers who have investigated scales of motion, with a particular process in mind, will be given. This additional information is desirable because of some lack of definition, imposed by availability of data, in the structure function results.

Horizontal structure. A structure function of the form

$D(r) = \langle[(V(x+r) - V(x)]^2\rangle$, where r is the magnitude of the vector separation of points of measurement, can be computed. For horizontal wind components, u and v, the function is

$$D(r) = \langle[u(x+r) - u(x)]^2\rangle + \langle[v(x+r) - v(x)]^2\rangle \quad .$$

Justus and Woodrum made use of "Robin" sphere data for the altitude range 50-65 km; and of chemical release trail data for the altitude range 80-140 km. Substantial aggregating in altitude is thus involved. Sphere data were acquired at latitudes up to 64N, and chemical release data were obtained up to 47N. No discrimination in respect to latitude was possible. It may be noted that, with the exception of work at Adelaide, 35S, most of

the drifts comparisons have been made above 50N. Figure 2.1 shows the functions for these two ranges. The value of L shown is appropriate to an exponential correlation, i.e. $\rho(r) = \exp(-r/L)$. The values of σ, standard deviation, were obtained from a separate daily difference analysis.

Blamont (1966) has presented results of simultaneous vapour-trail measurements at locations up to 2000 km apart, in the latitude range 26N to 43N. He found that the extent of correlation of horizontal velocities at the same altitude differed in separate experiments; identical hodographs resulting sometimes from firings separated by 600 or even 2000 km; while on other occasions hodographs at 600 km spacing, or even as little as 50 km, showed no correlation. The results of a spacing of 450 km are included in Figure 2.1.

Justus and Woodrum also obtained a horizontal structure function for the vertical component of wind, w. As is to be expected, the magnitudes, $\langle \Delta v^2 \rangle$, are some two or three orders less than for the horizontal winds, as is shown in Figure 2.2. To date, the significance of vertical components has not been assessed in comparison experiments.

Vertical structure

A vertical structure function has the form

$$D_F(\xi) = \langle [F(z+\xi) - F(z)]^2 \rangle .$$

Justus and Woodrum employed two sets of time separations; the first, of one day, being used to determine irregular (gravity

wave) components; while the second was 7-15 days for the altitude range 45-65 km, and 10-12 for 65-85 km. The difference between values for these two time intervals is attributable to planetary wave components. It may be noted that the technique differences data for times which are an integral number of days apart, in order to eliminate tidal and prevailing components. However the recent work of Fellous, Bernard, Glass, Massebeuf and Spizzichino (1975) has shown that at latitude 47N, the daily parameters of the tides are of great variability, beyond the limits of experimental error.

Hence some tidal contribution to the "irregular winds" determined by Justus and Woodrum is probable. Figure 2.3 shows the vertical functions for single day differences, and for 10-12 day differences.

Alternative approaches to the vertical structure of horizontal winds have been made by several workers. A study of small scale variations in winds to 70 km altitude has been made by Newell, Mahoney and Lenhard (1966). The measurements were derived from falling spheres ("Robin" balloons) tracked by radar. Due to smoothing of radar output data, some scales of wind structure were not available. Newell, et al identified the vertical spacing between successive maxima, in the vertical, of horizontal winds; equating these with a vertical half-wave length. The magnitude changes between successive maxima, Δu; the vertical spacing, ΔH_u and the shears, $\Delta u/\Delta H$ were established for 19 balloon soundings chosen on the basis that a further sounding occurred within two hours. The results of analysis show an

increase in Δu from 5 m/sec at 30 km to 6.5 m/sec at 60-70 km, for winter, and from 6.0 m/sec to 7.7 m/sec for summer, respectively. The vertical spacing, ΔH, increased from 0.27 km to 1.4 km (winter), and 0.34 km to 1.6 km (summer), over the same altitude range. The values of shears, $\Delta u/\Delta H$, tended to decrease, due to smoothing, with altitudes; but values of 25 m/sec/km were noted in the lower altitude ranges. Time resolution was not attempted, but wind features tended to persist for more than one hour. Newell, et al. related their measurements to the properties of gravity waves.

For altitudes above 70 km, (78-111 km), Manson, Gregory and Stephenson (1974) have made a study of "irregular winds" at 52N. These are defined as the difference between the wind determined by the radiowave drifts technique from a given 3-minute sounding of an altitude region 3 km in extent, and the median of twelve such soundings in one hour. The irregular winds show characteristics consistent with internal gravity waves; though they did not exhibit obviously monochromatic behaviour. Manson, et al. present data showing the change of amplitudes with altitude, for most months of one year; also the values of vertical shear, for summer, equinox and winter. These are shown in Figure 2.4. In general, the amplitudes are in the range 10-30 m/s at 78 km, increasing to 70-90 m/s at $\approx$110 km; while the median shears were in the range 15-20 m/s/km at $\approx$80 km, increasing to 40 m/s/km at $\approx$110 km in some seasons. The wind magnitudes quoted are appropriate to either r.m.s. values, or to the smallest 80% of data; these being essentially similar. In respect to shears,

maximum values are much higher than medians, reaching 100 m/sec/km, or more, at 110 km. These data suggest that gravity wave components of the wind field will provide the major perturbations, e.g. by comparison with tidal components, discussed below.

Justus and Woodrum computed the irregular component, ascribed to gravity waves, from daily differences for locations up to 70 latitude over the altitude range 35-170 km. These are shown in Figure 2.5. Blamont (1966) found oscillations of the velocity vector at vertical distances of 3 km at 90 km altitude, increasing to 8 km at 125 km. The largest mean gradient of magnitude of velocity from 31 chemical releases was found in the region 95-100 km, and was of value 2.5 m/sec/km. The contribution of the oscillatory component to the total speed was not more than 15-20% in these firings at 31°N.

Finally, it is instructive to examine a composite profile of velocity, derived from simultaneous chemical release, meteor trail, drift and rocket-parachute techniques, reported by Andreeva, Vugmeister, Ilyichev, Kazimirovsky, Katasev, Kokourov, Lifshitz, Pahomov and Uvarov (1973). This is shown in Figure 2.6.

The foregoing treatment of scales of motion has involved a suppression of some or all of the larger scales, which comprise the mean circulation including seasonal changes; planetary waves, including stratospheric warmings; and tidal motions. While the irregular components, of periods less than ≈1 day, are of greatest significance for recent comparisons of drifts and other techniques; earlier comparisons have utilized data separated substantially in time and distance. Hence a

summary of the characteristics of the larger scales is useful.

Mean circulation

A substantial summary of the mean circulation is available in the model by Groves (1969), which may be consulted for seasonal and latitudinal trends.

Gregory and Manson (1975b) have given examples of the effects of major warmings observed at 52N. Altitudes to 110 km are shown to be affected; the zonal flow being reversed for periods of the order of one week duration. However, the altitude variation of the winds during a warming is not to be described simply; there is evidence for alternating regions, of the order of 10 km thickness, in which the thermal wind has opposite sign. Gregory, Manson, Stephenson, Belrose, Burke and Coyne (1975) have further shown that the longitude extent of such effects may extend across Canada, from 105°W to 75°W, and cover latitudes from 59N to 45N. Additional studies of mean winds by Gregory and Manson (1975a) show that at altitudes above 80 km, the variation of flow from year to year in the months September - November, i.e. while the northern hemisphere winter circulation is building up, is considerable. Clearly, comparisons during summer months are more to be desired.

Planetary Waves

At mid-latitudes, the existence of planetary waves in the mesosphere and lower thermosphere has been inferred (Gregory and Manson, 1970), and indirectly demonstrated (Deland

1973). A direct demonstration has been given by Glass, Fellous, Massebeuf, Spizzichino, Lysenko and Portniaghin (1975) of the existence of periodicities, in the range 2 to 6 days , due to travelling waves. A significant feature is the change of spectral components from dominant to negligible within a height interval of 6-9 km, e.g. from 86 to 92, or to 95 km. Since the combined amplitudes were of the order of $\pm$ 20 m/sec, in both summer and winter, (though not around a solstice), they are significant in respect to averaging for longer term or mean winds. Some of the components showed negligible change of phase with altitude, i.e. they were in an evanescent mode.

As can be noted in Figure 2.3, Justus and Woodrum have also detected the presence of a spectrum of planetary waves in the time scale up to 12 days.

Tidal motions: Information on tidal components has been derived mainly from meteor-trail observations; and the extent of detailed knowledge has increased with the technical improvement of meteor systems. Thus for example, Fellous et al.(1975) have given data on diurnal and semi-diurnal tide, by season, at 47N, - which include the amplitude at 90 km, together with amplitude gradients and phase information. The diurnal tide had amplitudes, at 90 km, in the range 4-7 m/sec, with gradients 0.0 to 0.4 m/s/km, and wavelengths 23 to >100 km; while the semi-diurnal tide ranged from 8 to 20 m/sec, with gradients of 0 to 2 m/s/km, and wavelengths $\approx$ 100 km. However, Fellous, et al. have drawn attention to the fact that in 20 to 40% of their observations, there is evidence, deduced via vertical harmonic analyses, of the simultaneous

existence of several tidal wave motions, some of which are downwards propagating; also evanescent. The wave numbers lay in the range -0.3 (downwards) to +0.5 (upwards) km^{-1}, with maximum occurrence 0.1 to 0.2 km^{-1}. The existence of such additional modes is not predictable; and thus introduces further uncertainty into the consequences of finite height discrimination. Since there exists also the possibility that some modes may be non-migrating, the effect of horizontal separation over larger distances, $\approx$1000 km and more, is also uncertain. Agreement between the measurements of Fellous, et al, and theoretical studies, e.g. by Chapman and Lindzen, and Lindzen and Hong, is limited to only some aspects of the tidal motions.

2.3 Comparison experiments.

It is convenient to group these according to the techniques employed. The latter include chemical release trails and meteor trails; while the drifts measurements may be divided according as total or partial radiowave reflection occurred. The comparisons are limited to altitudes not above those of sporadic-E reflections.

Chemical release, meteor trails and drifts

An experiment which compared chemical release, meteor trail and drift techniques is described by Andreva, Vugmeister, Ilyichev, Kazimirovsky, Katasev, Kokourov, Lifshitz, Pahomov and Uvarov, (1973). The various equipments appear to have been

adjacent; and the meteor and drift measurements were made within a few minutes of the formation of the chemical trails. In respect to the values from drifts and the vapour clouds, quoted errors are ±6, ± 3 m/sec in magnitude; ± (4 to 6)° in azimuth, respectively; and in respect to heights, ± 2 km and ± 0.5 km. Two comparisons, on 6 July 1970 and 15 Octover 1971, at Volgograd, gave agreement within these limits for sporadic-E drifts at 2.27 MHz, and at 112 and 106 km respectively. It was further noted that when the collecting area for meteors overlapped the chemical cloud, on October 15, good agreement was found for one component; the other being unobtainable due to low meteor detection rate. A significant feature of the very complete wind profile, 7 to 140 km, obtained on 6 July is the existence of velocity shears, up to 25 m/sec/km, over regions of ≈5 km altitude extend in the altitude range 90-120 km. (See Figure 2.6).

An illustration of the discrepancies which are encountered when a spatial separation of observing locations exists, is provided by the work of Rees, Roper, Lloyd and Low (1972), and Lloyd, Low, McAvaney and Roper (1972). Comparisons were made between chemical release trails at Woomera, and meteor winds at Adelaide, the two sites being 450 km apart. For one (evening) comparison, magnitudes of velocities were in the same range, 70-100 km m/sec for each technique, but directions differed typically by 50-60°. In another (morning) flight, though discrepancies were tolerable around 94 km, they had reached 100 m/sec by 101 km. Lloyd, et al., rejected an

instrumental origin for the discrepancies.

Total reflection drifts and meteor winds

Three groups of total reflection drift measurements may be distinguished on the basis of the radio frequencies employed, and thus the heights investigated. The first, employing frequencies below 300 kHZ, includes the work of Sprenger and his collaborators (Sprenger and Schminder, 1968; Sprenger, Lysenko, Greisiger and Orljanski, 1971; Lysenko, Portnyagin, Sprenger, Gresiger and Schminder, 1972; Sprenger and Lysenko, 1972). The heights of reflection were estimated to lie in a relatively restricted range, 95-100 km; and data were available only for night hours, due to day-time absorption. First comparisons (Sprenger and Schminder, 1968) were between L.F. measurements based on Kuhlungsborn (54N), and meteor radar measurements at Jodrell Bank (52N) (Greenhow and Neufeld, 1961), for which the separation was ~ 900 km. Comparisons of mean values over years between 1956-65 (for the drifts) and 1953-55 (for the meteor winds) gave good agreement. "Obviously, there can be no longer any doubt that in this height range, the mean drift motion of the ionospheric irregularities as observed by the L.F. drift measurement, even though merely evaluated by the simple similar fade method, would not be nearly identical with the mean wind flow of the neutral gas as indicated by the meteor results." (Sprenger, et al., 1968). Later comparisons with meteor data from the Sheffield radar (Müller, 1968) for four nights showed "fairly close agreement" especially for the

amplitude and phase of the 12 hourly tidal component.

Data from the same L.F. winds systems were compared with radar meteor data obtained at Obninsk, 1600 km distant. (Sprenger and Lysenko, 1972). The agreement between mean monthly "prevailing" winds, for three years, is within about 20% on average; the data sets showing no consistent difference. In a further comparison, a meteor installation was arranged so that one of the two collecting areas (southeast) was coincident with the mid-point of a 185 kHz drifts path. (Lysenko, et al., 1972). It may be noted that the northeast collecting area, which contributed data for the second component of meteor drift, was 100-300 km distant from the coincidence region; and that alternate sampling, over half hour periods, was utilized. For 25 selected nights, the two sets of values show reasonable agreement; with no systematic trend towards larger values from the meteor systems, as is evident in the Adelaide partial reflection-meteor comparison (see below). When tidal components were compared, it was evident that over limited durations, consistent differences were present in both the 6- and the 12-hourly components. This suggested differences of a systematic nature in the motion in respective parts of the total observing area.

The second group of comparisons involved total reflection in E-region, by day; the heights of reflection being derived by means of an ionosonde. Müller (1968) compared Sheffield meteor data with drifts measured at Aberystwyth; whose location coincided with the southwest collecting area for the meteor system. The dominant meteor height was assumed to be

95 km, while the mean drift height was 103 km. For a comparison period of 24 hours duration, the meteor data were found to include a trend, which tended to invalidate a mean-wind comparison. A displacement in time, of some three hours, appears between the two sets of data in respect to the 12-hour component. There were also higher velocities in the drifts data, for 103 km, than in the "95 km" meteor data. By contrast, some additional L.F. drift data from the Kuhlungsborn measurements showed relatively good agreement with the meteor data. The discrepancies appeared consistent with an increase of the velocity of the 12-hour component with altitude over the 8 km height interval, 95-103 km, in accord with estimates from a standard atmosphere.

Felgate, Hunter, Kingsley and Müller (1975), have also made a comparison between E-region drifts and meteor winds; in which one meteor collecting region again coincided with the drifts measuring area, over Lancaster. However, in this comparison the height difference was reduced to ≈1 km on average, for heights around 97-98 km, but occasionally extending to 102 or 106 km. The comparisons were essentially between groups of 3-5 days of drift data, and single days of meteor data, centrally within these days. The drift values refer to 3-5 minute "runs", and meteor values to 10-30 minute intervals. Some 50% of days showed good agreement. In the remainder, there appeared strong discrepancies attributable to sudden changes in E-region height. Since data from separated collecting volumes also agreed well, it was concluded that the "scale" of the winds must be considerable, possibly exceeding several hundred kilometres. This was

considered difficult to explain on the basis of drift velocities which should be ascribed to wave motions; "drifts are representative of the flow of the neutral air masses (to 120 km)".

The third group of total reflection drift measurements was made on sporadic-E reflections, in order that local comparisons might be with a chemical release trail. Wright (1968) employed a variable frequency drifts equipment, and was thus able to make measurements at frequencies above and below the blanketing frequency, f_b. Heights of reflection were determined to better than 1 km. The chemical trails were released at Barbados, Yuma (Arizona) and Eglin (Florida), and winds at the time of drifts measurements were interpolated from a time cross-section built up from a series of trails. The comparisons were grouped according as the working frequency, f, was greater or less than f_b, the blanketing frequency. The results showed substantial scatter; but agreement was better than $f < f_b$ (total reflection) than when $f > f_b$ (partial reflection). For $f < f_b$, the comparison tended to favour the relationship U (neutral winds) = V (drifts velocity), rather than the expected U = V/2, leading Wright to suggest that the point source effect was invalid.

A separate investigation of the validity of the point source effect was carried out by Felgate (1970), using the facilities afforded for antenna switching and pattern sampling by the Buckland Park array. His findings showed, with little ambiguity, that for total reflection in E region, the point source effect was valid. Wright (1972) later came to the same conclusion; and in respect to the drifts technique, he stated

that "we believe we have demonstrated that the radio spaced-receiver method does indeed succeed in detecting neutral air motions at the radio reflection level in the E-region".

An investigation designed to test the measure of agreement between drift results obtained at a separation of 50 km for reflection "points" was carried out by Kokourov, Kazimirovsky, Jakharov and Jovty (1971). Vertical and oblique soundings were made at 2.2 MHz; with "lower ionosphere" data thus relevant to E and E-s regions. Some 2000 useable soundings were obtained for 4 one-monthly periods representative of the seasons. In general, this body of data agreed well with earlier, extensive data. In respect to the effect of separation, by 50 km horizontally and 3-10 km vertically (depending on ionospheric conditions) it was found that a measure of shear, $S = (\Delta u^2 + \Delta v^2)/d$, where u and v are wind components, and d is separation, was of order 10^{-3} sec^{-1}. The bulk of the distribution of S was within 3 m/sec/km. Angular agreement was generally within 30°; the bulk of the distribution being contained within $\pm$30°. These discrepancies were attributed to the vertical and horizontal separations.

Meteor winds and partial reflection drifts.

At Adelaide, S.Australia, a series of comparisons between meteor trail velocities and partial reflection drifts have been made since 1967. The locations of the two experimental systems are such that drifts are measured within the collecting area for meteors, of $\approx$200 km radius; but the majority of meteors

are detected outside the zone of drift measurements, which is ≃30 km in radius at the same height ≃90 km. Since the meteor system determined only the line of sight component of trail drift, it was necessary to use two trails, at the same altitude, but differing in location, and usually in time, to determine a single wind velocity. The components so combined might be derived anywhere in the collecting area. In respect to height agreement, individual meteor echoes were considered to be known to within ± 2 km; while the drifts were determined by grouping data within intervals initially 10 km, e.g. 80-90 km; and later within 5 km. In respect to times of measurement, a basic comparison interval of 3 hours, for averaging of velocities, was adopted. Within that interval, "the only (meteor) echoes may occur early, ---- whereas ionospheric conditons may dictate that drifts can be determined only in the last hour" (Stubbs, 1973).

Within this framework, the work at Adelaide has included a series of adjustments designed to improve the conditions for comparison studies. Thus the early work of Rossiter (1970) showed poor agreement between the results of the two methods, the drifts velocities tending to be less than meteor values. In this work, the comparisons were between a drifts velocity, and a velocity derived from the application of Groves' (1959) analysis to a set of meteor values, some of which would have occurred outside the time period for a comparison. Alternatively, a comparison was made between a line-of-sight meteor trail component, and a

drift velocity resolved along that line. The height increment for drifts was 10 km. Each procedure has evident disadvantages. Further, the receiving triangle used by Rossiter was right-angled, and of side 91 m; a distance which was acknowledged to be less than desirable.

Further investigations were conducted by Stubbs, (1973, 1975), and by Stubbs and Vincent (1973). In this work, the size of triangle was increased to 182 and 204 km (two adjacent triangles being employed, enabling a check for internal consistency of drift values); the shape of triangle was changed to more nearly equilateral (Barber, 1957), and a narrower beam width employed, using four parallel dipoles at the vertices of the triangle. Height increments were decreased to 5 km; and transmitter power increased. In respect to the meteor data, Groves' analysis was dispensed with, and comparisons made only with line-of-sight velocities averaged over three hours.

The limitations of space and time sampling, noted above, remained; and for the drifts, it was found that 50% of observations were not suitable for the derivation of "true" velocities by the full correlation analysis. The data accumulated for this work covered all months of 1972, for 3-6 days per month at 10-20 minute intervals, as well as special observations, made in July of 1970-72, for comparison with earlier observations in the same month of the year. The data available for these comparisons vary in quantity according to altitude range, being most frequent around 85-90 km.

An example of the results of the comparison studies is given in Figure 2.7 other similar figures appear in the works quoted. In summary, it is evident that there is substantial agreement between the two techniques. It is also evident that the drift values tend not to reach the peak values evident in meteor data by some 10%; and further, that the meteor data tend to be the more variable. With regard to the lesser velocities of drift, Stubbs suggests that effect of size of triangle has not been completely eliminated; and that the larger scales in the diffraction pattern have tended to produce lower velocities. Later work by M.J. Burke (private communication) suggests that if these larger scales are associated with longer fading periods, then the "true" velocity may be substantially underestimated. The variability of the meteor data is ascribed to the size of collecting area; and more specifically, to the fact that when internal gravity waves are present, velocities at the same heights, but at points separated by $\approx$100 km, may differ due to the slope of phase fronts. A seasonal change in the variability of the meteor results lends credence to this possibility. One of the conclusions reached by Rossiter (1970), that winds were mainly eastward during mid-day hours, is adequately substantiated by the 24-hour observations. For the month of July in years 1971 and 1972, the correlation coefficients of values from the two techniques for regions 85-90, and 90-95 km, were significant at better than 0-5% level, for zonal components; and at 10% level for meridional.

Stubbs' conclusion in respect to these comparisons is

"If the meteor technique measures the neutral wind (and it is widely agreed that it does) then it must be concluded that for much of the time so does the drift technique". In review, this conclusion appears justified; but it must be held with the recognition that by virtue of the differing sampling processes, in time and space, each technique determines a distinctive velocity which is merely representative of the actual velocity field. The latter remains the hypothesized true velocity; but in reality, there is available only a meteor technique velocity, or a drifts technique velocity.

Figures for Chapter 2

CAPTIONS

Figure No.

2.1 Horizontal structure functions, from Justus and Woodrum, (1972), for horizontal winds, 50-65 km, (top) and 80-140 km (bottom).

2.2 Horizontal structure function for vertical winds, from Justus and Woodrum, (1972).

2.3 Vertical structure functions for single day differences (solid dots), and for 10-12 day differences (open circles), from Justus and Woodrum (1972).

2.4 Irregular wind components, obtained by subtracting a median for one hour from individual (5-minute) winds, from Gregory and Manson, (1974).

2.5 Irregular wind amplitudes, for single day differences, from Justus and Woodrum, (1972).

2.6 Wind profile, from rocket head (□), chaff (△), drifts on E-S layer (0 ⌀), and chemical release trails (○), reported by Andreeva et al, (1973). Solid points show U-component; open points, V-component.

2.7 Comparison of meteor and partial reflection drift measurements for one month (July, 1972) at Adelaide. From Stubbs and Vincent (1973).

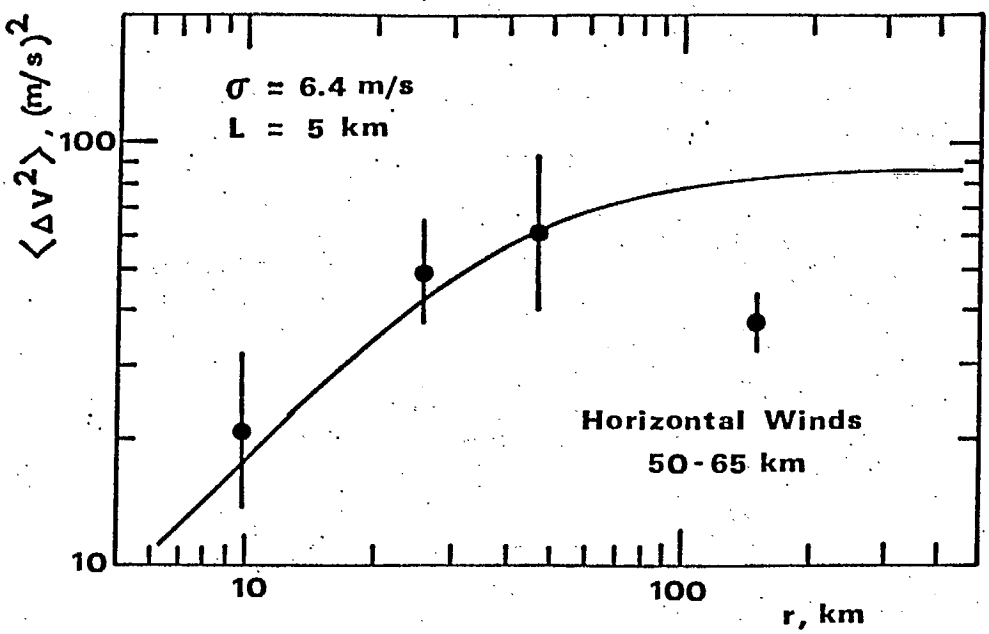
σ = 6.4 m/s
L = 5 km
100
10
10
100
r, km
⟨Δv²⟩, (m/s)²
Horizontal Winds
50-65 km

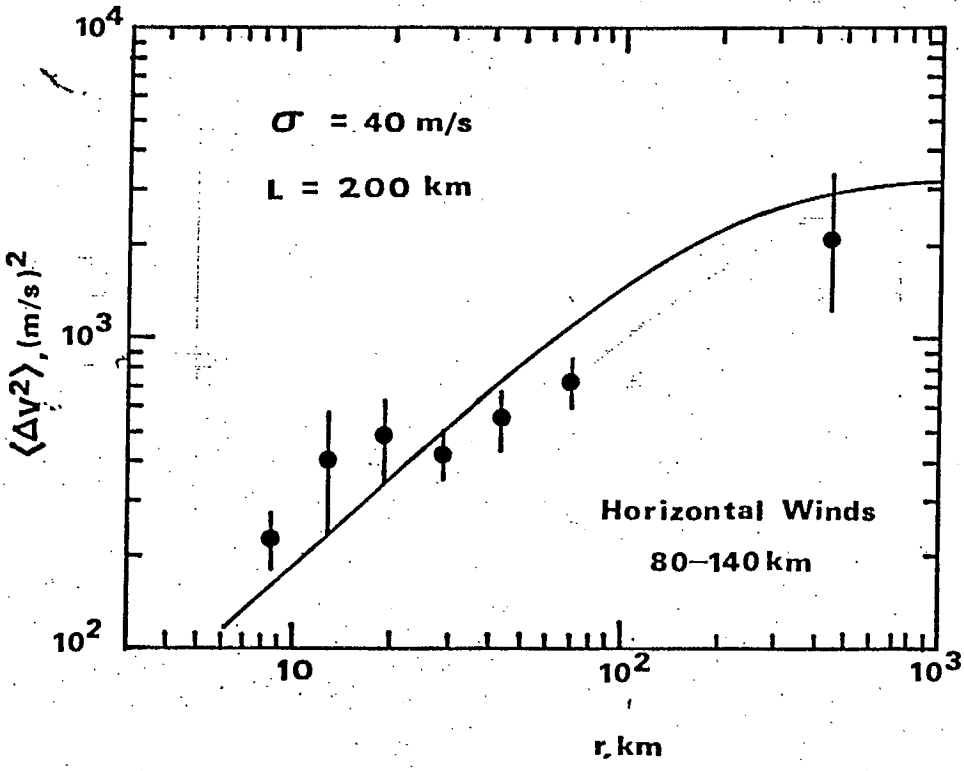
σ = 40 m/s
L = 200 km
10⁴
10³
10²
10
10²
10³
r, km
⟨Δv²⟩, (m/s)²
Horizontal Winds
80–140 km

Figure 2.1

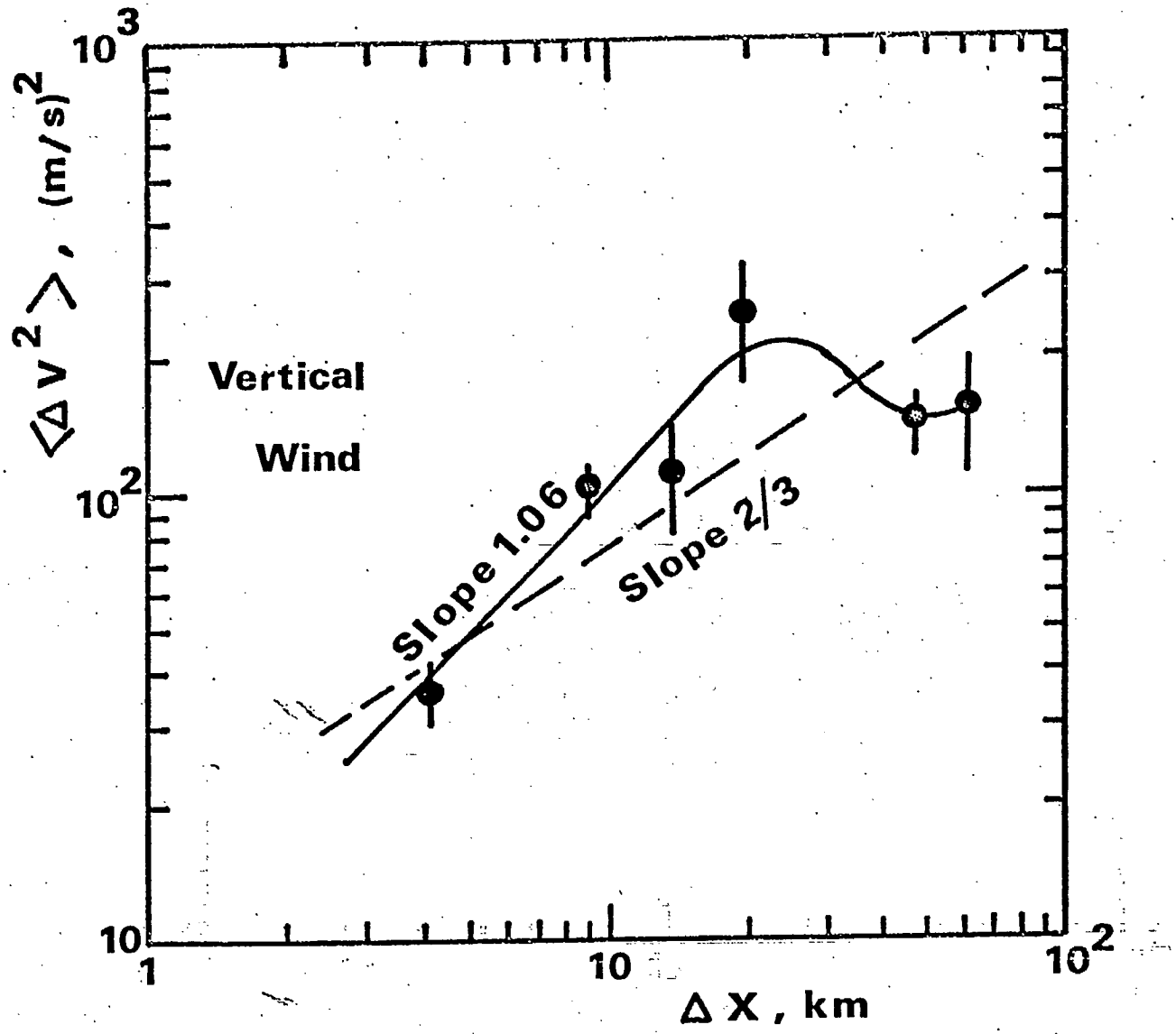
10^3
10^2
10
1
10
10^2
$\langle \Delta V^2 \rangle$, $(m/s)^2$
Vertical
Wind
Slope 1.06
Slope 2/3
ΔX, km

Figure 2.2

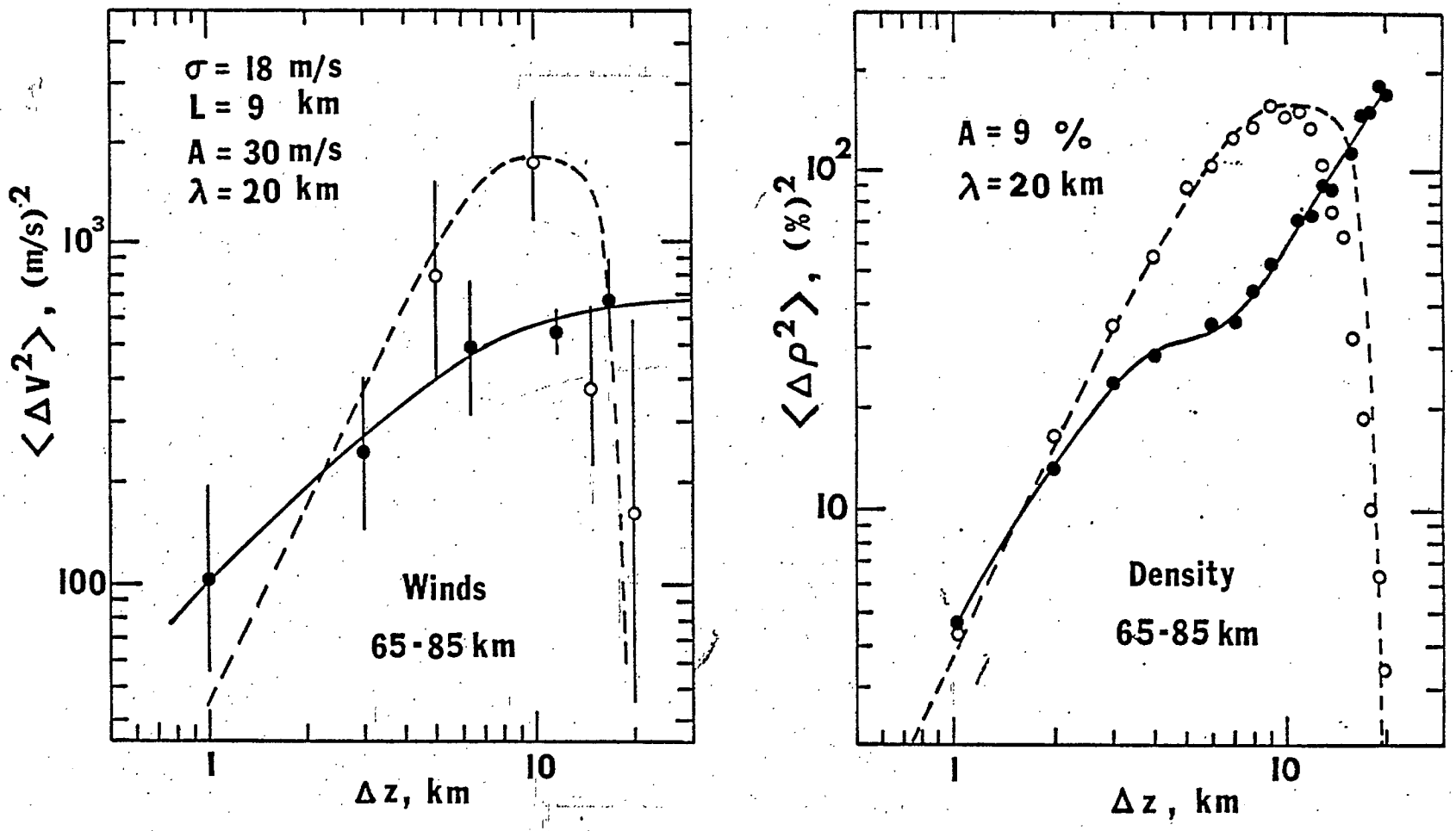
σ = 18 m/s
L = 9 km
A = 30 m/s
λ = 20 km
Winds
65-85 km
$\langle \Delta V^2 \rangle$, (m/s)^2
10^3
100
1
10
Δz, km
A = 9 %
λ = 20 km
Density
65-85 km
$\langle \Delta \rho^2 \rangle$, (%)^2
10^2
10
1
10
Δz, km

Figure 2.3

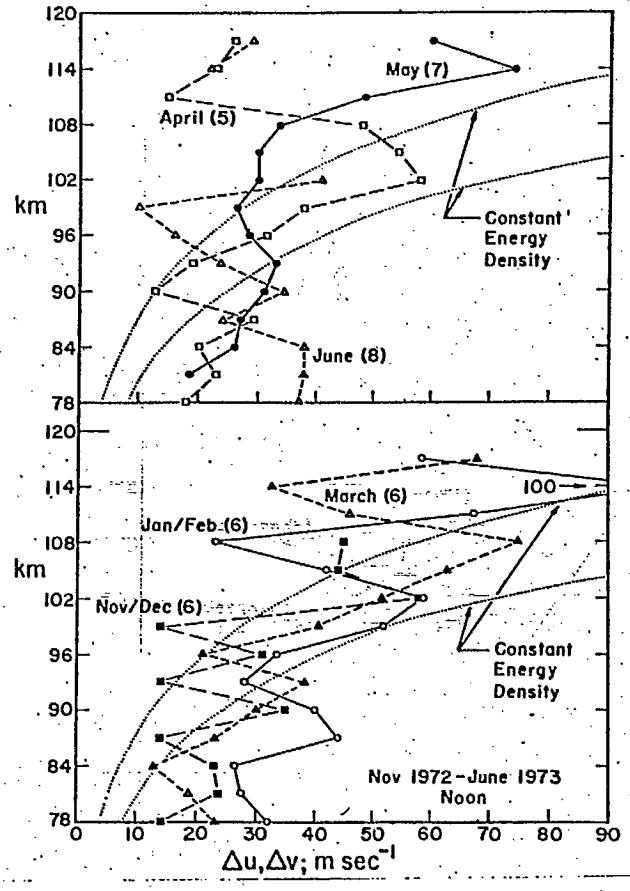
120
114
108
102
km
96
90
84
78
May (7)
April (5)
Constant
Energy
Density
June (8)
120
114
108
km
102
96
90
84
78
March (6)
100
Jan/Feb (6)
Nov/Dec (6)
Constant
Energy
Density
Nov 1972 - June 1973
Noon
0
10
20
30
40
50
60
70
80
90
Δu,Δv; m sec⁻¹

Figure 2.4

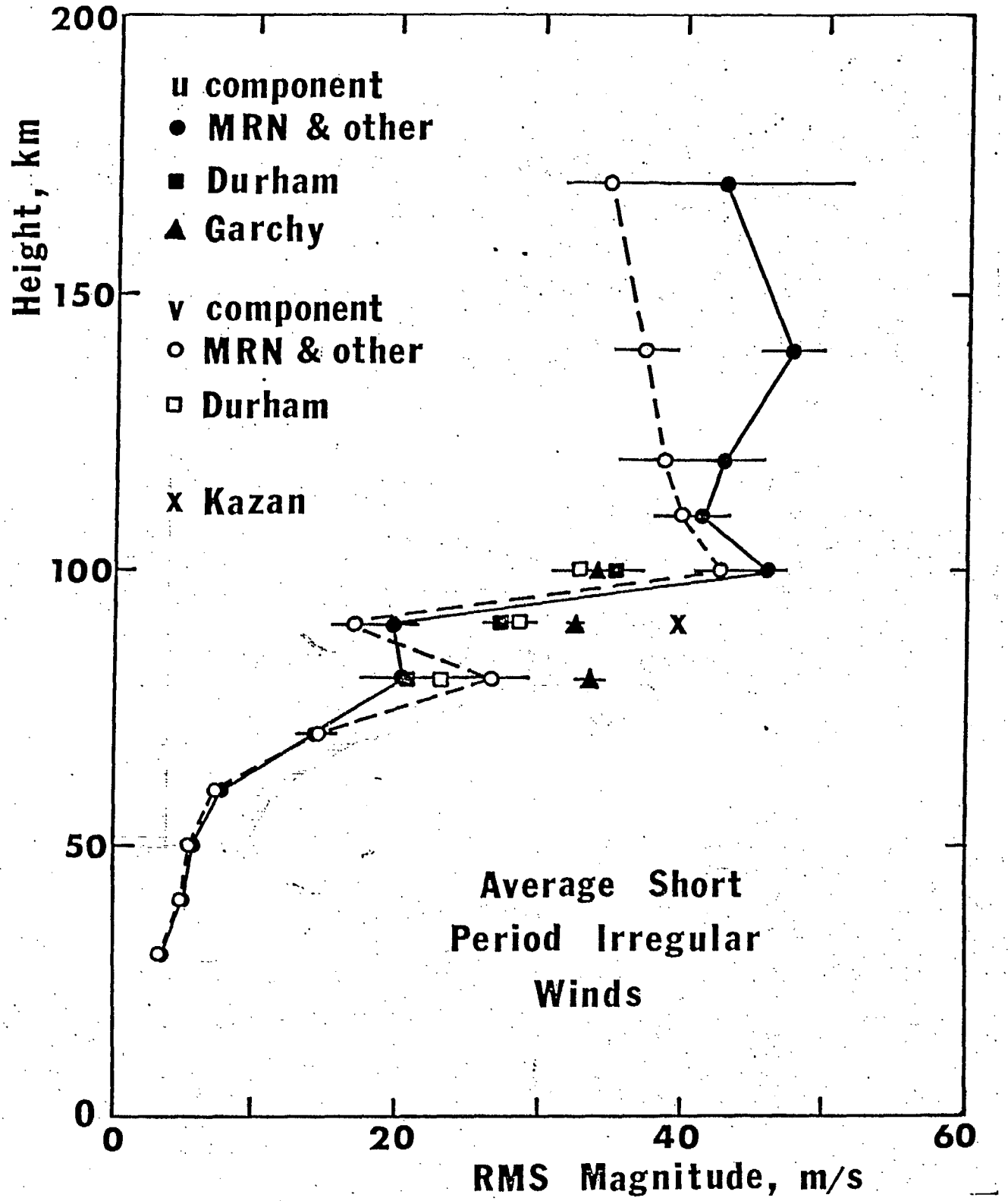
200
150
100
50
0
Height, km
u component
MRN & other
Durham
Garchy
v component
MRN & other
Durham
Kazan
Average Short
Period Irregular
Winds
0
20
40
60
RMS Magnitude, m/s

Figure 2.5

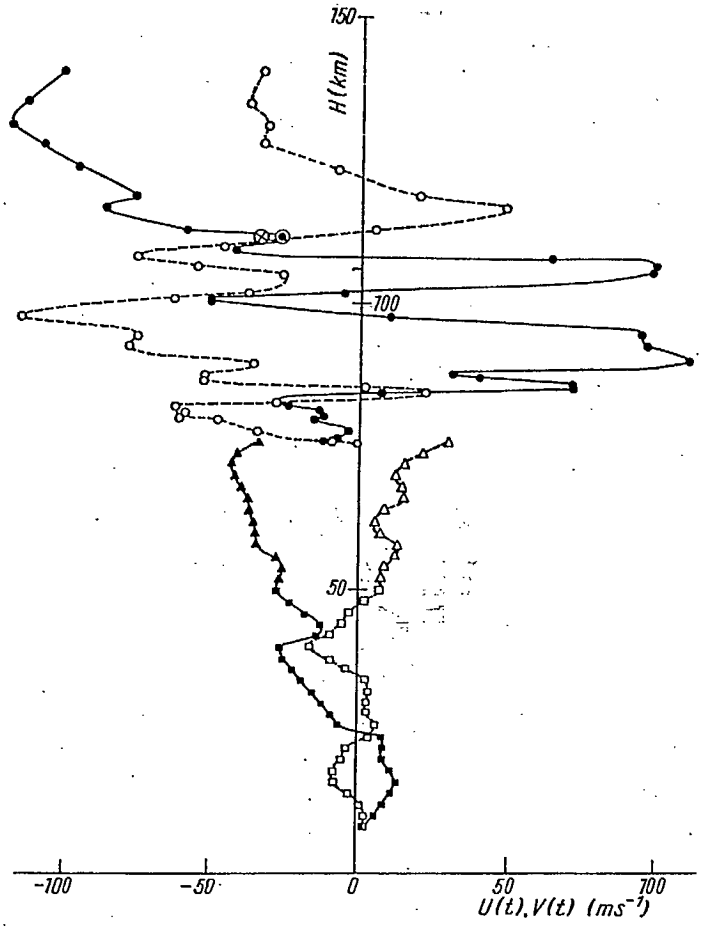

Figure 2.6

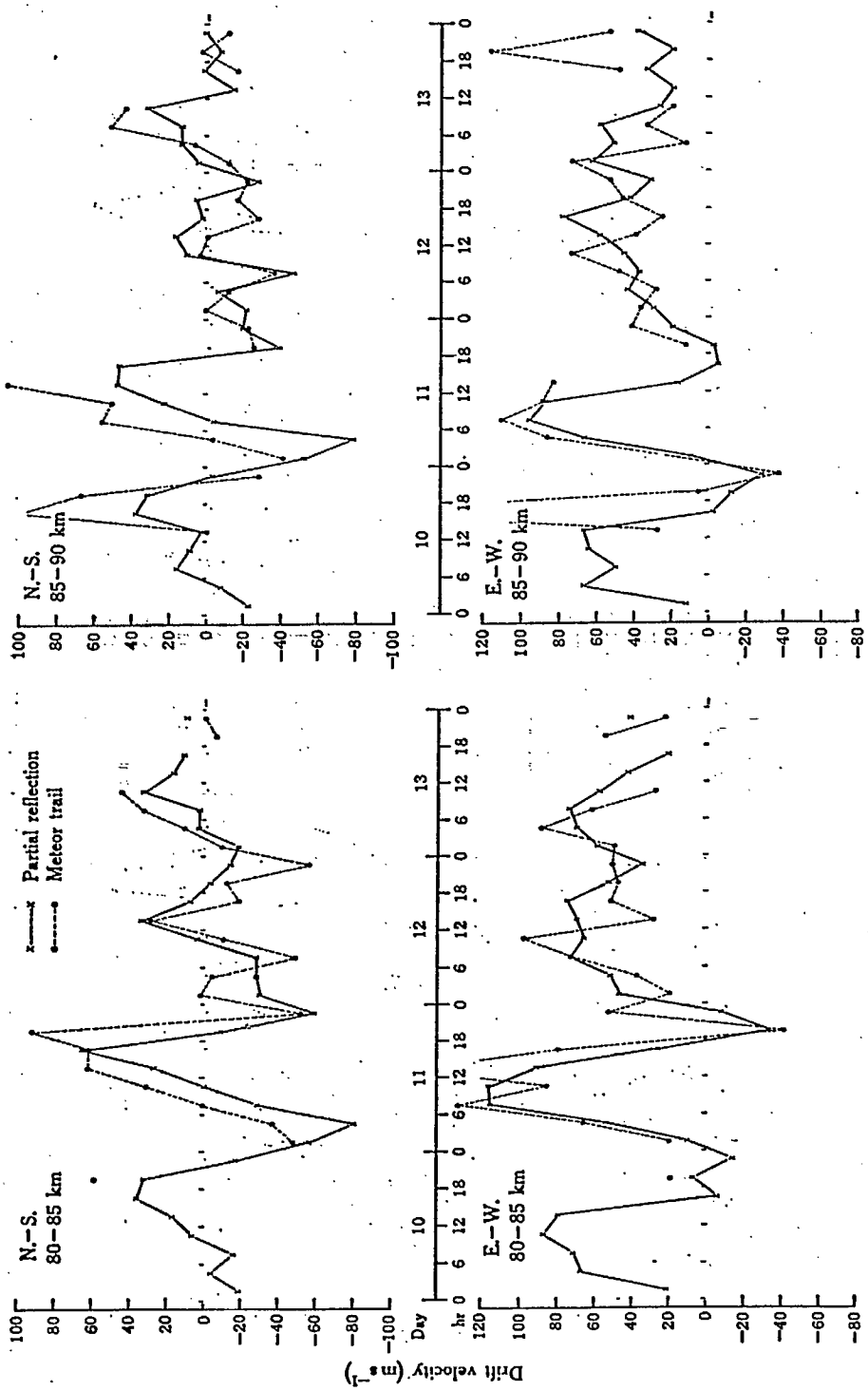
N.–S.
80–85 km
E.–W.
80–85 km
N.–S.
85–90 km
E.–W.
85–90 km
Partial reflection
Meteor trail
Drift velocity (m s⁻¹)
Day
hr

Figure 2.7

Chapter 3. Analysis by sample technique.

3.1 Introduction

The sample method attempts to obtain an apparent drift velocity by analysing relatively short "fading" sequences (10-20 sec) from a longer record of 3-5 minutes. Ideally, fading sequences at the three antennas should define the passage of a single maximum (called an 'irregularity') in the ground amplitude pattern. Difficulties arise when an irregularity cannot be uniquely defined on the three spaced antennas, either because the shapes of the three amplitude peaks are quite different, or because the irregularity size is smaller than the spatial separation of the antennas. Included in the latter are cases when one irregularity is not clear of the antenna array before the next one arrives.

3.2 Lines of maxima

A line of maximum is defined as the locus of maximum amplitude ('ridge') in the ground pattern of an irregularity. In cases where this is ambiguous (e.g. a perfectly circular pattern) it will be defined as a line travelling with the pattern, which crosses each antenna as the maximum amplitude occurs. For example, the line of maximum for a circular pattern would be a straight line perpendicular to the drift motion.

3.3 Normalized time discrepancy

A general criterion for determining whether the cal-

culated time delays of the pattern between a pair of antennas represents the passage of one irregularity is the normalized time discrepancy, denoted N.T.D. This will now be defined.

Figure 3.1 shows a line of maximum crossing the antenna array. The accompanying amplitude sequence plot, Figure 3.3 shows the instants of maximum amplitude in the three antennas. The interesting fact is that, as long as the line crosses each antenna only once, and the time of crossing can be measured, the equation $(T_1-T_2)=(T_3-T_2)+(T_1-T_3)$ holds, regardless of the shape of the line or its motion. This is true for any three times, one in each sequence. If the definition $T_{ij}=T_j-T_j$ is made, where T_{ij} is the time taken for the line of maximum to move from antenna i to antenna j, then; for these conditions,

$$T_{21} = T_{23} + T_{31}$$

$$\text{or:} \quad T_{12} + T_{23} + T_{31} = 0 \qquad (3.1)$$

However, in practice, the sum of the three time delays in this equation is rarely found to equal zero. The value of the sum will be called the time discrepancy. A normalized value which does not depend on the pattern speed is defined as follows:

$$\text{N.T.D.} = |T_{12}+T_{23}+T_{31}| / (|T_{12}|+|T_{23}|+|T_{31}|) \qquad (3.2)$$

This has values in the interval [0,1], and essentially indicates whether the three time delays are self consistent.

Of course, a low N.T.D. could occur sometimes if the time delays were entirely unrelated, i.e. not due to the passage of a single irregularity. For the situation in which the time delays are independent random values comprising a uniform distribution centered on zero delay, the probability density and distribution functions for the N.T.D. have been calculated. These are shown in Figure 3.2. A uniform distribution is reasonable because usually the time delays are selected from a finite time interval, given by the maximum lag of a cross-correlation sequence. These curves will be used later in comparisons with experimentally determined distributions of N.T.D.

3.4 Goodness of data criteria

The N.T.D. is the basic criterion of self-consistency in the time delays; however, conceptually, it does not give an indication of the expected errors in magnitude and direction of a deduced wind vector. The latter arise during the attempt to select a wind vector which agrees with the measured time delays.

It can be shown that, when the N.T.D. is zero, there is an equivalent straight line of maximum moving perpendicular to its length which would give the same time delays as those measured. The following equations, which refer to Figure 3.4, define the time delays in terms of the magnitude (V) and direction (α) of the motion of this line.

$$T_{21} = \frac{d}{V} \cos \alpha$$

$$T_{23} = \frac{d}{V} \cos (60° - \alpha)$$

$$T_{13} = \frac{d}{V} \cos (120° - \alpha) \qquad (3.3)$$

where d is the antenna separation.

Using equation 3.3, a least squares fit to the three times can be made, and the standard error in V, expressed as a percentage, can be determined. This is available as a criterion of consistency of times. It is used for example, at C.R.C. (M.J. Burke, private communication). An alternative criterion is the comparison of the angles between the three vectors (one of which is not independent, in theory); these being taken in pairs from equation 3.3. This criterion has been used at University of Saskatchewan.

These two criteria may be compared with the N.T.D., as indicators of data quality. Random sets of times, as used in compiling Figure 3.2, have been employed. The comparisons with the N.T.D. are shown in Figures 3.5 and 3.6. The relationships are not unique because in the first case errors in angle, and in the second, errors in speed, are ignored.

3.5 Reasons for non-zero N.T.D.

If the three peaks in amplitude due to one irregularity can be identified in the fading sequences, e.g. through similarity in shape, then a non-zero N.T.D. will be the result of computational problems in finding the delays. The maximum cross-correlation

will identify some sort of 'average' delay between antennas rather than the delay due to an unambiguous line of maximum. The time discrepancy would be expected to be proportional both to the width of the peaks in the cross-correlation and to the dissimilarity in the shapes of the peaks. Hence large N.T.D.'s could be generated if the time delays themselves were small.

If the three fading peaks are very dissimilar in shape, such as might be due to irregularity size much less than antenna spacing, it may happen that a higher cross-correlation is found between the sequences due to different lines of maximum at two antennas than due to the same line. If more than one peak in a fading sequence is involved, there exists the possibility of incorrect pairing of peaks. For example, in Figure 3.7, good correlation might be obtained between peaks b1 and b3, a1 and b2, and b2 and a3, leading to three independent time delays. However, the velocity so deduced would differ considerably from that based on correct identification.

3.6 Conversion of time delays to drift when N.T.D.~ 0

As stated previously, the deduced velocity when the N.T.D. is zero is just the motion of the equivalent line of maximum perpendicular to its length. The assumption is often made that the actual line of maximum is straight and perpendicular to the drift, as would apply if the irregularities were circular. Briggs and Page (1955) derived the distribution of angles of lines of maxima for irregularity patterns basically circular but with random deviations. It appears that the distribution

will be very dependent on the choice of model. Their probability density function f was given as

$$f(\tan \gamma) = \frac{1}{\sqrt{0.74\pi}} \; e^{-\tan^2\gamma/0.74} \qquad (3.4)$$

where γ is the angle deviation from perpendicularity to drift. This distribution does not appear to have been verified with experimental data.

Ratcliffe (1954) has compared an assumed uniform distribution of angles with experimental distribution of time delays between a pair of antennae for single irregularities in the E region. Some of his data shows fairly good agreement with this assumption. Other data indicate that the line of maximum was perpendicular to the drift less often than predicted by the uniform assumption. Still other data show skewed distributions which he suggests are probably due to a change in the drift during the recording, or to the presense of a non-perpendicular preferred direction.

Some possible effects on the deduced velocity of particular lines of maxima will now be discussed. It will be assumed that the line is fixed with respect to the drift motion, i.e. there is no time change in shape, or non-translational motion.

3.6.1 Straight line of maximum

Figure 3.8(a) illustrates the case of a straight line of maximum whose perpendicular is at an angle β with the drift. The deduced velocity is just the motion of the line perpendicular to its length, viz. the component of the actual drift along the

perpendicular to the line. It can be seen that, given a constant actual drift, and variable angles of the line, the deduced velocities for each line will lie on a circle passing through the origin whose diameter is the actual drift vector.

3.6.2 Curved line of maximum, with motion along an antenna pair.

Figure 3.8(b) shows an irregular line travelling along the direction defined by a pair of antennas. It can be seen that this irregular line is equivalent to the straight line shown, and that the conclusions of paragraph 3.6.1 apply.

3.6.3 Curved line, with drift not along an antenna pair.

No general conclusions can be drawn in this case. (See for example Figure 3.8(c), for which the deduced velocity could be in the opposite direction to the actual drift). However, if the line has a large radius of curvature (i.e. almost straight) the difference in deduced speeds between the actual curved and the approximating straight line is rather small, being of the order of $\Delta s/d$, where Δs is the departure from linearity over the antenna spacing d. (See Figure 3.8(d)) A particular calculation for a circular line with radius of curvature $(3/2)d$ gave a maximum difference in deduced speed of about 10%.

The conclusion to be drawn from the above three cases is that, for relatively straight lines, the deduced sample vector should lie on a circle whose diameter is the actual drift vector.

3.7 Combination of sample vectors.

The vector derived from that portion of a data sequence which corresponds to the passage of an irregularity over an antenna system will be termed a sample vector. In practice, it may not be possible to identify this situation; but the term sample will still be applied to a short portion of a longer, or total, record. Some methods for combining sample vectors will now be considered.

3.7.1 Mean vector method

This method averages the vectors (considered acceptable on the basis of the N.T.D. or other equivalent criteria) obtained from all samples in a record. The difficulty with this procedure is that the angular distribution of lines of maxima must be known, and a large number of samples (irregularities) must be included in the average to reduce statistical scatter. This, if the lines are assumed symmetrically distributed about the perpendicular to the drift, the direction of the mean vector will be a good approximation to that of the actual drift, but the magnitude will be lower than the actual drift by a factor which depends on the angular distribution of lines. If all lines are assumed to be perpendicular to the drift, the required factor is 1. If a uniform distribution of angles is assumed it can be shown that the factor is 0.5. Von P. St. Pütter (1955), (a reference suggested by M.J. Burke) assumes a probability density proportional to $\cos(\beta)$ (β is defined in Figure 3.8(a)), and finds a factor of 2/3. The distribution used by Briggs and Page (1955)

(Reference Equation 3.4) can be integrated numerically. It yields a factor of 0.8.

3.7.2 Straight line fit to inverted sample vectors.

Since the sample vectors $\vec{V}_s$ lie on a circle, the vectors $\frac{1}{V_s}\vec{V}_s$ (where the hat represents a unit vector) lie on a straight line, illustrated in Figure 3.9. The perpendicular to the straight line has the direction of the actual drift $\vec{V}_s$ and a magnitude of $1/V_D$.

The main difficulty with this procedure is that the fit will be very sensitive to low magnitude sample vectors. The advantage is that only two samples (with differently oriented lines)are needed to define the actual drift.

3.7.3 Mean times

This mean was first used by Ratcliffe (1954) and later by Briggs and Spencer (1955) to determine apparent drift velocities. Basically the same assumptions are made as in the mean vector method, viz. a symmetrical distribution of lines about the perpendicular to the drift, but in this case the form of the distribution is not required. The method averages the three separate time delays for the three pairs of antennas and calculates the drift from the resulting three mean times. Again, a large number of samples is required, but rejection of samples on the basis of the N.T.D. may not be necessary because only one of the time delays may be in error. Rejection of individual delays on the basis of the value of maximum cross-

correlation found might be a better procedure. The N.T.D. criterion is applied to the final mean times to gauge the consistency of the data.

3.7.4 Mean cross-correlation method

This method averages the cross-correlation function for a pair of antennas over all samples, and then uses the time delays determined by the positions of the maximum cross-correlation to determine the drift. Essentially, the result should closely approximate the results obtained with longer sequences which will be discussed in the next chapter. The N.T.D. is still used as a criterion of goodness but the justification is no longer simple. This topic will be developed further in later chapters.

Figures for Chapter 3

CAPTIONS

Figure No.	
3.1	Line of maximum crossing, antennas 1-3.
3.2	Probability distribution and density function for N.T.D.
3.3	Sequence of amplitudes at antennas 1-3.
3.4	Time delays for equivalent perpendicular line of maximum.
3.5	Relation between N.T.D. and % standard error of $\|V\|$, computed from random times.
3.6	Relation between N.T.D. and maximum angle between vectors determined by pairs of Equation 3.3.
3.7	Sequence of amplitudes permitting alternative grouping of peaks.
3.8(a)	Straight line of maximum, with perpendicular at angle B to drift vector.
3.8(b)	Curved line of maximum, and equivalent straight line.
3.8(c)	Hypothetical curved line, with deduced drift opposite to actual drift.
3.8(d)	Approximation of curved line to straight line.
3.9	Straight line fit to inverted sample vectors.

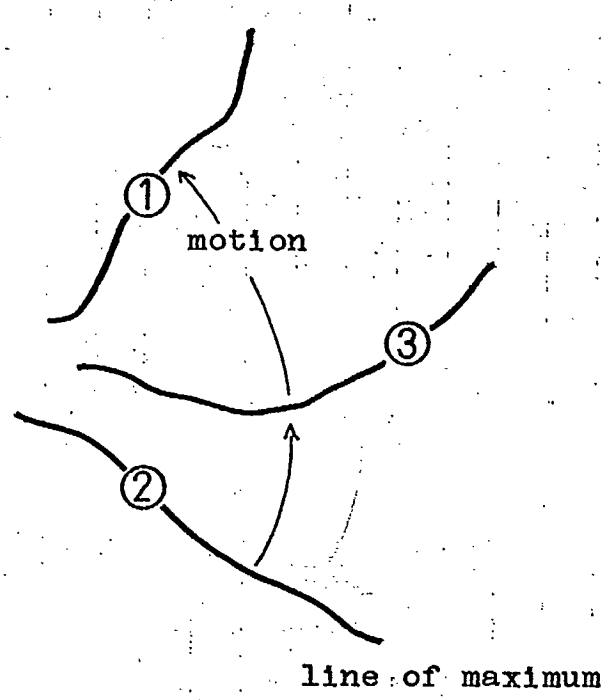

Figure 3.1

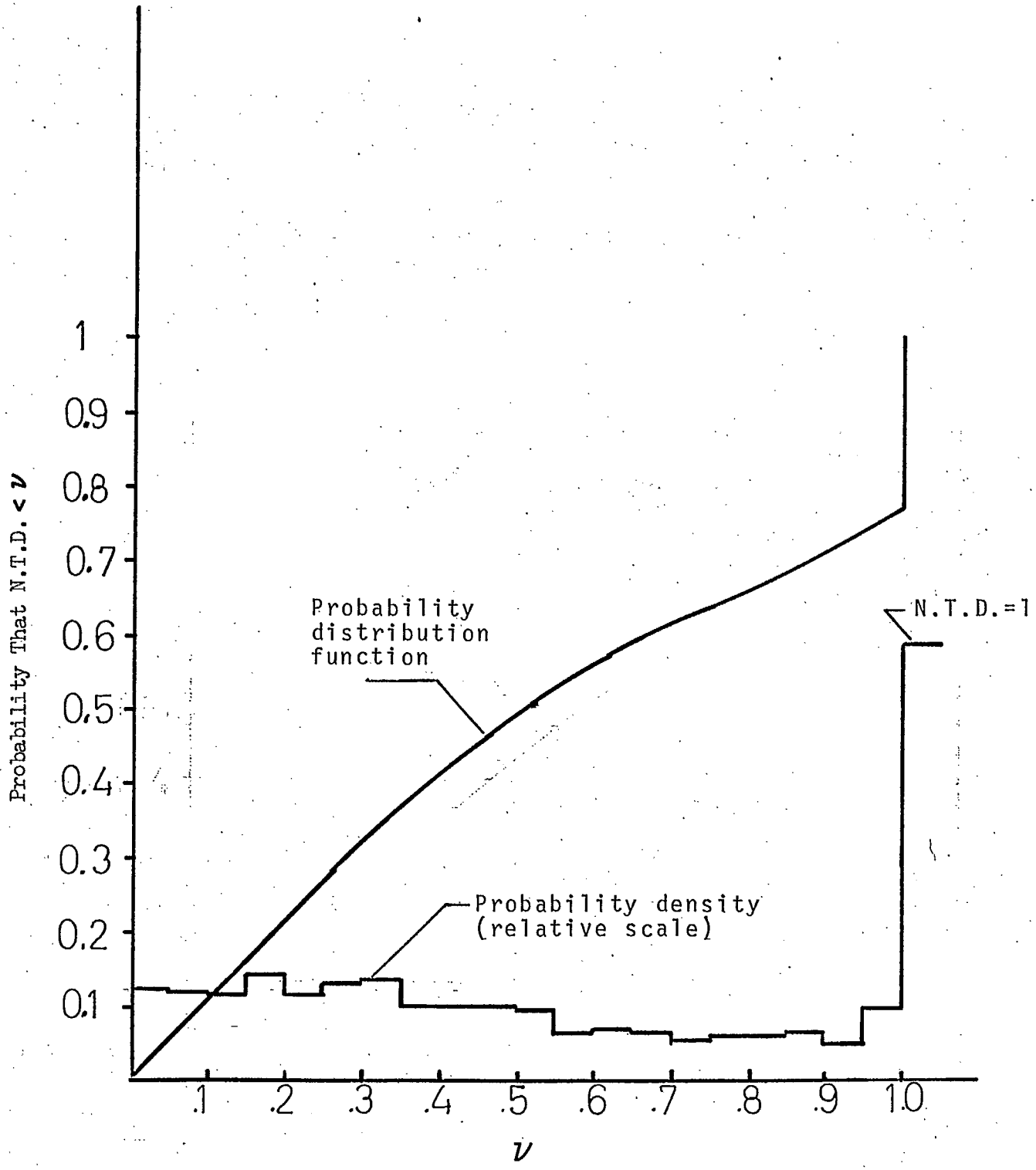
Probability That N.T.D. < ν
1
0.9
0.8
0.7
0.6
0.5
0.4
0.3
0.2
0.1
Probability distribution function
N.T.D.=1
Probability density (relative scale)
.1
.2
.3
.4
.5
.6
.7
.8
.9
1.0
ν

Figure 3.2

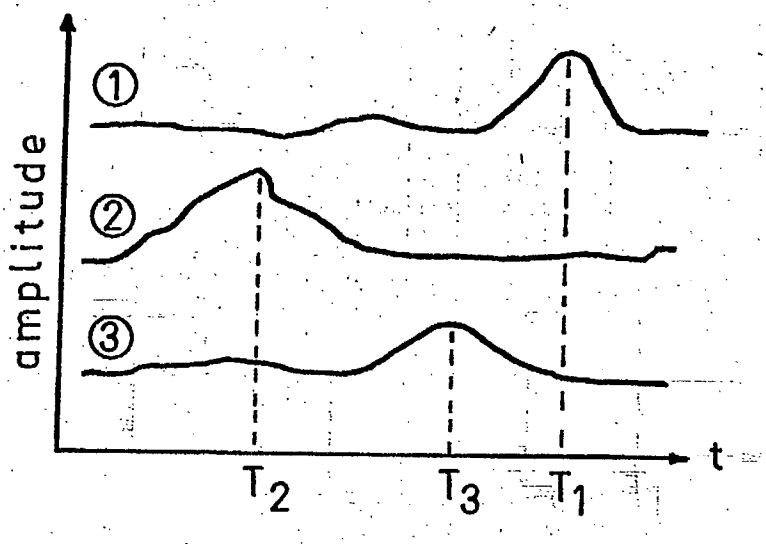

Figure 3.3

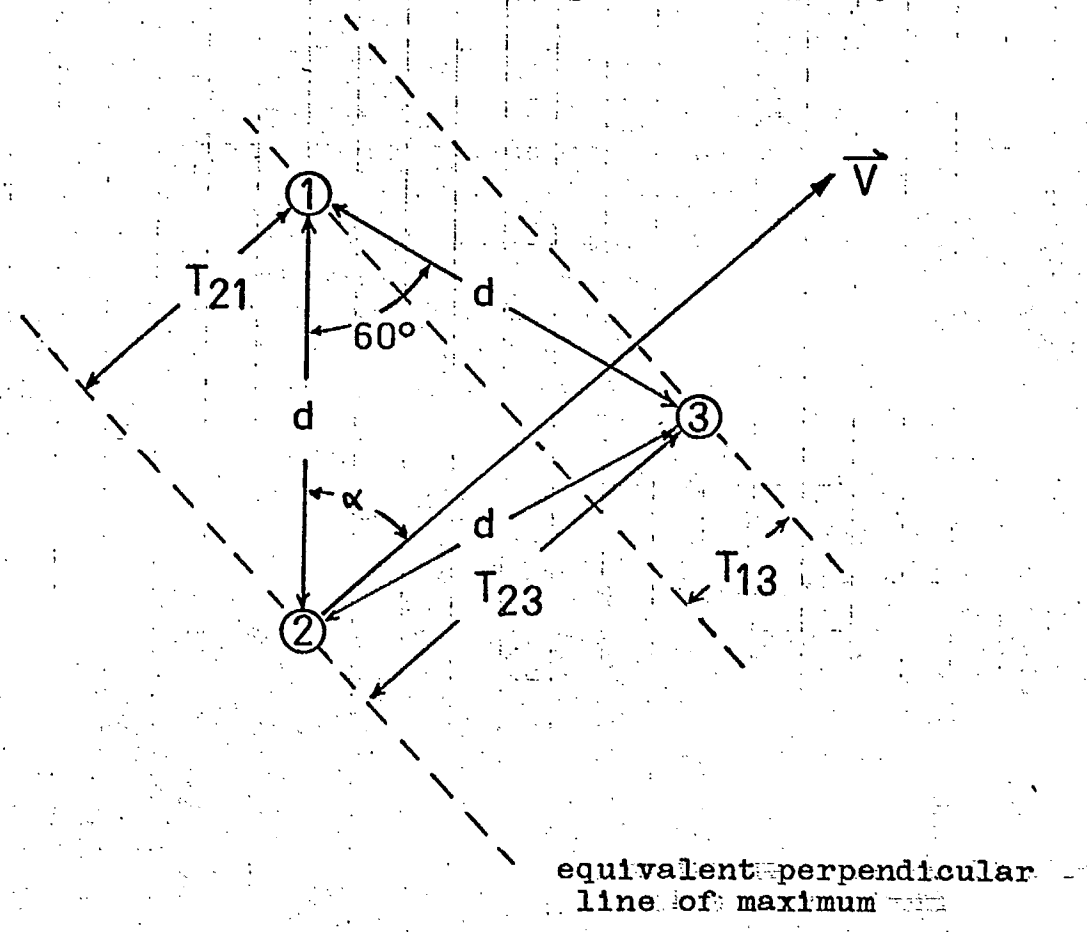
1
2
3
T_{21}
T_{23}
T_{13}
d
d
d
60°
α
$\vec{V}$
equivalent perpendicular
line of maximum

Figure 3.4

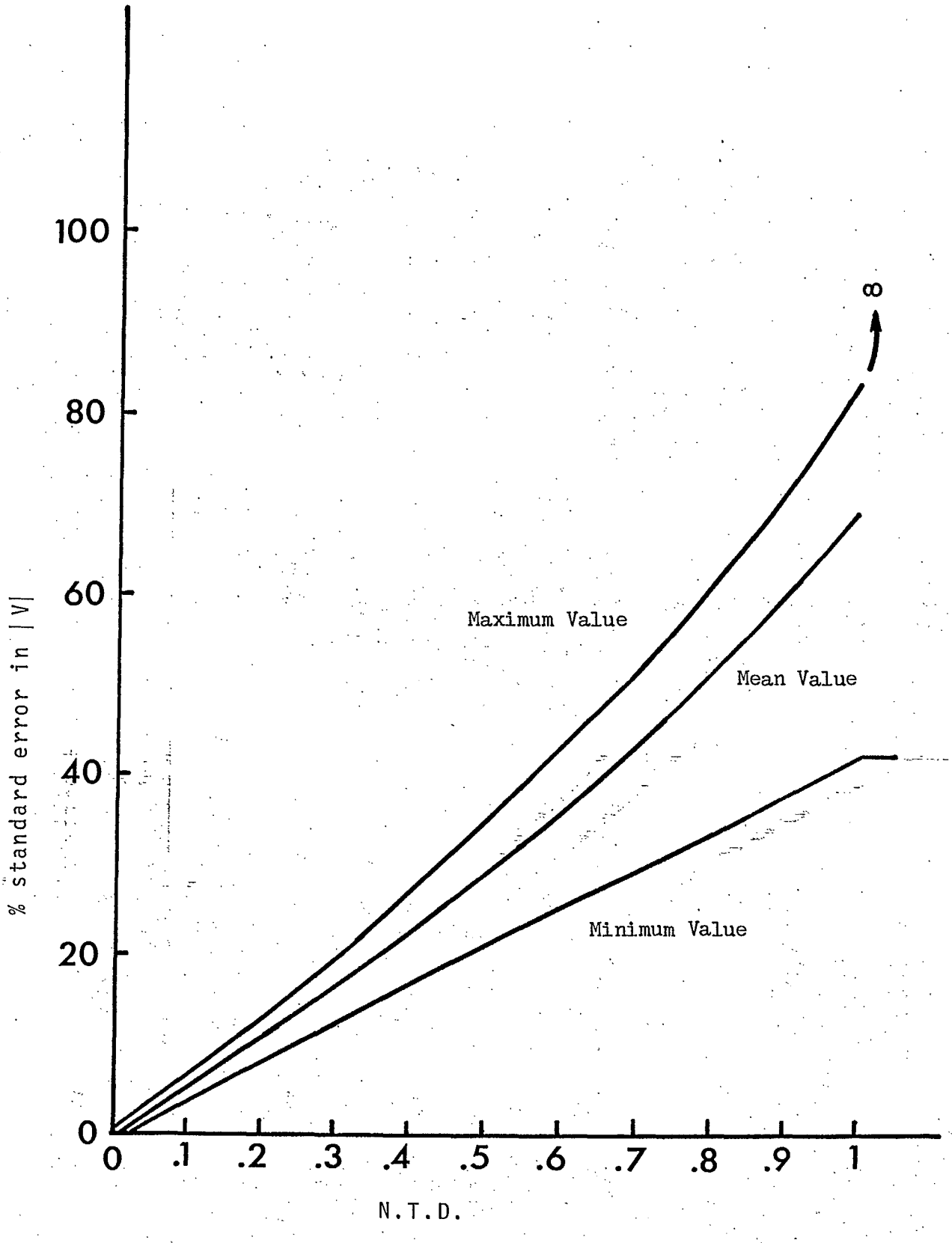
100
80
60
40
20
0
% standard error in |V|
∞
Maximum Value
Mean Value
Minimum Value
0
.1
.2
.3
.4
.5
.6
.7
.8
.9
1
N.T.D.

Figure 3.5

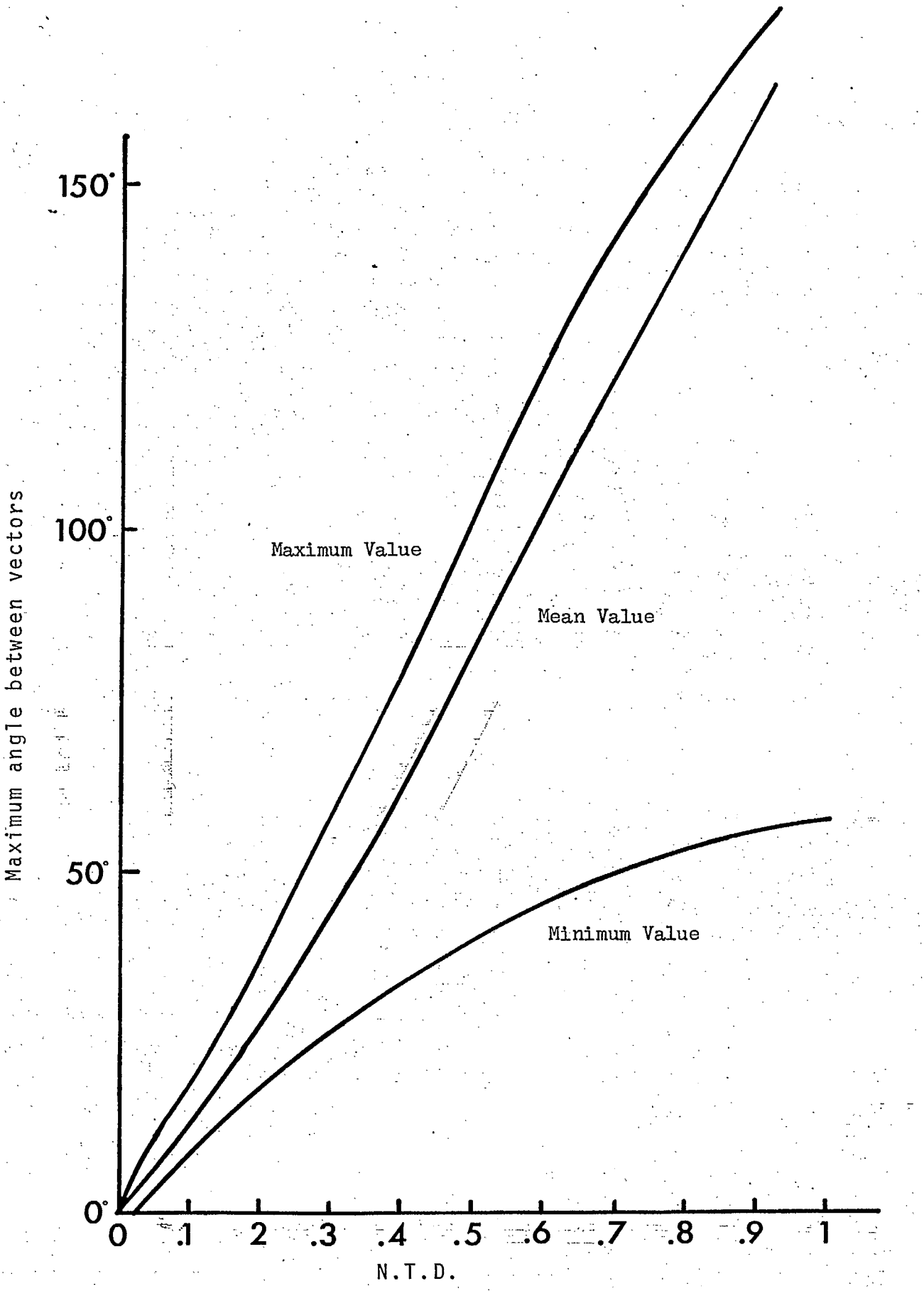
150°
100°
50°
0°
Maximum angle between vectors
Maximum Value
Mean Value
Minimum Value
0
.1
2
.3
.4
.5
.6
.7
.8
.9
1
N.T.D.

Figure 3.6

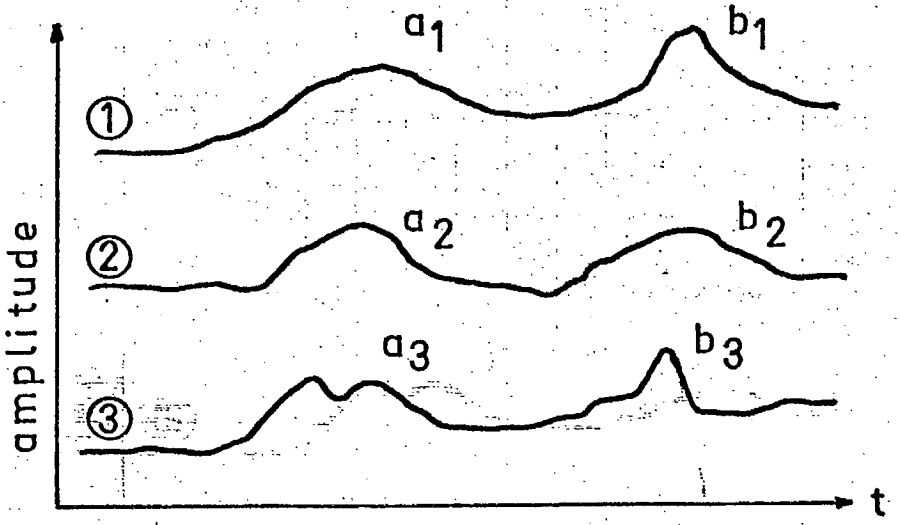

Figure 3.7

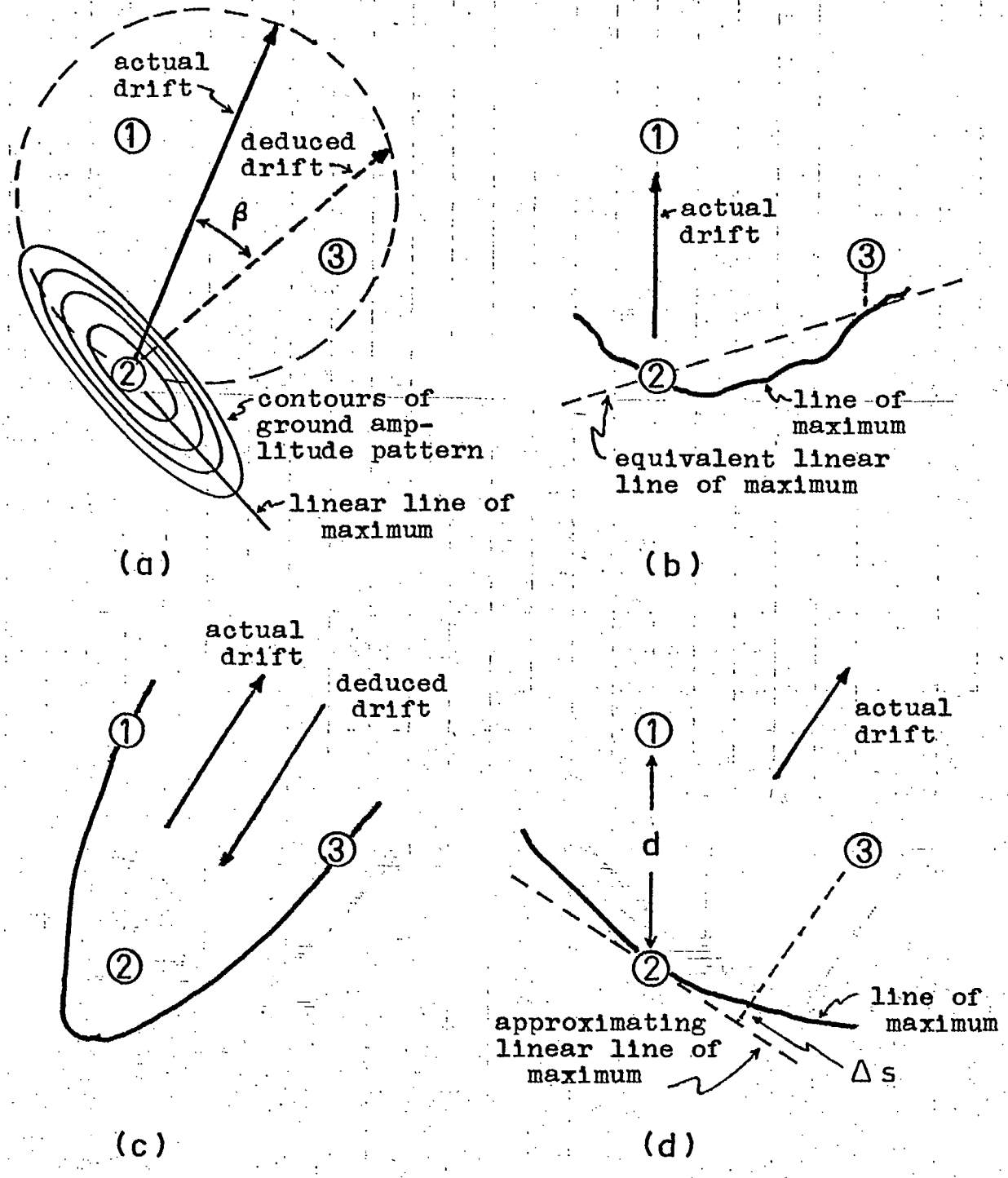
actual drift
①
deduced drift
β
③
②
contours of ground amplitude pattern
linear line of maximum
(a)
①
actual drift
③
②
line of maximum
equivalent linear line of maximum
(b)
actual drift
deduced drift
①
③
②
(c)
actual drift
①
d
③
②
line of maximum
approximating linear line of maximum
Δs
(d)

Figure 3.8

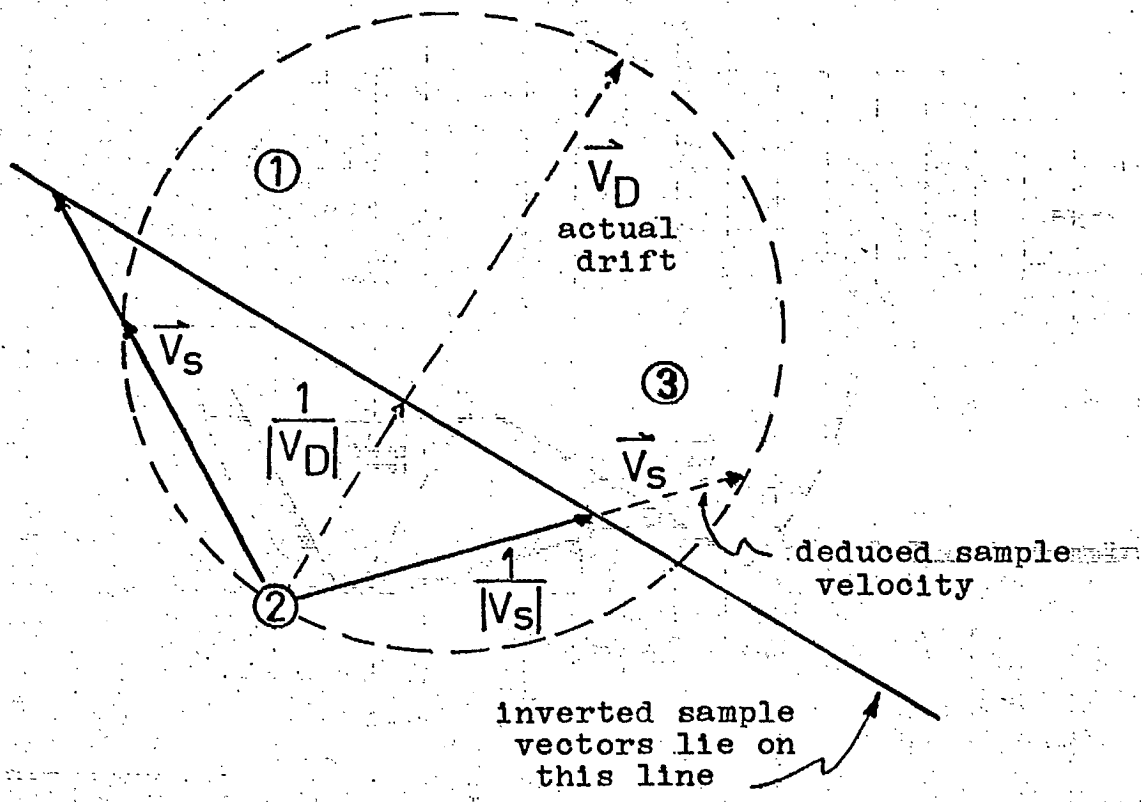
①
$\vec{V}_D$
actual
drift
$\vec{V}_S$
$\frac{1}{|V_D|}$
③
$\vec{V}_S$
deduced sample
velocity
②
$\frac{1}{|V_S|}$
inverted sample
vectors lie on
this line

Figure 3.9

Chapter 4. Analysis of long data sequences.

4.1 Introduction

The term 'long sequence methods' will be used to denote analyses where data sequences consisting of many 'fades' or irregularities are used as a whole. A typical sequence duration is five minutes. Of course, these terms have no absolute definition since irregularities may simply be aspects of a larger pattern.

The methods to be discussed here would work equally well on samples except that they would then be rather expensive in computor time. The usual procedure is to calculate the cross correlation between pairs of sequences, and to calculate time delays based on these functions. Once the time delays are determined, calculation of drift vectors parallels that for samples.

The N.T.D. is still used as a criterion of data consistency. It is difficult to see why it should be a good criterion, since strong evidence will be presented later that lines of maximum for samples are not all perpendicular to the drift. However, inspection of wind values indicates that, when the N.T.D. $\simeq$ 0, wind vectors from sequences are very similar on records which are adjacent in height and time, and in fact are more consistent than any of the sample methods tried (Ref. Chapter 3).

Plots of N.T.D. to be shown in Chapter 5 will indicate that the long sequence method fails, i.e. shows a high N.T.D., when the fading rate is fast. Whether this is just due to

difficulty in identifying the 'correct' peak from among many in a cross-correlation sequence or whether it is a basic flaw in the method is not clear.

Several methods have been developed at U. of S. to obtain the "apparent" velocity. (Ref. Section 1.2) The final judgement of any particular method, or combination of methods, must be based on the scatter in vectors between adjacent records.

4.2 Median angle method

This method has been used extensively at U.of S. Effectively the choice of a vector is based on the N.T.D. and the magnitude of drift. The actual criteria are as follows. $\vec{V}_1$, $\vec{V}_2$, $\vec{V}_3$ are the three dependent vectors calculated with pairs of time delays according to equation 3.3. Data are rejected if any one vector has magnitude greater than 250 m/s, or if the three do not lie in a half-plane, or if the angle between any two is greater than 145°. Then the median vector in angle, $\vec{V}_m$, is selected. If the difference in magnitude between $\vec{V}_m$ and either of the other two vectors is greater than 200 m/s, or if both differences are greater than 150 m/s, then the data are rejected. Otherwise, the $\vec{V}_m$ is used as the drift vector. These criteria are empirical, and are essentially based on knowledge of wind velocities as revealed by alternative techniques of measurement.

4.3 Least squares fit to times (LSFIT)

This method is used by M.J. Burke (private communication)

in a different formulation to determine sample vector velocity, and assumes that the three determinations of time delay are equally accurate. The fit minimizes the mean squared error, $\Sigma e_i^2/3$, in the time of the computed drift vector. From equation 3.3:

$$\Sigma\, e_i^2 = (T_{21} - \frac{d}{V}\cos\alpha)^2 + (T_{23} - \frac{d}{V}\cos\,(60°-\alpha))^2 + (T_{13} - \frac{d}{V}\cos\,(120°-\alpha))^2 \qquad (4.1)$$

For minimum error:

$$\frac{\partial}{\partial Q}\,\Sigma\, e_i^2 = 0$$

and

$$\frac{\partial}{\partial \alpha}\,\Sigma\, e_i^2 = 0\ , \qquad (4.2)$$

where $Q = d/V$.

The solution of these equations is:

$$\alpha = \tan^{-1}\,\frac{(T_{23} + T_{13})\sqrt{3}}{2T_{21} + T_{23} - T_{13}}$$

$$Q = \frac{2}{3}\,(T_{21}\cos\alpha + T_{23}\cos\,(60°-\alpha) + T_{13}\cos\,(120°-\alpha)), \qquad (4.3)$$

where the quadrant of α is taken from the signs of the numerator and denominator, and V is the pattern speed.

4.4 Weighted least squares fit to times (WLSFIT)

A better method is to weight the errors in time according to the confidence placed in each time delay. Some function of the maximum cross-correlation appears to be the

best weight, since one would have most confidence in the time delay associated with the greatest maximum cross-correlation.

In this case the weighted error is

$$\Sigma\, w_i e_i^2 = X(T_{21} - \frac{d}{V}\cos\alpha)^2 + Y(T_{23} - \frac{d}{V}\cos(60°-\alpha))^2 + Z(T_{13} - \frac{d}{V}\cos(120°-\alpha))^2 \qquad (4.4)$$

where X is the weight associated with T_{21} etc.

The solution of

$$\frac{\partial}{\partial\alpha}\Sigma\, w_i e_i^2 = 0$$

$$\frac{\partial}{\partial Q}\Sigma\, w_i e_i^2 = 0 \qquad (4.5)$$

is given by the equations:

$$\cos\alpha\,\frac{\sqrt{3}}{4}\,(XYT_{21} - XZT_{21} - YZT_{13} - YZT_{23} - 2XYT_{23} - 2XZT_{13}) + \sin\alpha\,\frac{3}{4}\,(YZT_{23} - YZT_{13} + XYT_{21} + XZT_{21}) + \cos^2\alpha\,\sin\alpha\,\frac{XT_{21}}{2}\,(2X - Y - Z) = 0, \qquad (4.6)$$

and

$$Q = \frac{2[C(2XT_{21} + YT_{23} - ZT_{13}) + \sqrt{3}\,S(YT_{23} + ZT_{13})]}{C^2(4X+Y+Z) + 3S^2(Y+Z) + 2\sqrt{3}\,CS(Y-Z)}, \qquad (4.7)$$

where $S = \sin\alpha$ and $C = \cos\alpha$.

Equation 4.6 is a cubic in $\sin^2\alpha$. Selection of the right value for α is based on the value of error calculated by equation 4.4.

4.5 Method of least N.T.D.

Sometimes there are several almost equally significant peaks in a cross correlation sequence. This method identifies several peaks in each sequence and selects that combination of peaks one from each of the three sequences, which gives the least N.T.D. As will appear later this method has been discarded.

4.6 Method of zero N.T.D.

This method is similar in intent to the method of least N.T.D. except that a reverse procedure is used. The time discrepancy is set equal to zero, and the set of times, one in each of the three sequences, for which the sum of the cross-correlation values is a maximum, is found. This is done by a search over all possible values of two of the time delays. The third is determined by N.T.D. = 0. Figure 4.1 shows a contour plot of the sum of the cross correlations versus the two time delays. The 'corners' of this plot are missing because here the third value of time defined by N.T.D. = 0 is beyond the set value of maximum lag for the cross-correlation sequences. When the maximum has been found, a paraboloid fit is used to determine the exact times.

In U. of S. data, there are usually more peaks than shown in Figure 4.1.

Figure for Chapter 4

CAPTION

Figure No.

4.1 Computer plot of sum of values of cross-correlation coefficients which occur throughout the correlogram. Refer to text, Section 4.6.

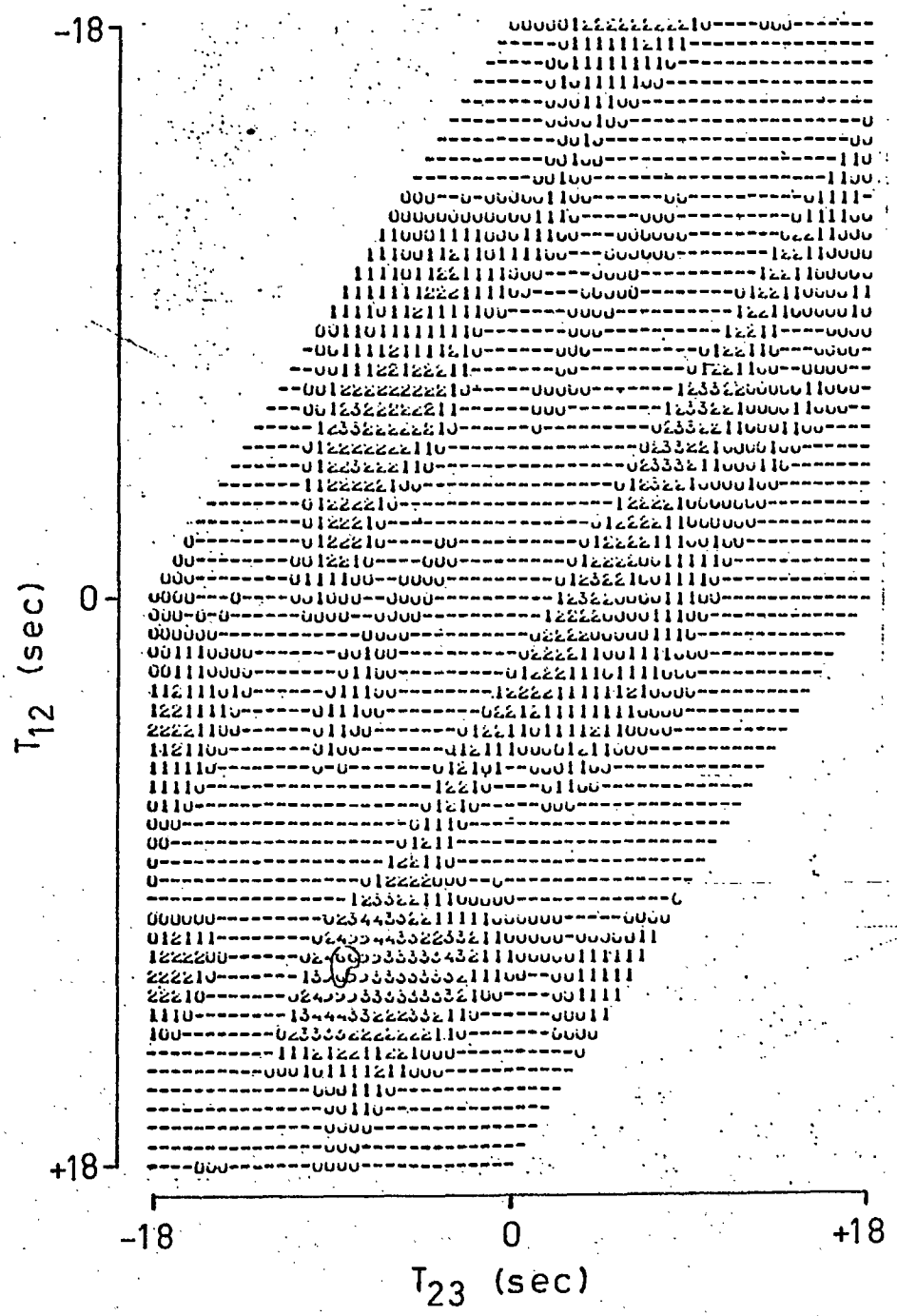

Figure 4.1

Chapter 5. Equipment and Data Comparison, C.R.C. & U. of S.

5.1 Introduction

Comparisons of data sequences obtained at the above locations will now be considered. The most striking differences in the data from the two locations are the higher cross-correlations and the preponderance of low N.T.D. values obtained at C.R.C., as compared with U. of S., using long sequence (5 minute) methods of analysis. These may be due to equipment differences or geomagnetic/geographic location.

5.2 Equipment and preliminary processing.

Diagrams of the antenna arrays at the two locations are shown in Figure 5.1. One difference is in the size of triangle, in terms of wavelength. However, orientation may be one of the factors influencing maximum cross-correlation value (ρ_{max}), since, with a prevailing E-W drift, the pattern will be travelling more nearly along the direction of two antennas in the C.R.C. array than in the U. of S. array. This would tend to reduce variations between amplitude sequences due to spatial differences in the pattern, and give a high value of ρ_{max} between these two antennas. Some data will be presented in Chapter 7 which illustrates this effect.

Table 5.1 compares the usual arrangements for observation and analysis at the two locations. Important differences in Table 5.1 appear to be sequential vs. simultaneous measurement at the three antennas, and time spacing of measurements. These will be discussed at the end of the chapter.

Table 5.1. Comparison of Equipment and Preliminary Processing.

	C.R.C.	U. of S.
T_x frequency	2.66 MHz	2.219 MHz
R_x, T_x mode	O-mode	linear (N-S)
T_x array	-	16 dipole (4x4 square) beamwidth 45°
R_x array	-	3 of 4-dipole squares
T_x power	-	40 kw
Pulse width	50 μsec	20 μsec
Normal height range	44-98 km (Noise value placed in 42 km ht. gate)	52-118 km (No noise measurement)
Amplitude measurement	Simultaneous at three antennas, 1 sec spacing with point skipped every 60th sec for time info. filled in by interpolation. 40 minutes continuous.	Sequential among 3 antennas at 15 Hz, 192 sec/file (960 pts. per sequence averaged in 3's to give 0.6 sec spacing) comprising 8 records (with 60 msec inter-record gap - not corrected for) 1 file every 5 min.
Initial data rejection	Based on mean signal strength (< 5μV)	Based on depth of fading (standard deviation of a sequence) and fading rate (reject if mean auto-correlation <0.61 at 0.6 sec lag)

Figure 5.2 compares N.T.D. distributions for C.R.C. and U. of S. data and includes those from Figure 3.2, based on random time distribution. Here, 5 minute segments of C.R.C. data were used, and the N.T.D. were calculated from the times of ρ_{max} between pairs of antennas. The few cases in which $\rho_{max}<0.1$ or ρ_{max} occurred at maximum lag (18 sec) are included; these were rejected in U. of S. data.

If the criterion, N.T.D. ≤ 0.1, is adopted, 60% of the C.R.C. values are 'good' as compared to only 20% of the U. of S. values. This disparity suggested further observations at Saskatoon. Several sets of observations were made, utilizing different arrangements of transmitter and arrays. The corresponding N.T.D. distributions are shown in Figure 5.3. For these observations, the sequence of data was rejected if the mean auto-correlation coefficient was less than 0.4. The slight increase in low N.T.D. values compared with Figure 5.2 is probably due to increased care in monitoring the observations, e.g. in setting receiver gain.

Figure 5.4 compares values of ρ_{max} at C.R.C. and U. of S. These may be somewhat dependent on the particular data used, as opposed to the N.T.D. distributions which appear to be characteristic of the equipment and/or location. It can be seen that the median value of ρ_{max} for U. of S. is about 0.25 whereas that for C.R.C. data is 0.4; - quite a large difference. As noted before, the difference may be due to antenna spacing orientation but factors dependent on location may also be involved.

5.3 Data comparison using N.T.D. and ρ_{max}

As stated previously, the N.T.D. is a measure of the difficulty in defining a drift vector, and in addition appears to be a criterion for consistency of drift values at different heights or time intervals.

5.4 Comparison of fading rates.

A parameter which may be used to compare data independently of equipment is the fading rate. This can be defined from the mean auto-correlation function over the three antennas if the function is assumed to have a gaussian shape. The mean fading period (MFP) is defined as 3.62σ (M.J. Burke, private communication). σ is found from

$$\rho(\tau) = e^{-\frac{\tau^2}{2\sigma^2}} \qquad (5.1)$$

where ρ is the mean auto-correlation at lag τ.

Histograms of the MFP, as defined by ρ at unit lag, are shown in Figure 5.5. Again, these are probably relevant only to the particular data used, but the difference is very pronounced. This could be partly due to aliasing in the C.R.C. data because of the time spacing, which gives a Nyquist frequency of 0.5 Hz. U. of S. data effectively has a Nyquist frequency of 2.5 Hz, so that aliasing is probably not important. The sharp cutoff in U. of S. data at low MFP's is due to the rejection criterion on $\rho(\tau)$. Roughly speaking, the higher fading rate and lower cross correlations of U. of S. data probably combine to give a poor N.T.D. distribution in the following way.

The high fading rate means that there are more peaks within a given maximum lag in the cross correlations, and the lower cross correlation values mean that the 'real' peak will be chosen less often.

Some support for this explanation is given in Figures 5.6, 5.7, 5.8, which show respectively the N.T.D., MFP, and signal strength vs. height profiles for unsmoothed C.R.C. data. The band of high N.T.D. values (day 35, 78-86 km) roughly corresponds to a drop in MFP at these heights, and also to the 'upper part' of an echo structure. In this case, fast fading is probably due to interference of oblique rays from the strong reflector. Note that the effective pulse width of the C.R.C. equipment is 7.5 km; i.e. a measurement of amplitude at a given nominal height includes contributions from a range of 7.5 km about this height.

The same results have been noted in U. of S. data, viz. faster fading occurs on the 'upper part' of a reflecting structure.

Possible reasons for a greater fading rate at U. of S. are more rapid time changes in the pattern or smaller irregularity size. The dynamical origins of the processes involved are unknown.

5.5 Comparison of data consistency

In the following chapters comparisons of analysis methods will use unsmoothed C.R.C. data exclusively. Hence comparisons of the consistency of U. of S. drift values with those from smoothed C.R.C. data, and also with the Method of

least N.T.D. will be made here.

The smoothed C.R.C. data was produced with 4 passes of a 3-point binomial filter on 5-minute segments of data. This filter has an attenuation of about 3 dB at 0.1 Hz, and roughly approximates the filter used at C.R.C. for analysis by the sample method. The N.T.D. distribution for this data is shown in Figure 5.2.

In the case of the method of least N.T.D., the two most significant peaks with $\rho_{max} > 0.1$ were chosen in each of the three cross-correlation sequences, and the set of time delays with minimum N.T.D. were used through the LSFIT method to give a drift vector. The median vector method was chosen for comparison in both U. of S. and C.R.C. data as the best available. In this method, the worst data are rejected (whereas in the other methods all data are accepted.)

Figure 5.9 shows the distribution of angle differences between drift vectors for adjacent records in height and time for the foregoing analyses. The distribution would be expected to be better in adjacent heights, because in the C.R.C. data the height increment is 2 km, with an effective pulse length of 7.5 km, while in the U. of S. data, the height increment was 1 1/2 km with an effective pulse length of 3 km. Thus the records for adjacent heights are not independent. However, in the C.R.C. data, the distribution for adjacent times is actually a little better. In Figure 5.9, the number of 'cases possible' is just the number of instances when data in accord with the rejection criteria in Table 5.1 could be found adjacent in height

or time records. The 'cases accepted' were those for data remaining after applying the median vector criteria. In addition, ρ_{max} values were required to be >0.1 for both this and the method of least N.T.D. Also shown in Figure 5.9 is the expected distribution if the drift angles are independent, uniformly distributed, random values.

It can be seen that the consistency of smoothed data is worse than that of the unsmoothed, as would have been expected by the comparison of N.T.D. distributions. The same results were obtained for all the other methods (sample and long sequence), except for the mean times sample method (Ref. 3.7.3) in which, as will be shown in the next chapter, the distribution of angles was close to random.

Apart from magnitude criteria, the median vector method rejects data with N.T.D. $\gtrsim$ 0.8, as well as requiring that ρ_{max} should not occur at the maximum lag. This explains the large number of values rejected in U. of S. data, and also the disparity between U. of S. and C.R.C. distributions, since, after rejection of data, there is still a greater fraction of high N.T.D. values in U. of S. data than in that of C.R.C.

Figure 5.9 provides the justification for discontinuing use of the method of least N.T.D.

5.6 Simultaneous vs. sequential antenna sampling.

Examination of C.R.C. data showed that when the signal strength was small (< 58 km) there was usually a very high cross correlation at zero lag in 5-minute sequences, and that sometimes

at other heights individual sample speeds were very high.

These can be explained as a result of the simultaneous measurement of amplitudes. Any interfering signal or sferic will occur at the same time in the three amplitude sequences, and if ionospheric echoes are not sufficiently strong by comparison, ρ_{max} will occur at zero lag. Thus the time delays, which are found by curve fitting around ρ_{max}, will be small. Probably the N.T.D. distribution such a case would be close to the random. It is difficult to estimate the effect on the drift vectors in general, except to say that in cases where noise and interference is a problem, then the speeds will tend to be high; i.e. the peak of the cross-correlation sequence will be distorted towards zero lag.

Examination of the analyses indicates that this effect is probably important in the 5 min. methods only when the signal ~ noise. However, plots of sample vectors (see Chapter 7) show some cases of high speed which may be attributed to atmospherics. Plots of the amplitude sequences were not made, so that verification of this suggestion is not possible. Figure 5.10 shows a partial plot of the cross correlation sequences for a case in which atmospherics are thought to be important. If the measurement is sequential, atmospherics would have very little effect because the peaks would not all line up at one lag value; however, the possibility of noise or interference which synchronizes with the antenna sampling frequency of the equipment may not be overlooked.

5.7 Effect of antenna sampling rate.

For the purposes of this section, it will be assumed that the cross-correlation sequence gives the correct values of ρ, and that an approximation to the true cross-correlation function may be made by curve fitting. These assumptions will hold if the antenna sampling rate is much greater than the fading rate, i.e. there are no aliasing problems. Whether they continue to hold approximately when the fading rate approaches the sampling rate would be a study in itself, and so will not be discussed further in this report. The question is not merely academic, because in both U. of S. and C.R.C. data there are instances when the fading interval appears to be close to the lag unit used to determine the cross-correlation sequences.

The choice of unit of time between sampling at antennas determines the approximate location of ρ_{max} in the cross-correlation sequence. A large unit will mean that, for a reasonable range of wind values, ρ_{max} will often occur in the first lag. In the case of C.R.C. equipment (1 sec. spacing), assuming that the line of maximum is perpendicular to the drift, values of drift > 71.5 m/s will cause the three values of ρ_{max} to occur in the first lag. The corresponding value for U. of S. equipment is 202 m/s. If these conditions occur, it is reasonable to ask whether the calculated value of drift depends on the curve fitting procedure used to locate ρ_{max}.

In order to give a partial answer to this question, two types of curve, parabolic ($\rho = at^2 + bt + c$), and Gaussian ($\rho = a \exp(b(t-c)^2)$), were chosen, and the pattern was assumed

to be travelling along the line of two antennas. The two cases (A and B) when the maximum is expected to occur in the first lag are shown in Figure 5.11. For case 'A', the expected maximum falls between 1/2 and 1 lag, and in case 'B' between 0 and 1/2 lag.

The position of the maximum for the Gaussian curve, relative to the lag at which ρ_{max} (shown as C_2 in Figure 5.11) occurs, is given by:

$$\mu_G = - \ln(R_1/R_2)/(2 \ln(R_1 R_2)), \qquad (5.1)$$

and for the parabolic curve it is

$$\mu_P = (R_2-R_1)/(2(R_1+R_2-2)) \qquad (5.2)$$

where R_1 and R_2 are as defined in Figure 5.11.
The contour plots give the percentage difference (relative to the Gaussian) in predicted time delay for ρ_{max} for these curve types. In case 'A', the maximum difference is about 20%, and occurs when $C_1 \sim 0$, $C_3 \sim 1/2 C_2$. These fast changes in ρ do occur when the fading rate is high. For a low fading rate, the difference is negligible.

In case 'B', larger differences can occur; however, if predicted times less than 1/4 lag are rejected as indicating too high a drift speed (330 m/s on C.R.C. equipment), then the differences are of about the same magnitude as in case 'A'. This may be seen in Figure 5.11, in that area of the plot between the 1/4 lag line, plotted for the parabola fit, and the 1/2 lag line.

In summary, it appears that, for most of the U. of S. and C.R.C. data examined, the above considerations are not

important; but a larger unit of sampling time would not be recommended.

Figures for Chapter 5

CAPTIONS

Figure No.	
5.1	Comparison of antenna geometries, C.R.C. and U. of S.
5.2	Comparison of N.T.D. distribution, from C.R.C., U. of S., and random times as in Figure 3.2.
5.3	Probability distributions of N.T.D.'s, for data taken at U. of S. under the equipment arrangements shown.
5.4	Probability distributions of maximum cross-correlation values, for C.R.C. and U. of S. data.
5.5	Probability distributions of mean fading periods (M.F.P.) at C.R.C. and U. of S.
5.6	Profiles of N.T.D. versus height, C.R.C. data.
5.7	Profiles of M.F.P. versus height, C.R.C. data.
5.8	Profiles of signal strength versus height, C.R.C. data.
5.9	Probability distribution of angle differences, C.R.C. and U. of S. data. (NOTE: "Method #1" is the method of least N.T.D., (Reference Section 4.5)).
5.10	Plot of correlograms in which interference is believed responsible for the peak at zero lag.
5.11	Comparison of interpolation methods for ρ_{max}. Reference Section 5.7.

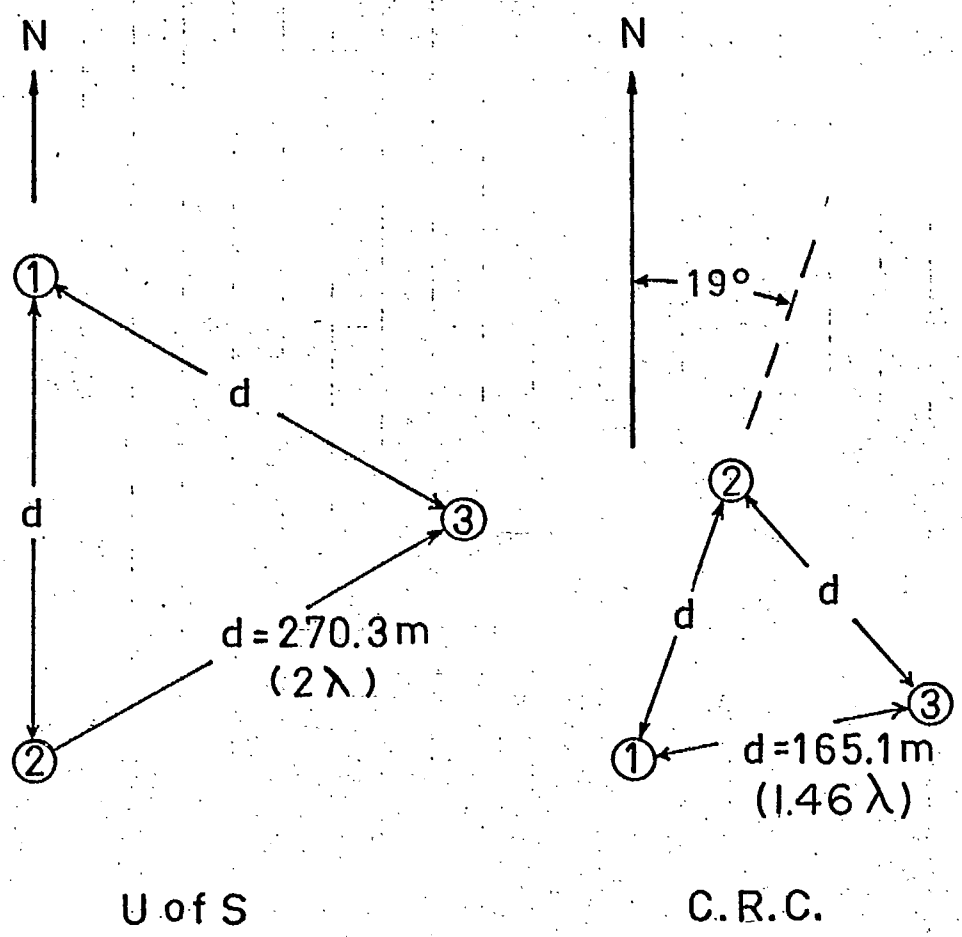

Figure 5.1

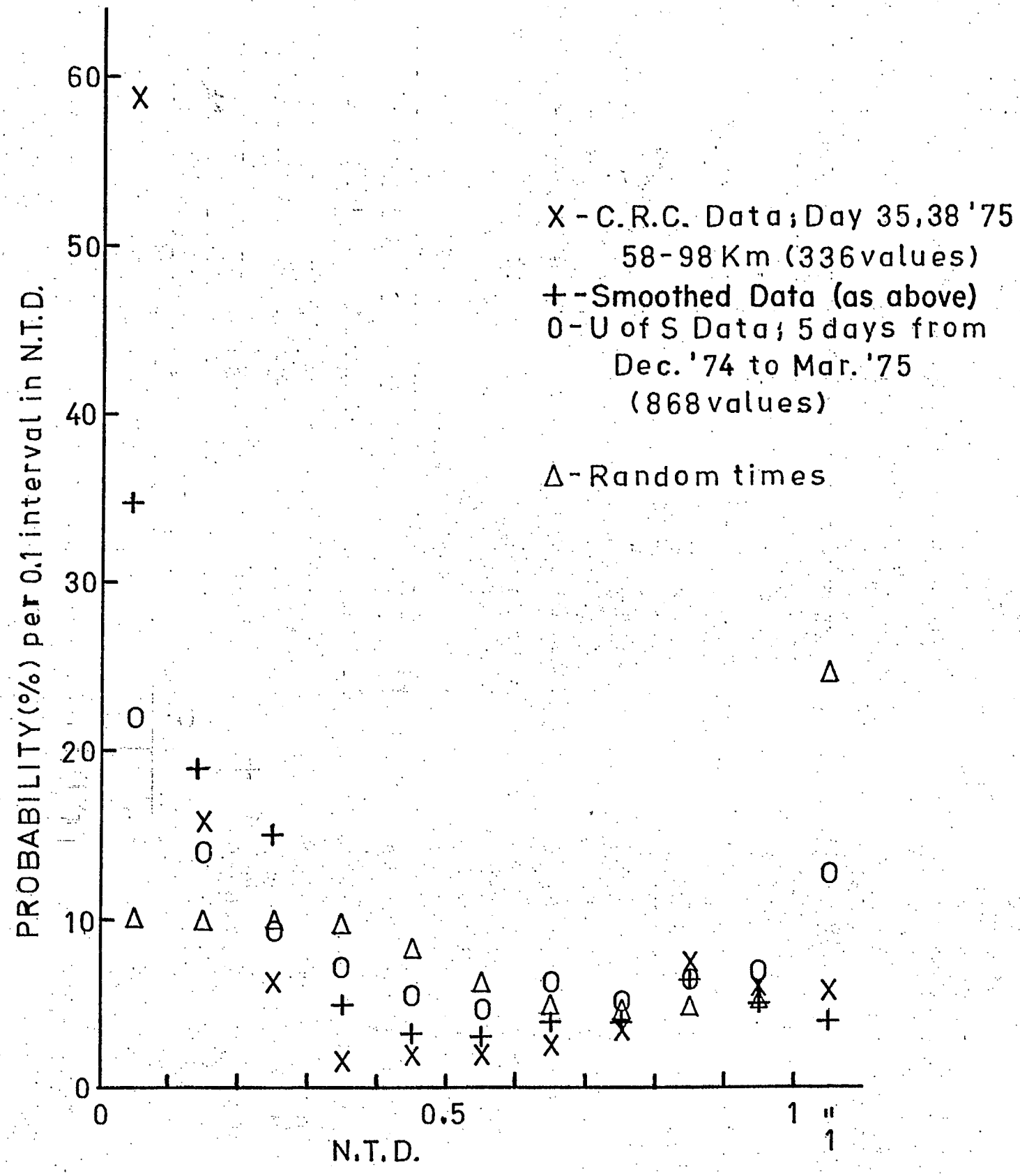
X - C.R.C. Data; Day 35,38 '75
58-98 Km (336 values)
+ - Smoothed Data (as above)
0 - U of S Data; 5 days from
Dec. '74 to Mar. '75
(868 values)
Δ - Random times
PROBABILITY(%) per 0.1 interval in N.T.D.
60
50
40
30
20
10
0
0
0.5
1 = 1
N.T.D.

Figure 5.2

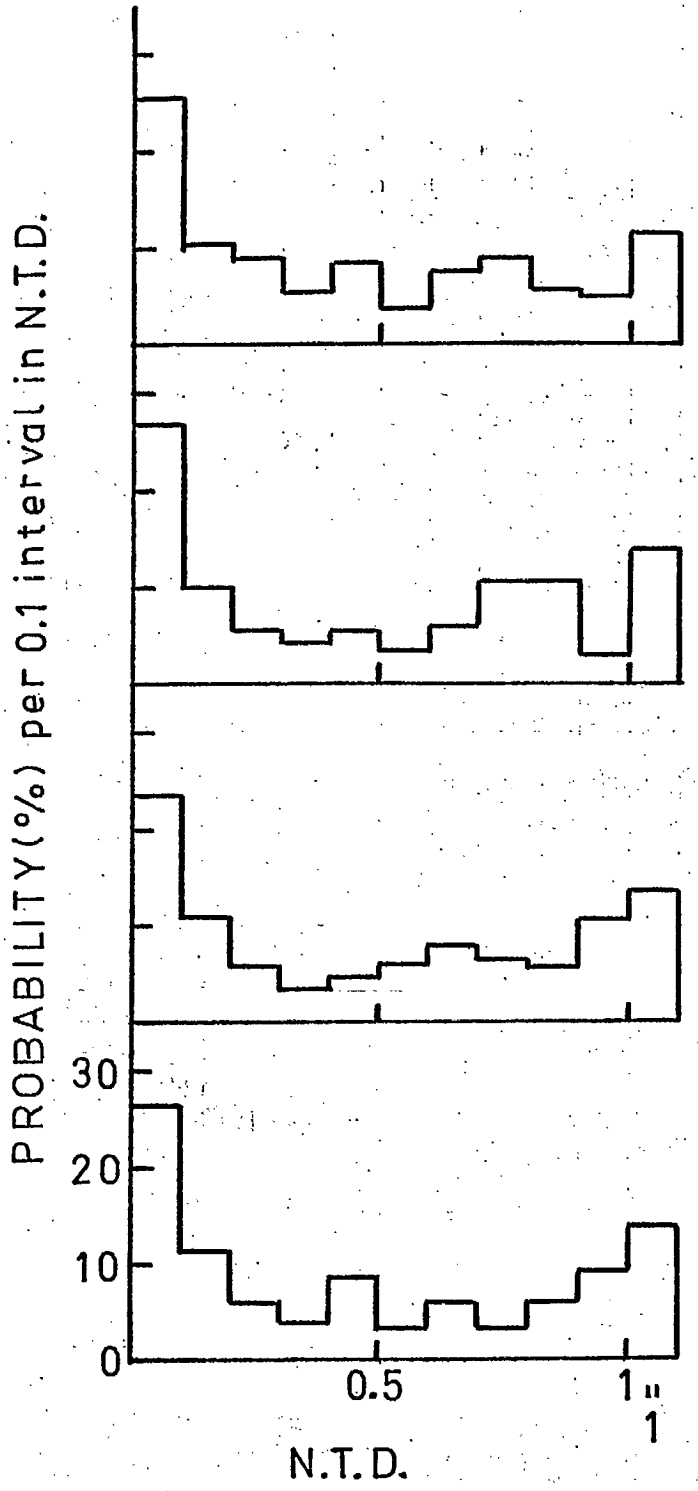

105 values
O-mode Rx

130 values
50 μsec pulse

104 values
O-mode Rx, Tx
50 μsec pulse

117 values
8 min run (600 pts/seq)
0.8 sec spacing
no average of data

Figure 5.3

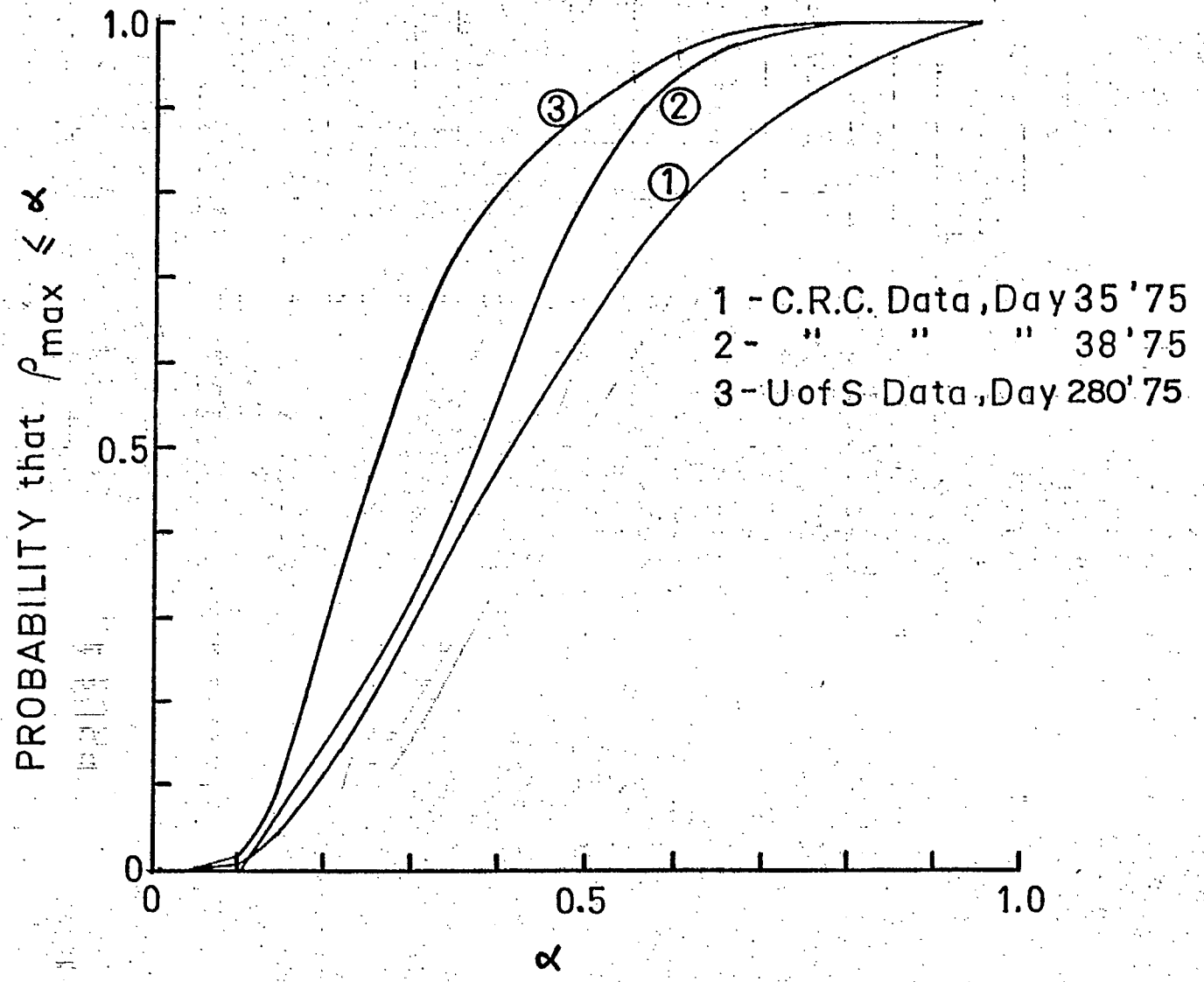
1.0
0.5
0
0
0.5
1.0
PROBABILITY that $\rho_{max} \leq \alpha$
α
③
②
①
1 - C.R.C. Data, Day 35 '75
2 - " " " 38 '75
3 - U of S Data, Day 280' 75

Figure 5.4

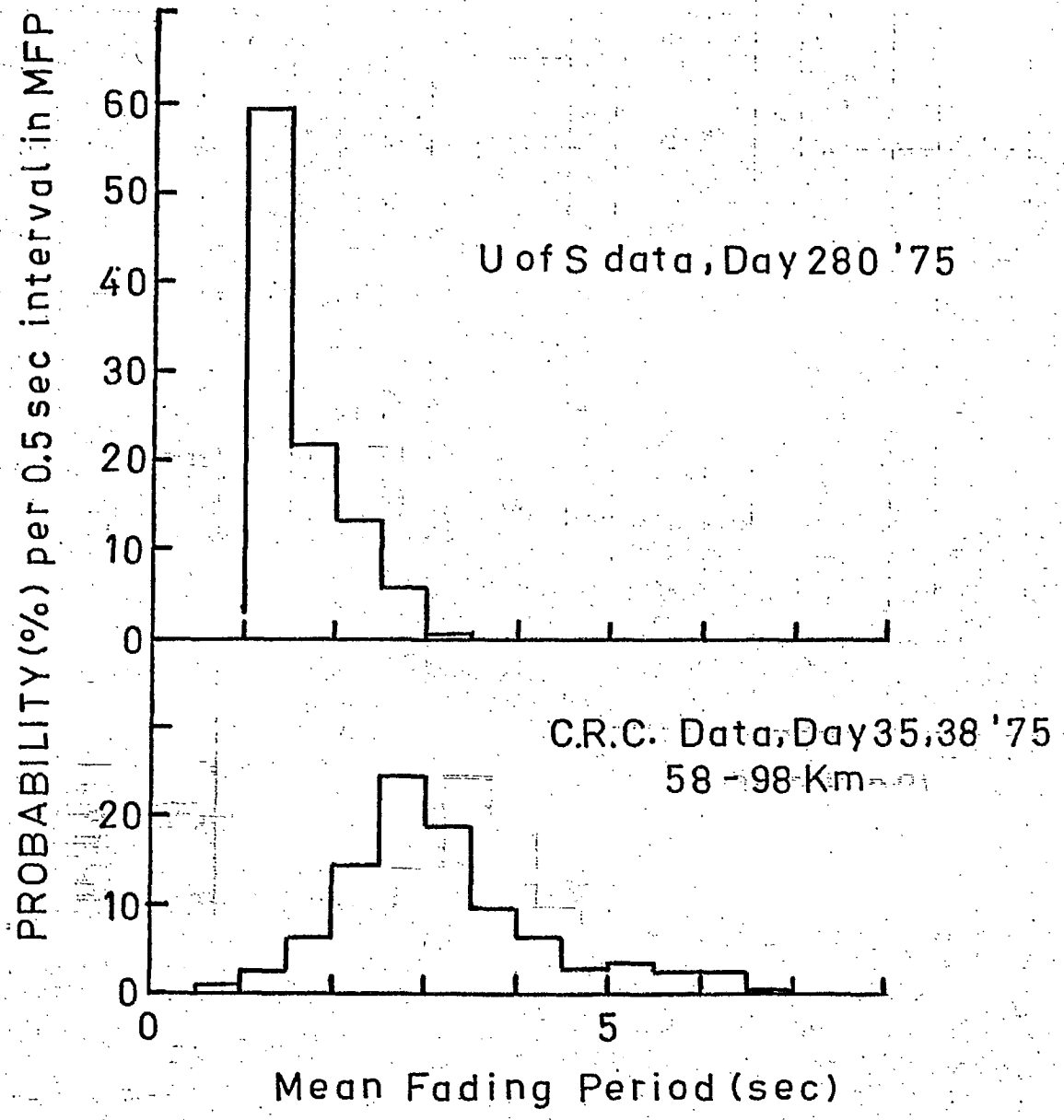
PROBABILITY (%) per 0.5 sec interval in MFP
60
50
40
30
20
10
0
U of S data, Day 280 '75
C.R.C. Data, Day 35, 38 '75
58 - 98 Km
20
10
0
0
5
Mean Fading Period (sec)

Figure 5.5

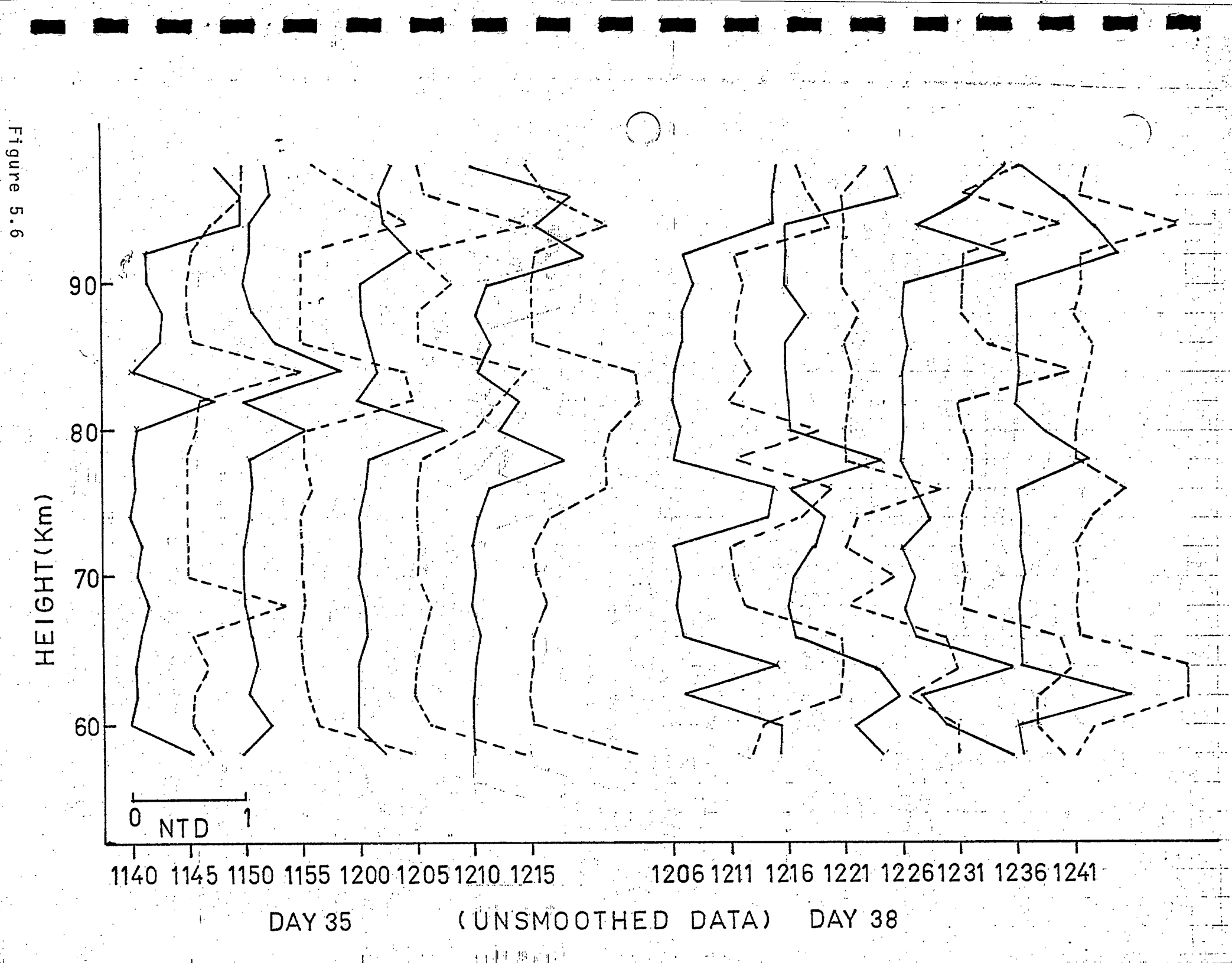
HEIGHT(Km)
90
80
70
60
0 NTD 1
1140 1145 1150 1155 1200 1205 1210 1215
1206 1211 1216 1221 1226 1231 1236 1241
DAY 35
(UNSMOOTHED DATA)
DAY 38

Figure 5.6

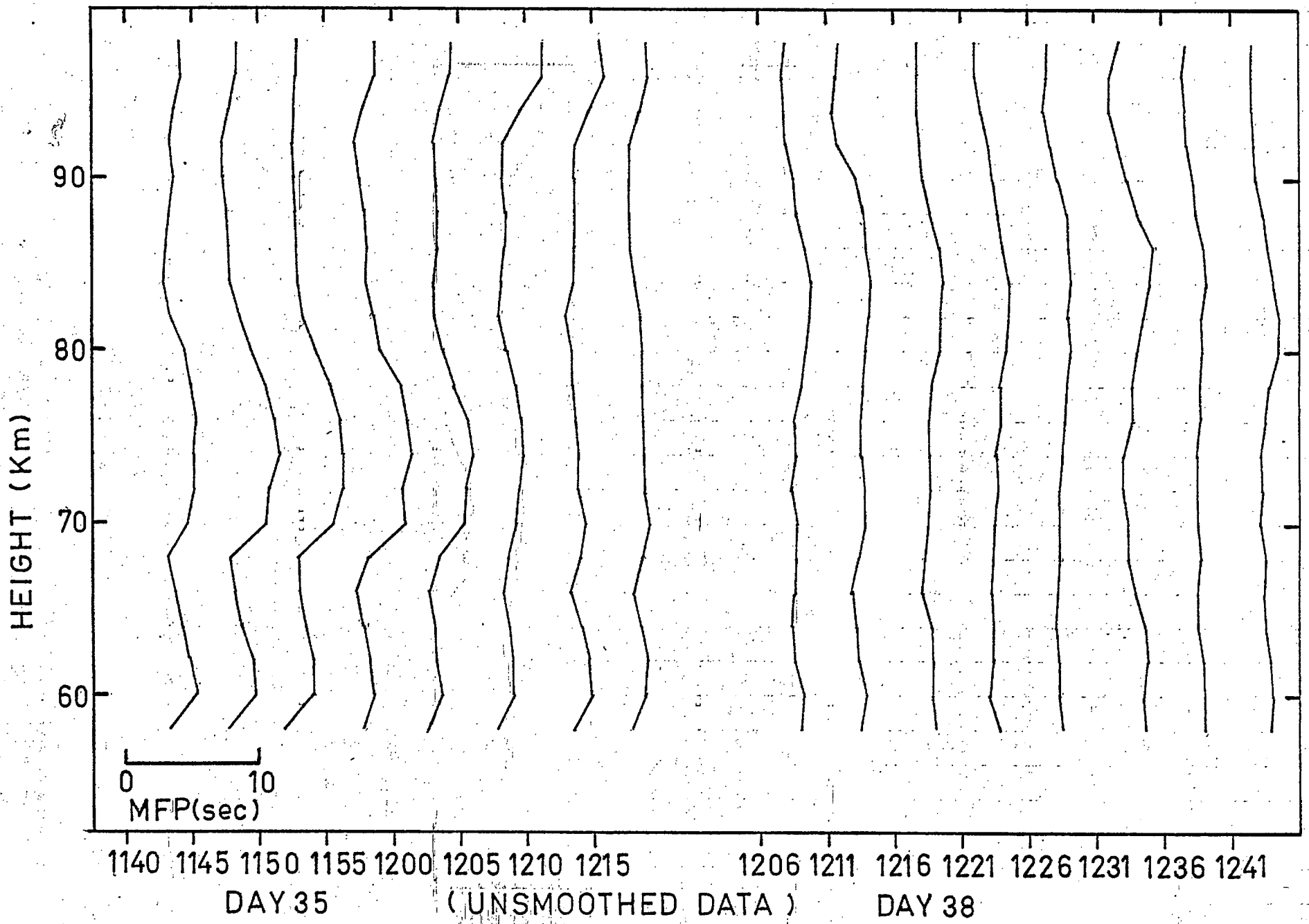
HEIGHT (Km)
90
80
70
60
0
10
MFP(sec)
1140 1145 1150 1155 1200 1205 1210 1215
1206 1211 1216 1221 1226 1231 1236 1241
DAY 35
(UNSMOOTHED DATA)
DAY 38

Figure 5.7

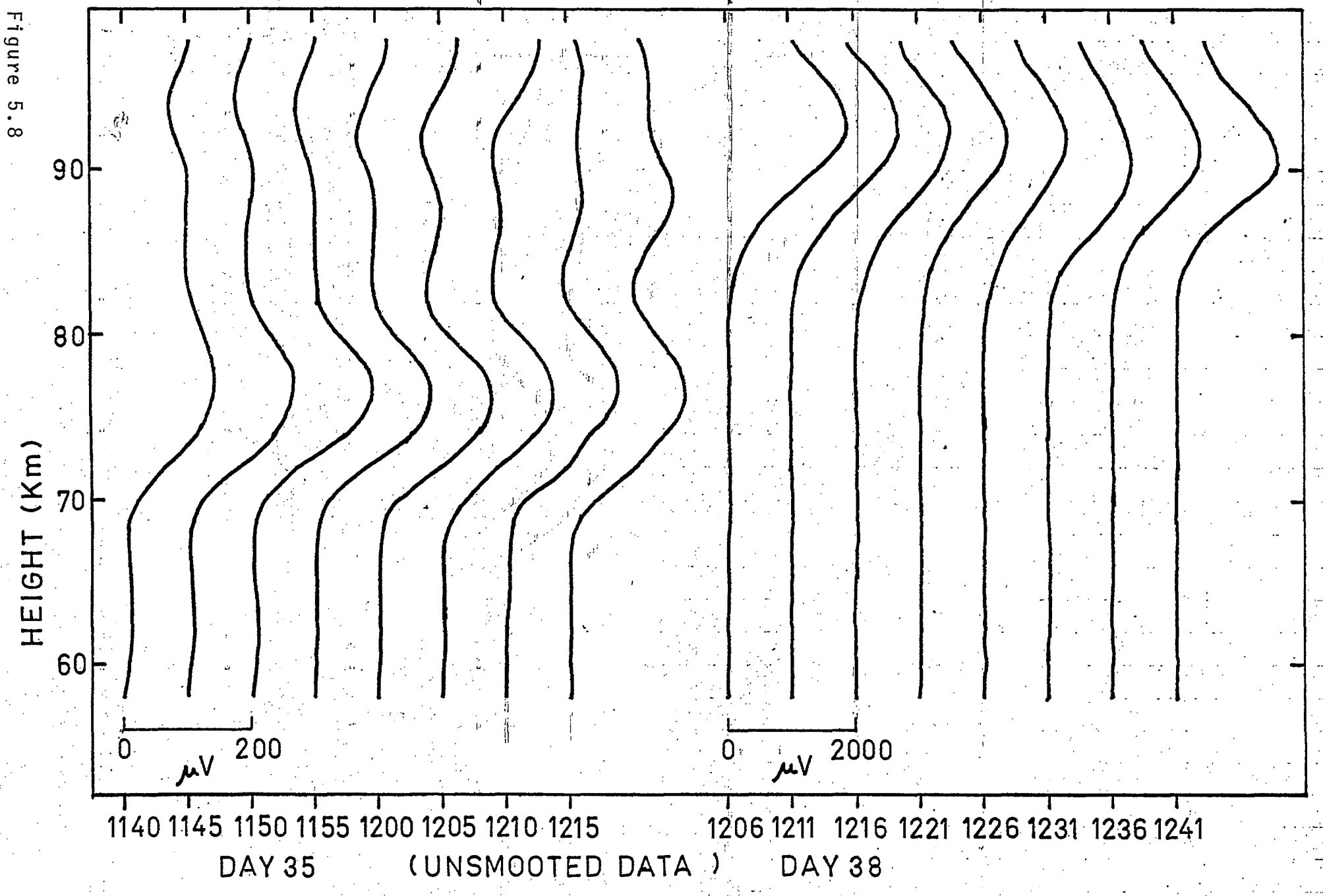
HEIGHT (Km)
90
80
70
60
0
200
μV
0
2000
μV
1140 1145 1150 1155 1200 1205 1210 1215
DAY 35
(UNSMOOTED DATA)
1206 1211 1216 1221 1226 1231 1236 1241
DAY 38

Figure 5.8

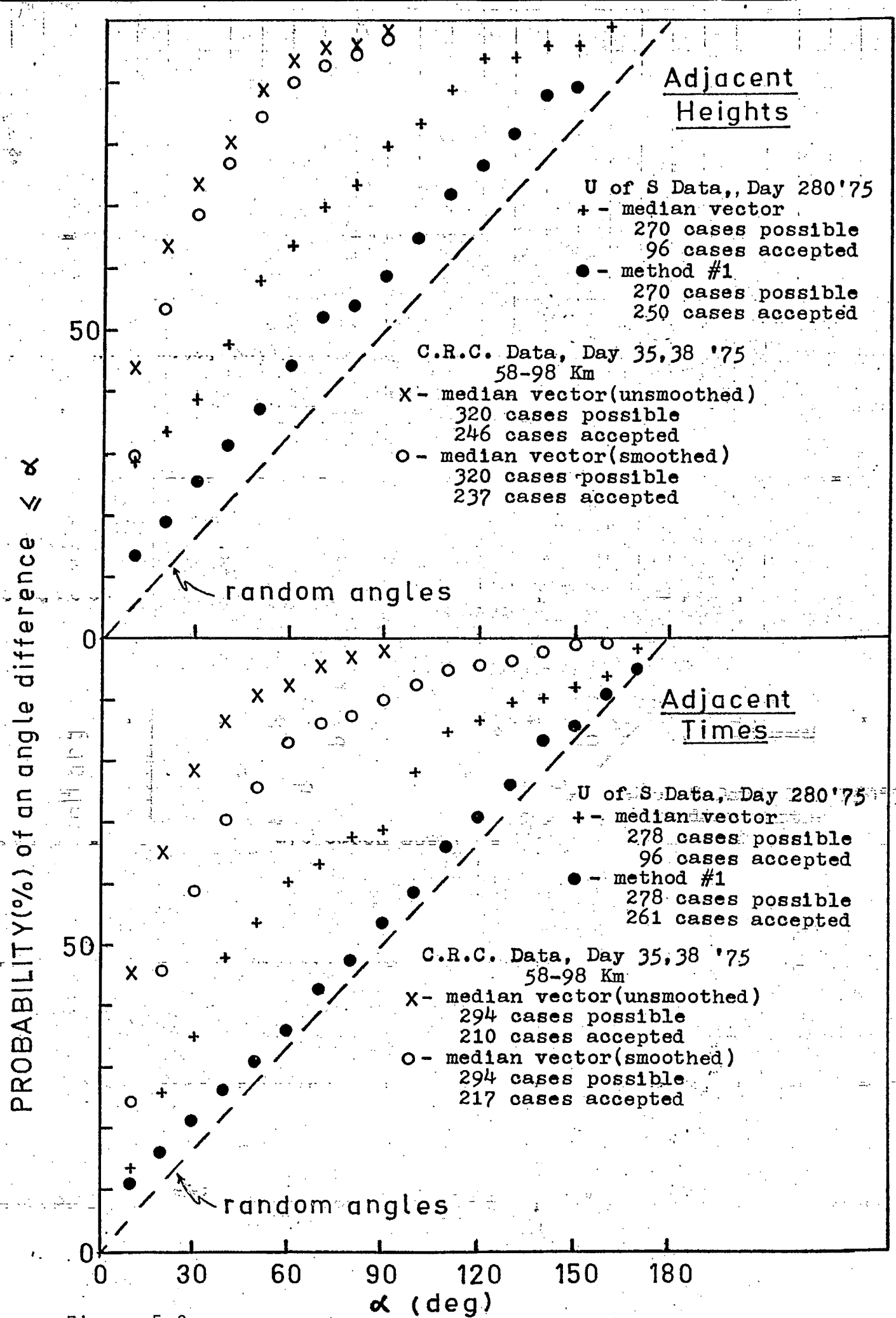
Adjacent Heights
U of S Data,, Day 280'75
+ - median vector
270 cases possible
96 cases accepted
● - method #1
270 cases possible
250 cases accepted
C.R.C. Data, Day 35,38 '75
58-98 Km
X- median vector(unsmoothed)
320 cases possible
246 cases accepted
o- median vector(smoothed)
320 cases possible
237 cases accepted
random angles
Adjacent Times
U of S Data, Day 280'75
+ - median vector
278 cases possible
96 cases accepted
● - method #1
278 cases possible
261 cases accepted
C.R.C. Data, Day 35,38 '75
58-98 Km
X- median vector(unsmoothed)
294 cases possible
210 cases accepted
o- median vector(smoothed)
294 cases possible
217 cases accepted
random angles
PROBABILITY(%) of an angle difference ≤ α
0
50
0
50
0
30
60
90
120
150
180
α (deg)

Figure 5.9

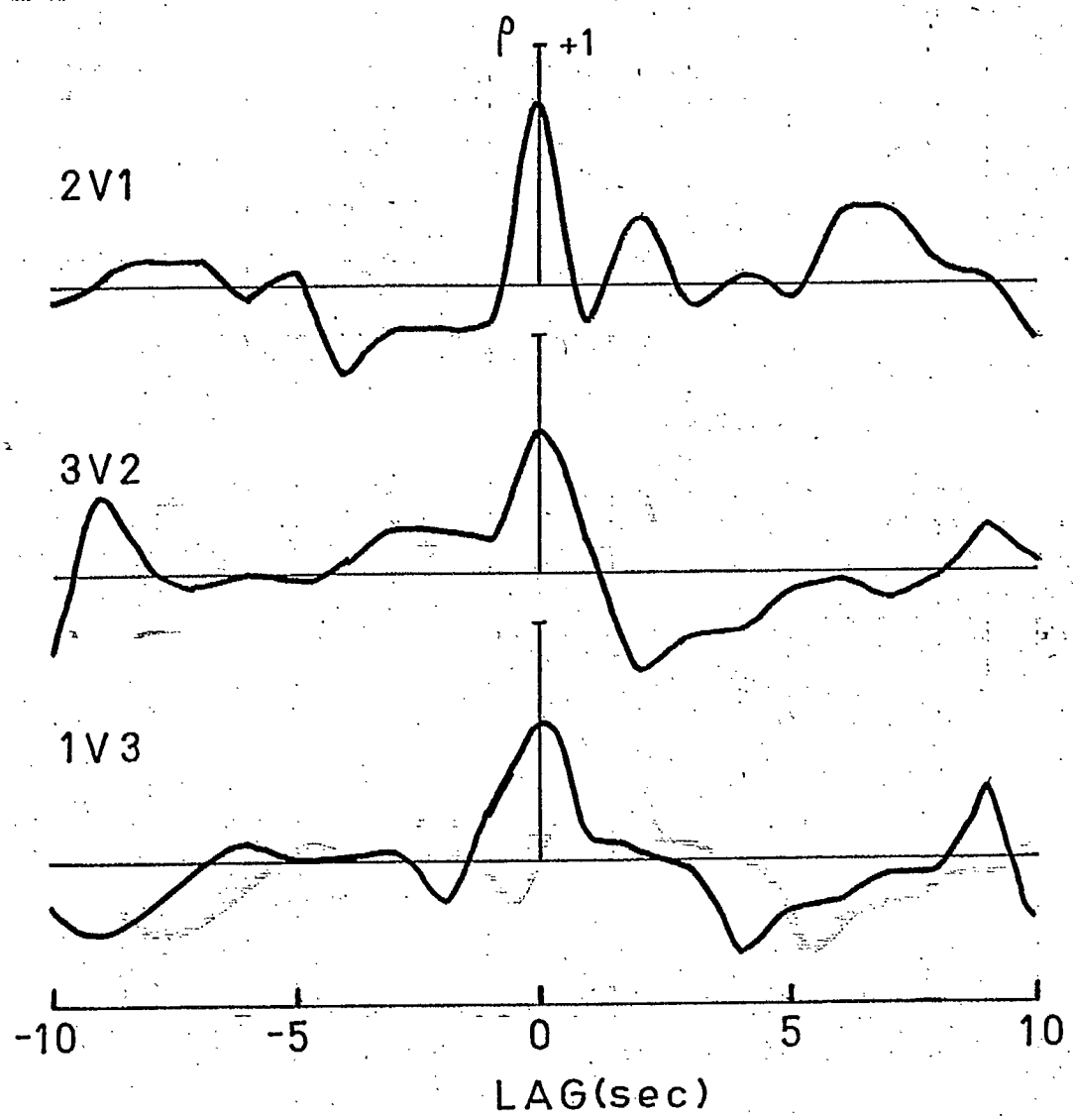

mean signal = 5.4 μV DAY 35 1140
mean noise = 3.6 μV 58 Km, sample#4

Figure 5.10

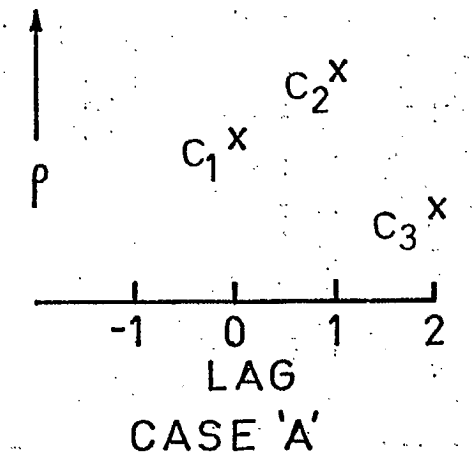

$$R_1 = \frac{C_3}{C_2}$$

$$R_2 = \frac{C_1}{C_2}$$

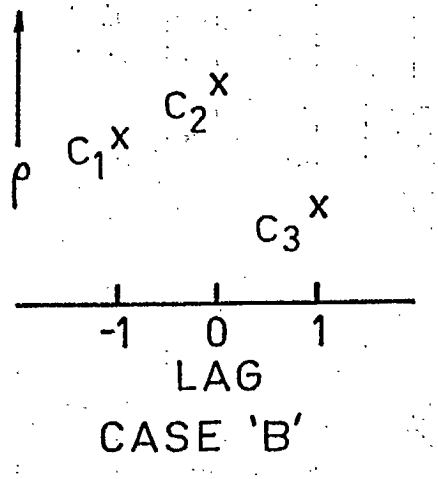

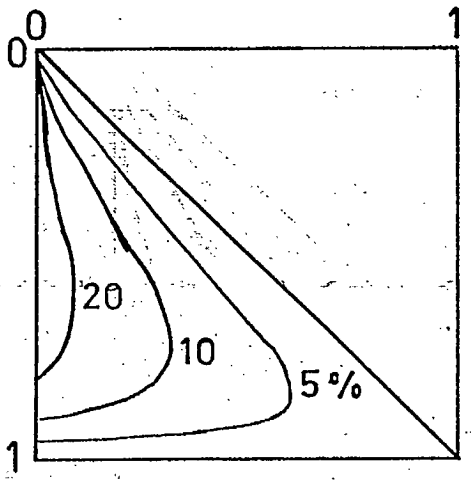

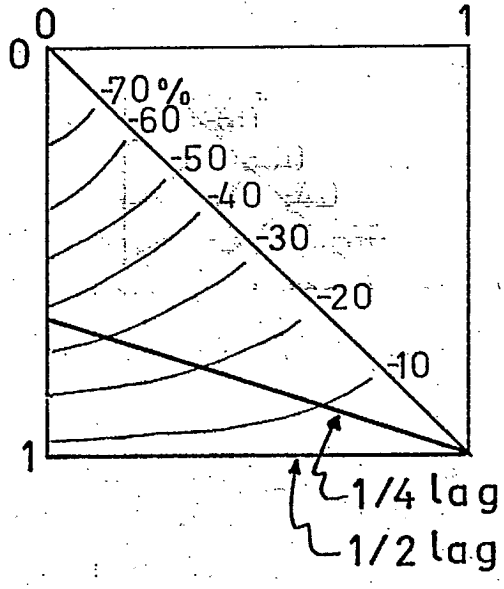

Figure 5.11

Chapter 6. Comparison of analysis methods.

6.1 Introduction

This chapter will discuss the practical details involved in the application of the analysis methods outlined in Chapters 3 and 4, and will compare the consistency of the drift values produced by the various methods. Comparison of daily averages will be made at the end of the chapter.

6.2 Choice of maximum lag used in the analyses.

The value of maximum lag must be based on the expected value of maximum delay between any two antennas. The long sequence methods appear to give the correct drift velocity, which is the same as the deduced velocity of an irregularity for which the line of maximum is perpendicular to the drift (Ref. Chapter 7). Hence the required maximum delay is a direct function of the minimum drift speed. It can be shown that, for an equilateral triangle array, delays up to a maximum value of $t = d/(2\ V_{min})$, where d is the antenna spacing, must be measured for drift speeds greater than V_{min}.

This relation does not apply to single irregularities for which the line of maximum is not perpendicular to the drift, since time delays could then have any value. However, if the lines are assumed to have limited angular distribution about the perpendicular to the drift, then the maximum delay required is $t = d/(2V_{min} \cos \beta)$, where β is the largest angle with the perpendicular.

For the purposes of comparing C.R.C. with U. of S. data, a maximum lag of 18 seconds was used on both long sequence and sample methods. Because of the smaller C.R.C. antenna spacing, this should have been scaled down to 11 sec; but in the long sequence methods, ρ_{max} is usually well defined, at least in the case of slow fading, so that the difference is not important.

For the sample methods, excepting perhaps the mean-cross-correlation method, the maximum lag is very important, since it sets a limit of measurement on the deduced velocity of separate samples. The deduced velocity of an irregularity could be smaller than this limit, even with a reasonable drift speed, if the line of maximum made a large angle β with the drift direction.

Figure 6.1 illustrates some of the difficulties in finding ρ_{max} for a sample as compared with the ease of locating it in the long sequence methods. It can be seen that the chosen values of time delay will, in some cases, depend on the maximum lag utilized; so that for a larger maximum lag, the deduced sample velocities will tend towards lower values.

6.3 Parameters for long sequence methods

Five-minute segments (299 points) of data were used to calculate the cross-correlation sequences for the three pairs of antennas, and maximum lag was set at 18 sec.

Three methods are compared; median vector, method of zero N.T.D., and weighted least squares fit (WLSFIT2).

The median vector method required that the three values of ρ_{max} be greater than 0.1, and that ρ_{max} not occur at maximum lag. A parabolic fit around ρ_{max} was used to find the time delay.

The method of zero N.T.D. required that the separate values of ρ which gave the maximum sum for N.T.D. = 0 should each be greater than 0.1.

The method of least squares used the values of ρ_{max}^2 for purposes of weighting. All data, including those cases where $\rho_{max} < 0.1$, or where ρ_{max} occured at maximum lag, were used.

6.4 Sample methods.

Detailed comparison of these methods is based on a sample program which was written at U. of S. for this purpose. However, M.J. Burke has supplied daily averages for the C.R.C. method, the parameters of which will be briefly described at the end of this section.

The U. of S. program used 13 equal sample lengths per 5-minute segment of data. This number was chosen so that, on smoothed data, a maximum lag of 18 seconds could be used without any overlapping. As it turned out, the unsmoothed data was found to be more consistent, so that the maximum lag actually used was 20 sec.

Samples were accepted if all values of ρ_{max} were greater than 0.3, and did not occur at maximum lag. This criterion rejected about 20-30% of the samples on the average.

a.) Mean vector method

This method used a least squares fit to the

time delays for each accepted sample and then averaged the vectors over the 5-min record. No additional rejection criterion (e.g. N.T.D.)was used.

b) Mean times

The time delays for each pair of antennas were averaged over all accepted samples, and the least squares fit applied to the mean time values to give a drift velocity.

c) Mean cross-correlation

The cross-correlation sequences for each pair of antennas were averaged over all accepted samples, then the maximum average cross-correlations, ($\bar{\rho}_{max}$), were found. A least squares fit to the resulting time delays gave a drift vector. All the values of $\bar{\rho}_{max}$ were accepted (i.e. no rejection if $\bar{\rho}_{max}$ <.1 or $\bar{\rho}_{max}$ at maximum lag).

There was an error in the computor program which resulted in the inclusion of some cross-correlations from rejected samples in the average, but this is not expected to influence the results. In fact, it would have been more satisfactory to have averaged over all samples.

d) Straight line fit to inverted sample vectors

This method was developed after the data had been analysed, so that statistical comparisons are difficult. It is felt that because of its strong dependence on low velocity vectors, a very stringent rejection criterion (e.g. N.T.D.< 0.1) should be used. Some examples of its application to daily drifts will be shown in the following chapter.

e) C.R.C. method

The method used at C.R.C. is a mean vector method, but the data are smoothed before analysis, and the sample lengths chosen so that an amplitude peak occurs in at least one of them. More samples are made available by choosing three sets of samples based on inspection of the three fading sequences. Maximum lag is 10 seconds.

6.5 Comparison of consistency between methods.

Figure 6.2 shows the distribution of N.T.D. for the sample methods. It can be seen that the distribution for the mean times is close to the random one, indicating that the mean times are probably random.

Two types of comparison were made. The first compares the distribution of angle differences between drift vectors calculated at adjacent records in height and time, as was done in the previous chapter, and provides a very well defined, as well as conceptually useful, indication of the differences between methods. The second uses the average % difference from the mean of the two adjacent vectors, defined as

$$\frac{|\vec{V}_1 - \vec{V}_2|}{|\vec{V}_1 + \vec{V}_2|} \times 100\%$$

Figure 6.3 shows the distribution of angle differences for the various methods used on C.R.C. data (unsmoothed, Day 35, 38; 58-98 km). The number of cases of adjacent vectors for all

methods except median vector and method of zero N.T.D., are 320 and 294 for heights and times respectively. These include all the data. The corresponding values for the median vector and method of zero N.T.D., which reject some data, are (246, 210) and (288, 263) respectively.

Figure 6.4 shows the distribution of the % average vector difference from the mean for just the best and worst (below the 50 percentile) methods. It appears that this distribution is very insensitive to method.

6.6 Discussion

Figure 6.3 shows that the median vector method gives the most consistent drifts, and that all the long sequence methods are better in this sense than the sample methods used.

It is possible that there would be some improvement in the mean vector sample method if 'bad' (high N.T.D.) vectors were rejected. However, given that there may be scatter in the sample angles due to orientation of the irregularities, many vectors would have to be averaged to give the correct drift direction; and these are not available after rejection.

There seems to be no possibility of improving the mean times method because large values of time delay have a strong influence on the mean time which is usually small for expected drift speeds. Figure 6.5 shows rough histograms (about 80 values in each plot) of sample times for one height and day, for which the drift, according to the long sequence methods, was relatively constant towards east. In

this direction (T13) the time delays are seen to be almost constant, as would be expected no matter what the orientation of the irregularities relative to the drift. In the other directions there are delays scattered across the available lag interval. Whether this is just due to accidentally high correlations between different lines of maximum because of spatial variation in the pattern, or to differently oriented lines, will be discussed in the next chapter. The important point is that these large delays occur sufficiently often independently of maximum lag interval, to make the mean times method worthless for 5-minute segments of data and also for daily averages. This will be shown in the next section.

6.7 Comparison of daily averages

Daily averages for the analyses used are shown in Appendix 1, along with the C.R.C. values.

All long sequence methods agree well in direction, but the method of zero N.T.D. gives slightly higher magnitudes. The mean times method gives apparently random values. The mean vector method agrees roughly in direction with the long sequence methods but the magnitude is much smaller. This is also the case with the C.R.C. mean vector values (the table gives pattern velocity instead of drift) but the magnitudes are higher, being of the order of 0.5 or less with respect to the 5-min. methods. The difference between the two mean vector methods is probably due to choice of maximum lag. The mean cross-correlation method agrees fairly well in magnitude and direction with the long

sequence methods.

The following chapter will discuss reasons for the difference between mean vector and 5 min. methods.

Figures for Chapter 6

CAPTIONS

Figure No.	
6.1	Data sequences for sample method and long sequence method, illustrating the uncertainty in position of ρ_{max}.
6.2	Distribution of N.T.D.'s for sample methods, C.R.C. data.
6.3	Distribution of differences in angles of vectors for sequences adjacent in height and time, C.R.C. data. (NOTE: "Method #2" refers to the method of zero N.T.D.).
6.4	Distribution of percentage average vector difference for mean, for sequences adjacent in height and time as for Figure 6.3
6.5	Distributions of sample times (for one height and day as shown).

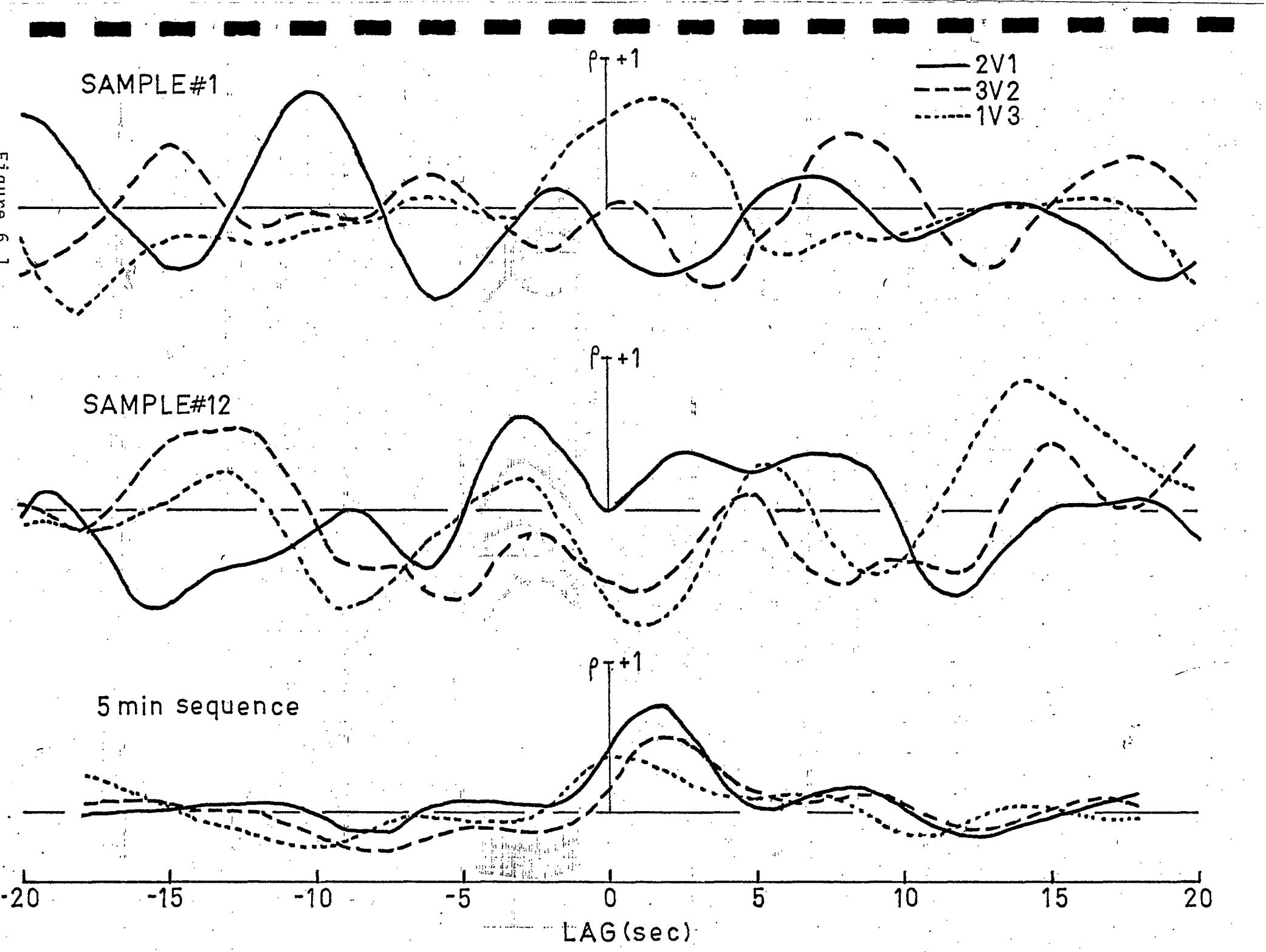
SAMPLE#1
ρ +1
2V1
3V2
1V3
SAMPLE#12
ρ +1
5 min sequence
ρ +1
-20
-15
-10
-5
0
5
10
15
20
LAG (sec)

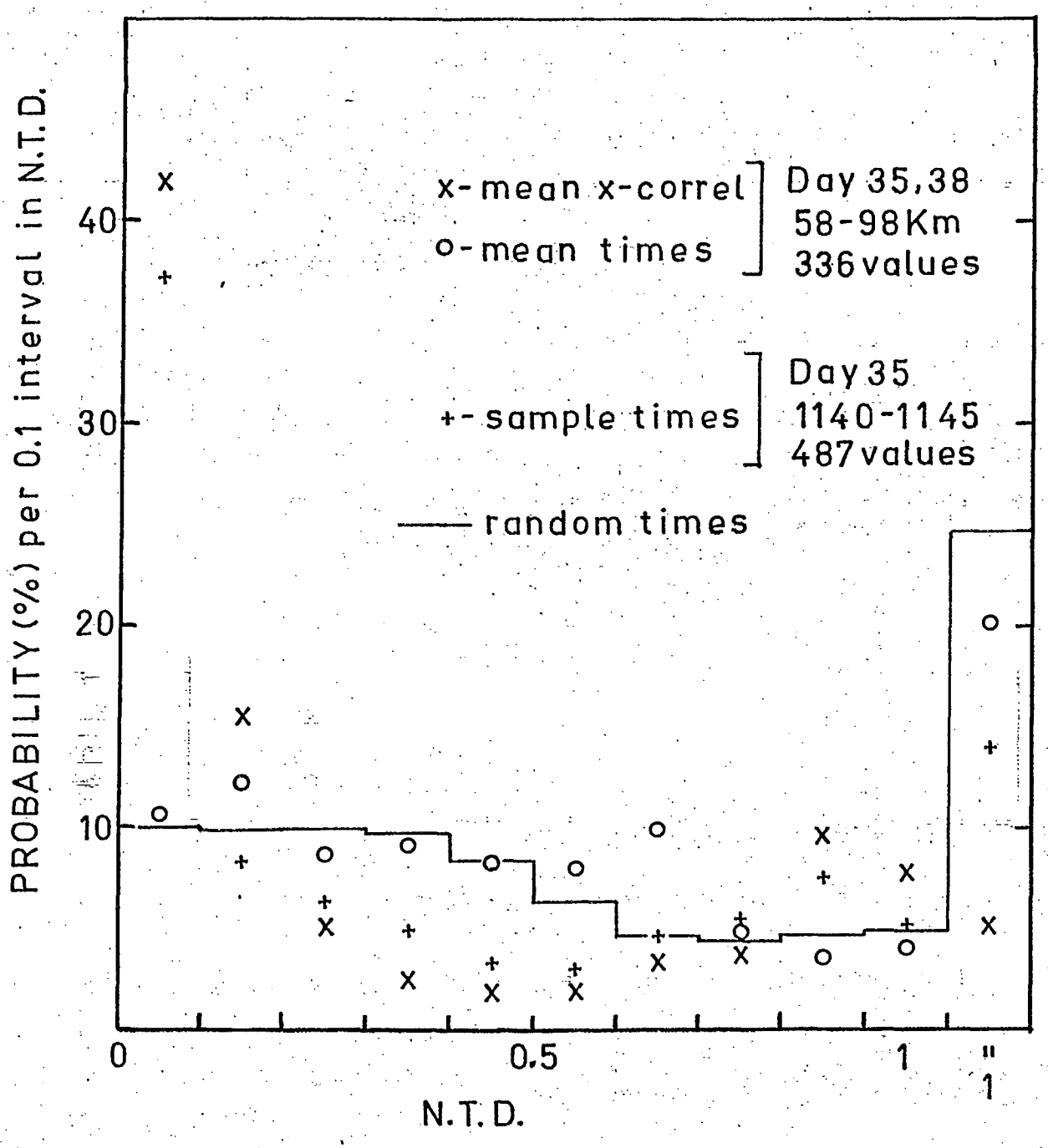
x-mean x-correl
o-mean times
Day 35,38
58-98Km
336values
+-sample times
Day 35
1140-1145
487values
random times
PROBABILITY (%) per 0.1 interval in N.T.D.
40
30
20
10
0
0.5
1
N.T.D.

Figure 6.2

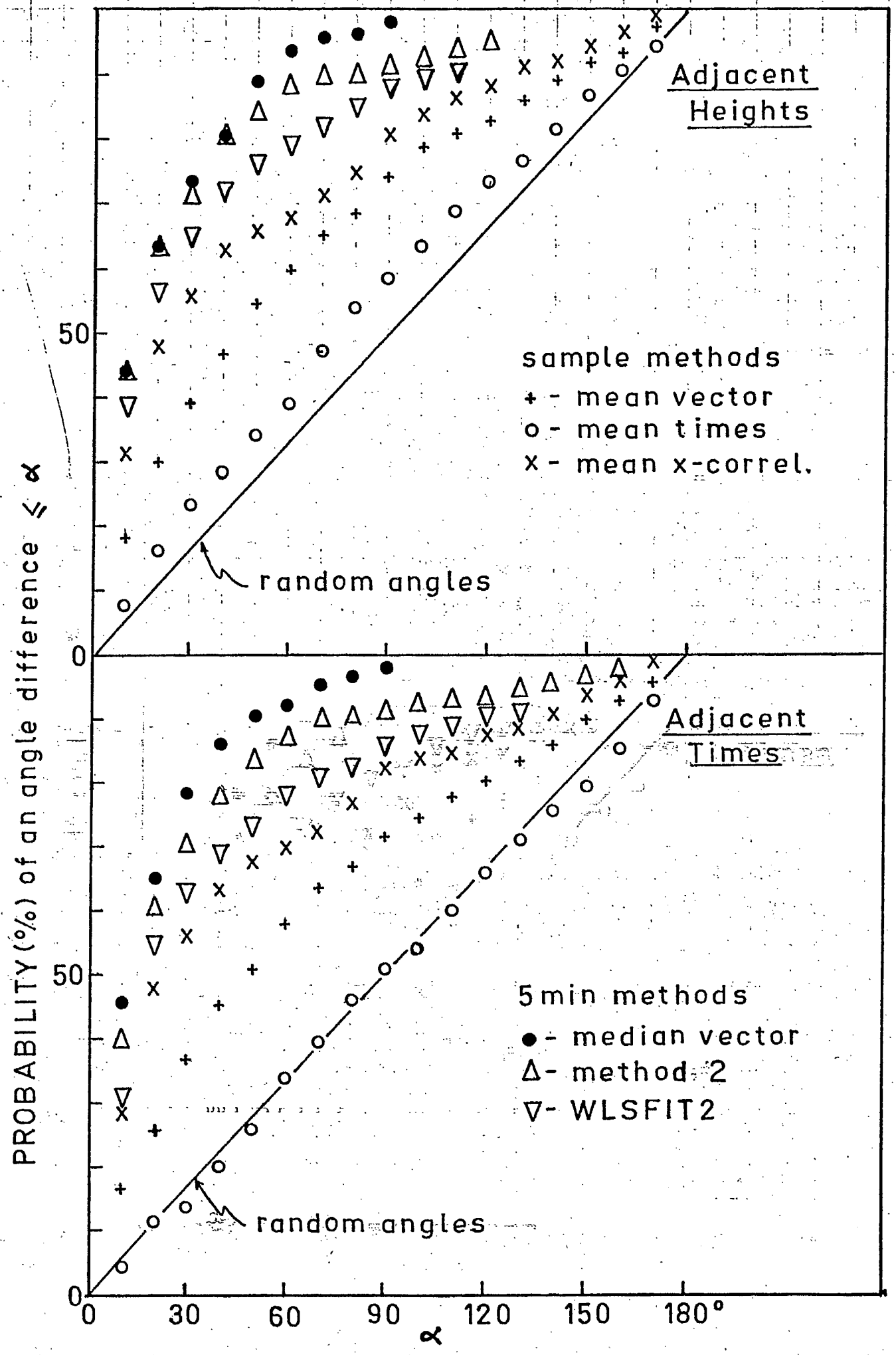
Adjacent Heights
sample methods
+ - mean vector
o - mean times
x - mean x-correl.
random angles
Adjacent Times
5min methods
● - median vector
Δ - method 2
▽ - WLSFIT2
random angles
PROBABILITY (%) of an angle difference ≤ α
0
50
0
50
0
30
60
90
120
150
180°
α

Figure 6.3

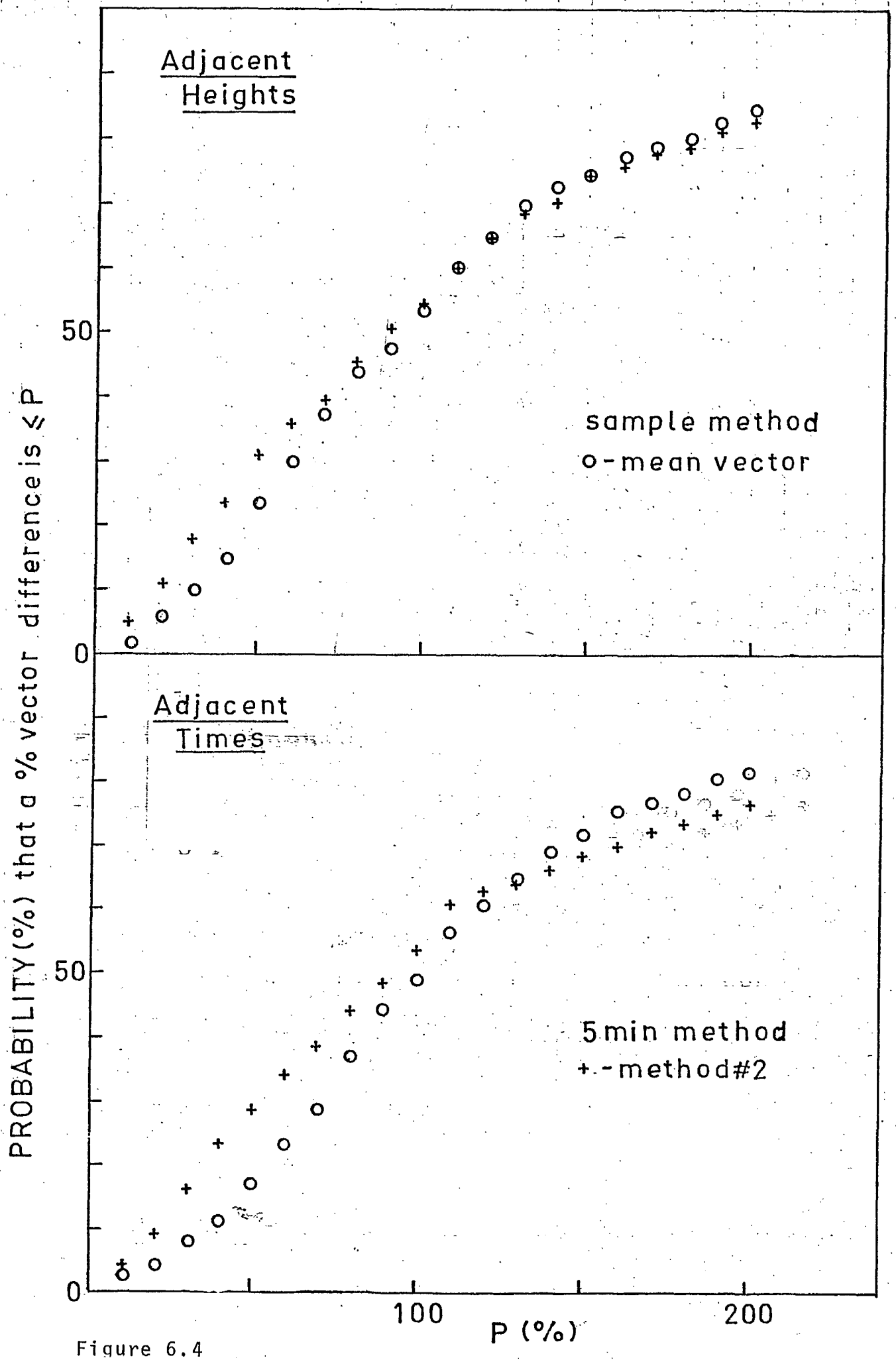
Adjacent
Heights
sample method
o-mean vector
50
0
Adjacent
Times
5min method
+-method#2
50
0
100
200
P (%)
PROBABILITY (%) that a % vector difference is ≤ P

Figure 6.4

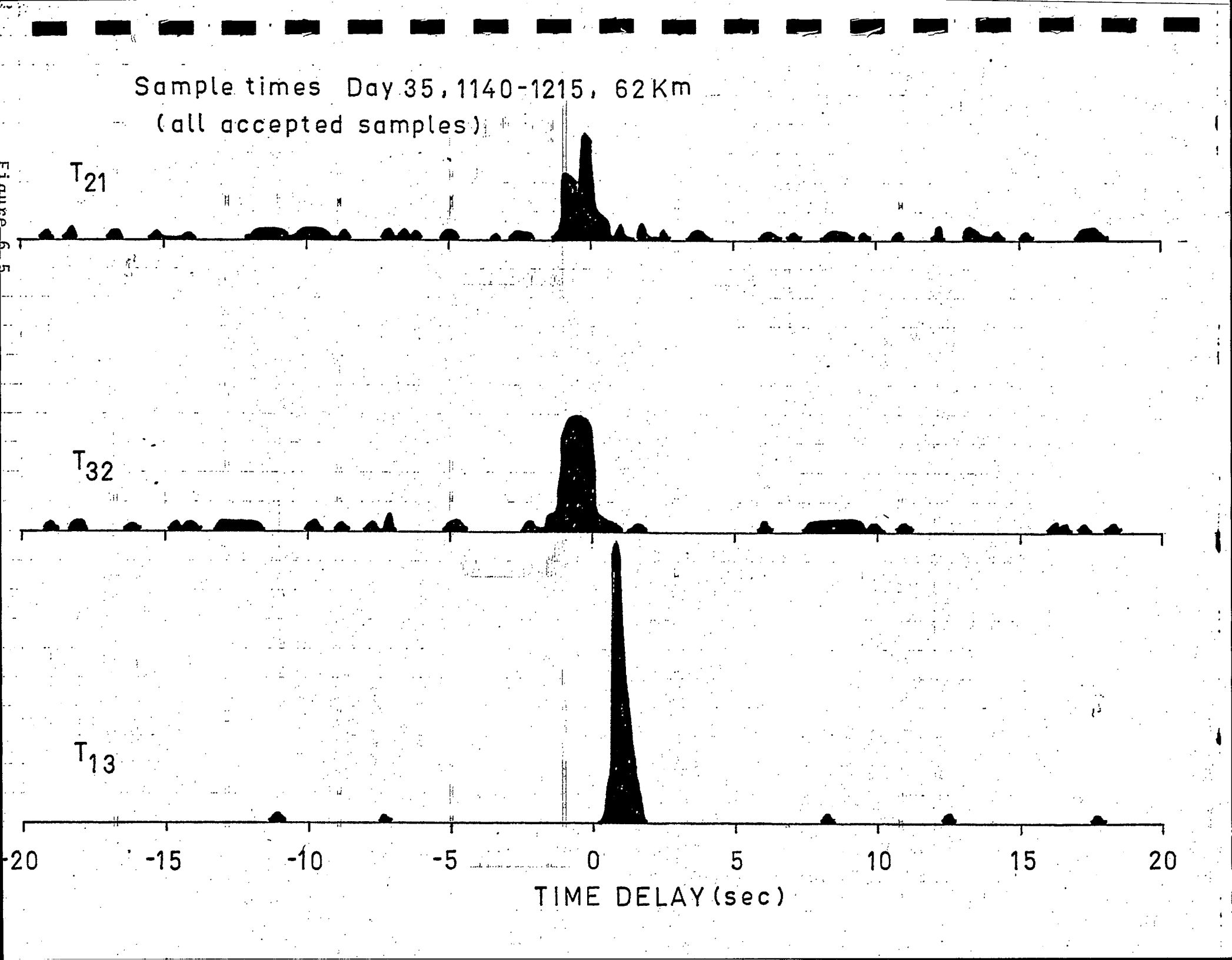
Sample times Day 35, 1140-1215, 62 Km
(all accepted samples)
T_{21}
T_{32}
T_{13}
-20
-15
-10
-5
0
5
10
15
20
TIME DELAY (sec)

Figure 6.5

Chapter 7. Relation between mean sample vector and long sequence vector.

7.1 Introduction.

The major difference between the mean vector method and long sequence methods for long term averages is the magnitude of drift obtained. This has also been noted by M.J. Burke (private communication).

Evidence to be presented indicates that the long sequence methods give the correct magnitude of apparent drift velocity. Some reasons for the low magnitudes given by the mean vector method will be discussed. Since sample vectors are not available for the C.R.C. method, all sample vectors presented are selected from the equal length samples by the criterion N.T.D. < 0.2. This ensures that a large proportion of the vectors represent the passage of single lines of maximum, although some low N.T.D. values could be accidental.

7.2 Determination of the correct magnitude

5-minute records were selected for which the sample times between one pair of antennas were almost constant, and for which the long sequence methods had a low N.T.D. The constancy of the sample times almost certainly means that the pattern is travelling along the direction of the antenna pair since neither off-perpendicular lines nor spatial pattern differences would affect the values of delay.

Table 7.1 shows the sample times, vectors, and N.T.D.'s for three such records. There is some small scatter in times,

60 Km 35/1140

SAMPLE APPAR VEL

SAMPLE#	T21	T32	T13	MAG	DIR	AN	AE	RMS	AVGXC	DISCREP(SEC)	NTD
1	-1.417	17.155	1.218	7.1	326.5	5.9	-3.9	5.65	.69	16.96	.86
2	-2.803	-.946	.830	39.3	48.3	26.2	29.4	.97	.87	-2.92	.64
3	-.209	-.742	1.269	68.6	93.8	-4.6	68.5	.11	.82	.32	.14
4	6.851	-.283	.935	18.7	189.8	-18.5	-3.2	2.50	.65	7.50	.93
5	7.865	-9.213	1.330	8.3	161.3	-7.9	2.7	.01	.64	-.02	.00
6	-1.216	.040	1.208	59.0	47.8	39.6	43.7	.01	.79	.03	.01
7	5.958	-7.210	.972	10.8	161.0	-10.2	3.5	.09	.60	-.28	.02
8	-.052	-.742	1.136	75.3	100.3	-13.5	74.0	.11	.80	.34	.18
9	10.977	-12.141	1.122	6.2	164.1	-5.9	1.7	.01	.77	-.04	.00
10	-.492	-.485	1.090	78.4	78.8	15.3	76.9	.04	.70	.11	.05
11	10.387	-6.713	-9.003	6.7	205.2	-6.1	-2.9	1.78	.52	-5.33	.20
12	-.998	-.130	1.053	69.4	54.1	40.7	56.2	.03	.91	-.08	.03
13	-.965	-.285	1.222	63.9	61.3	30.7	56.0	.01	.90	-.03	.01

70 Km 35/1140

SAMPLE APPAR VEL

SAMPLE#	T21	T32	T13	MAG	DIR	AN	AE	RMS	AVGXC	DISCREP(SEC)	NTD
1	REJECTED: ERROR MESSAGE= -10 (DIGIT GIVES ERR#, ,POSITION GIVES XCOR#)										
2	REJECTED: ERROR MESSAGE= -10 (DIGIT GIVES ERR#, ,POSITION GIVES XCOR#)										
3	-1.427	-.106	1.666	46.1	53.8	27.2	37.2	.04	.91	.13	.04
4	-1.276	-5.283	1.253	21.7	116.4	-9.7	19.4	1.77	.81	-5.31	.68
5	-1.420	-9.622	16.137	5.4	97.2	-.7	5.4	1.70	.64	5.09	.19
6	-1.245	-.047	1.318	55.8	51.2	35.0	43.4	.01	.84	.03	.01
7	-1.094	5.773	-10.763	8.6	283.4	2.0	-8.4	2.03	.71	-6.08	.35
8	REJECTED: ERROR MESSAGE= -10 (DIGIT GIVES ERR#, ,POSITION GIVES XCOR#)										
9	-1.490	3.902	-1.979	21.9	314.7	15.4	-15.6	.14	.52	.43	.06
10	-1.053	-.578	1.069	64.2	66.7	25.4	58.9	.19	.68	-.56	.21
11	-1.365	.535	.898	58.8	27.6	52.1	27.2	.02	.69	.07	.02
12	-1.037	-.692	1.146	60.9	70.6	20.3	57.4	.19	.68	-.58	.20
13	-.885	-.524	1.331	60.1	70.3	20.3	56.6	.03	.78	-.08	.03

92 Km 35/1140

SAMPLE APPAR VEL

SAMPLE#	T21	T32	T13	MAG	DIR	AN	AE	RMS	AVGXC	DISCREP(SEC)	NTD
1	8.895	-1.354	-7.922	8.4	221.8	-6.3	-5.6	.13	.66	-.38	.02
2	1.633	-1.948	.577	38.9	155.7	-35.4	16.0	.09	.63	.26	.06
3	18.118	-1.886	-17.170	4.0	224.6	-2.9	-2.8	.31	.52	-.94	.03
4	-13.177	-1.174	-13.011	10.4	319.7	7.9	-6.7	9.12	.57	-27.36	1.00
5	10.755	-1.303	-19.445	4.7	235.6	-2.7	-3.9	3.33	.53	-9.99	.32
6	2.822	-1.947	12.725	9.6	97.6	-1.3	9.5	4.53	.58	13.60	.78
7	REJECTED: ERROR MESSAGE= -1 (DIGIT GIVES ERR#, ,POSITION GIVES XCOR#)										
8	-.192	-.981	.037	134.0	126.6	-79.9	107.6	.38	.66	-1.14	.94
9	REJECTED: ERROR MESSAGE= -100 (DIGIT GIVES ERR#, ,POSITION GIVES XCOR#)										
10	-10.014	-1.746	2.328	11.4	37.9	9.0	7.0	3.14	.54	-9.43	.67
11	.747	5.860	.817	24.4	319.7	18.6	-15.8	2.48	.63	7.43	1.00
12	.761	5.522	-5.153	13.4	285.4	3.6	-12.9	.38	.54	1.13	.10
13	REJECTED: ERROR MESSAGE= -1 (DIGIT GIVES ERR#, ,POSITION GIVES XCOR#)										

Table 7.1

apart from obviously spurious values, which could be due to several causes. These include time changes in the pattern, a direction of travel not quite along the antenna pair, with the differences in delay caused by differently oriented lines, and scatter in calculation of the cross-correlation at fixed lag values. This scatter in delays arises because of the different shapes of cross correlation sequences obtained for each sample; i.e. the peak value, which would be unity if no differences occurred in the pattern between antennas, will occur between lags, and so the calculated position of the peak will depend on values adjacent to the peak. The scatter in times is only of the order of $\pm$ 0.2 lag.

Table 7.2 gives the median times (neglecting the spurious values) and expected drift components along the corresponding antenna pair ——

Table 7.2 Median times and calculated drift components (day 35, unsmoothed data)

Height (km)	Median time (sec)	Drift component (m/s)
60	T_{13} = 1.10	75
70	T_{21} =-1.27	65
92	T_{32} =-1.55	53

Table 7.3 shows the corresponding magnitude and direction given by the long sequence methods, along with those for the mean cross correlation sample method.

Table 7.3 Vectors (mag(m/s) and direction (deg E of N) for 5-min methods (day 35, unsmoothed data)

Height (km)	Median vector	WLSFIT2	Method of zero N.T.D.	LSFIT	N.T.D.	Mean-xcorrel	N.T.D.
60	76,66°	74,68°	76,66°	74,67°	0.02	68,63°	0.01
70	57,37°	63,33°	66,35°	62,38°	0.06	62,36°	0.06
92	41,117°	53,116°	56,120°	48,113°	0.14	48,112°	0.12

In these cases, the LSFIT method was also used on the three time delays produced by the 5-min segments of data.

Figure 7.1 shows plots of the sample vectors, the LSFIT vector, and a superposed, numbered, antenna diagram. Also shown are the values of ρ_{max} for the 5-min methods. As would be expected, the values of ρ_{max} are highest in the direction of drift because spatial differences in pattern are not involved.

Comparison of Tables 7.2 and 7.3 show that in these cases the correct magnitude of drift is given by the 5-min methods. Inspection of the sample vectors in Figure 7.1 shows why the mean sample vectors would give a low magnitude. These low values of sample drift are usually prevalent on all the records, even after rejection of those with high N.T.D. values, and will be discussed in the next section.

7.3 Reasons for low magnitude in the mean sample vector method.

Preliminary inspection of the data indicated that quite often, the sample vector with maximum magnitude agrees fairly well in magnitude and direction with the 5-min. value. This would be expected if the lines of max. had different orientation, since the maximum deduced velocity of an irregularity would be equal to the drift.

Figure 7.2(a) shows a plot of all sample vectors (N.T.D. < 0.2) for one height over a 40 minute time period. This particular record was chosen because the 5-min. methods gave relatively constant vectors and the N.T.D.'s were low. The mean 5 min. drift (median vector) is shown with bars indicating the standard deviation in North and East components. The C.R.C. vector is taken from Appendix ..I... Also indicated is the vector produced by a straight line fit (which minimized perpendicular deviations) to the inverted sample vectors. The equations for this type of fit have been derived by Kenny (1947).

The sample vectors apparently fall on a circle whose diameter is the mean 5 min drift vector, as would be expected from the discussion in Chapter 3. There is also an abundance of low values. However, the distribution of lines of maximum does not appear to be random, which might have been predicted from the factor of $\sim$ 1/2 between mean vector (C.R.C.) method and 5-min. methods.

Plotted in Figure 7.2ais the density of off-perpendicular angles (assuming that the correct angle is given by the mean 5-min vector). There appears to be a decrease in number with increasing

off-perpendicular angle, but the number of samples is not high enough for a conclusive statement. Also, the true pattern drift would have to be assumed constant.

There are also some 'impossible' (> 90°) angles. These are thought to be due to errors arising from a non-zero N.T.D., or 'accidentally' low N.T.D.'s, i.e. more than one irregularity is involved in the sample length.

Explanation of the angular distribution by a variable drift angle does not appear reasonable because separate plots of 5-min data segments also showed the same features, viz., a scattering of angles of sample vectors with large magnitude, and a disproportionate number of low values. In each case, the sample vectors appeared to be scattered around a circle whose diameter was the 5-min. vector.

Figures 7.2(b) and 7.2(c) show three other similar sets of data. These show much more scatter in sample vectors and many of the low values do not seem to lie on the circle.

In these as well as Figure 7.2(a), there are a few large magnitude sample vectors which are thought to be due to effects of simultaneous measurement of amplitudes.

An important question is whether these low vectors are just due to the choice of a large maximum lag. Since these sample vectors are all 'good' (low N.T.D.), and are assumed to be due to approximately straight lines of maximum, the maximum time delay, for a particular irregularity with speed > V_{min}, is related to V_{min} by $t < d/2V_{min}$). Thus, sample vectors lying outside a circle radius 8.3 m/s in Figure 7.2(a), (b), (c)

would still apply if a maximum lag of 10 seconds had been used, instead of 20 sec. Of course, some of the samples inside the circle, as well as those which had been rejected because of high N.T.D., might produce good vectors under the reduced maximum lag. The main point is that there are still many remaining low values, and it appears that even if a smaller maximum lag had been used, a similar quantity of low values would occur. The minimum magnitude of these would be greater, of course.

Some of these low values are certainly 'accidental', and do not represent a single irregularity. As shown in Figure 3.2, even if the times were random, there would still be 20% of the samples with N.T.D. < 0.2; and since $V \sim d/2t_{max}$) where t_{max} is the maximum of the three time delays, most of these would produce low velocities. However, it is difficult, if not impossible, to tell what fraction of the plotted vectors could be ascribed to 'random' times.

7.4 Conclusions

The discussion in this chapter leads to the following conclusions.

There is some evidence to indicate that the irregularities have some sort of distribution of lines of maximum about the perpendicular to the drift. There are not enough samples to draw conclusions about the form of the distribution, except that it is probably symmetrical about the perpendicular to the drift, since sample and 5-min. methods tend to agree in direction.

The sample method produces many low velocity vectors,

which may partially be due to unrelated values of time delays accidentally giving a low N.T.D., but this is expected to occur with any set value of maximum lag.

An average of sample vectors gives a reasonable approximation to direction (at least over a large number of samples) because the random vectors cancel, as do the components perpendicular to the drift direction of 'good' vectors.

The magnitude of the mean sample vector is less than the actual drift, because of the many low magnitude vectors obtained. It would be less, even if all vectors represented deduced irregularity velocities, because of the angular distribution of lines.

There appears to be no evidence for a preferred direction of lines, e.g. along the magnetic field, since this would show up as a concentration of sample vectors along the perpendicular to the preferred direction. (The perpendicular is about 108^{o} or 288^{o} east of north, in the case of the magnetic field, whichever is within 90^{o} of the drift direction).

These conclusions were formed purely with the equal sample method. However, given that the C.R.C. method gives lower magnitudes than the long sequence methods by a factor of one-half or less, the same considerations discussed above would likely apply.

Figures for Chapter 7

CAPTIONS

Figure No.

7.1 Sample vectors (solid dots), least squares fit mean (arrow) vector, and antenna geometry, for three sets of observations.

7.2(a) Plot of all sample vectors (solid dots), over 40-minute period, with mean vectors (arrows).

7.2(b) Further plot as in (a), at different height and time.

7.2(c) Further plots as in (a).

Table 7.1 Sample times and velocities. Reference Section 7.2.

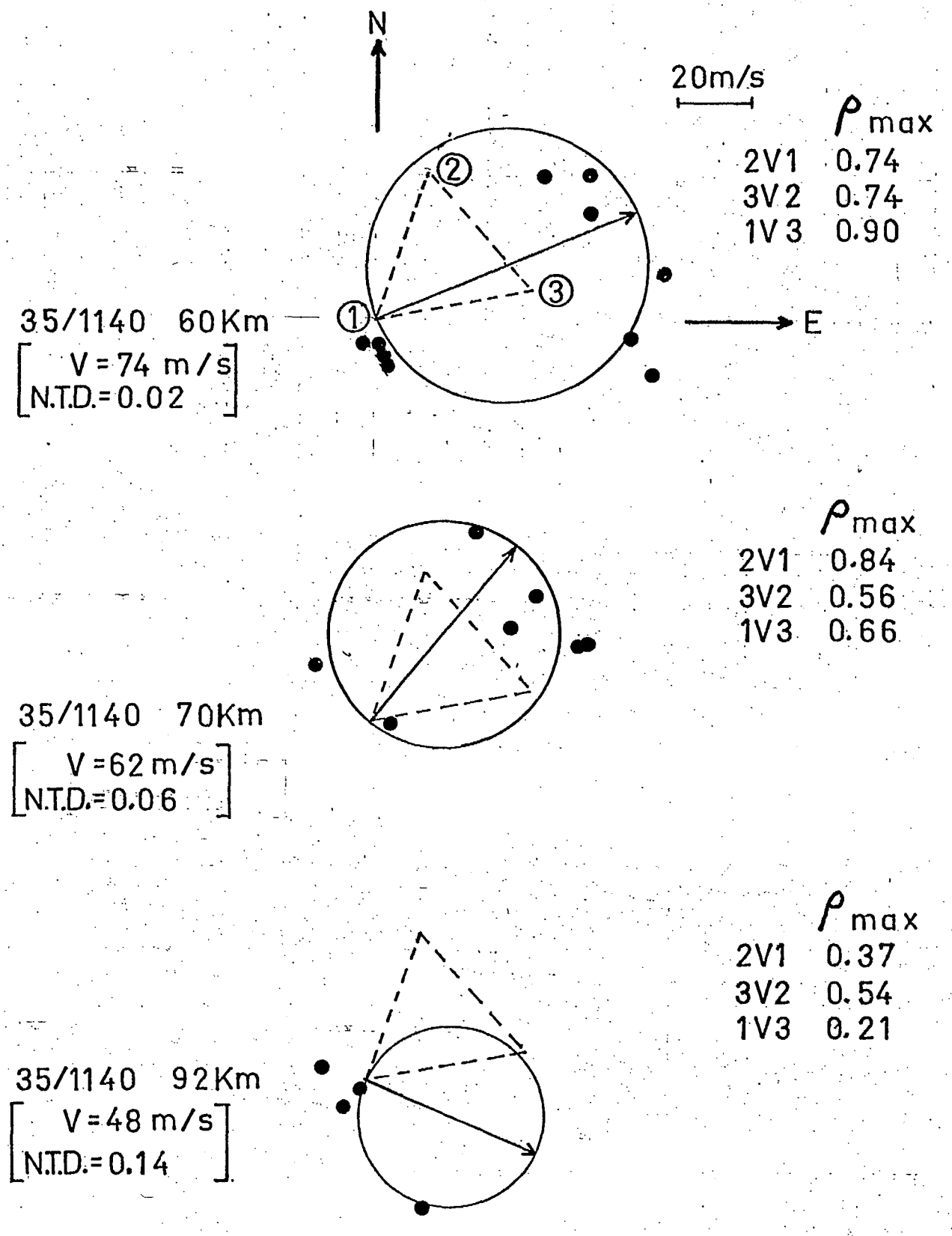
N
20m/s
ρmax
2V1 0.74
3V2 0.74
1V3 0.90
35/1140 60Km
[V=74 m/s
N.T.D.=0.02]
①
②
③
E
ρmax
2V1 0.84
3V2 0.56
1V3 0.66
35/1140 70Km
[V=62 m/s
N.T.D.=0.06]
ρmax
2V1 0.37
3V2 0.54
1V3 0.21
35/1140 92Km
[V=48 m/s
N.T.D.=0.14]

Figure 7.1.

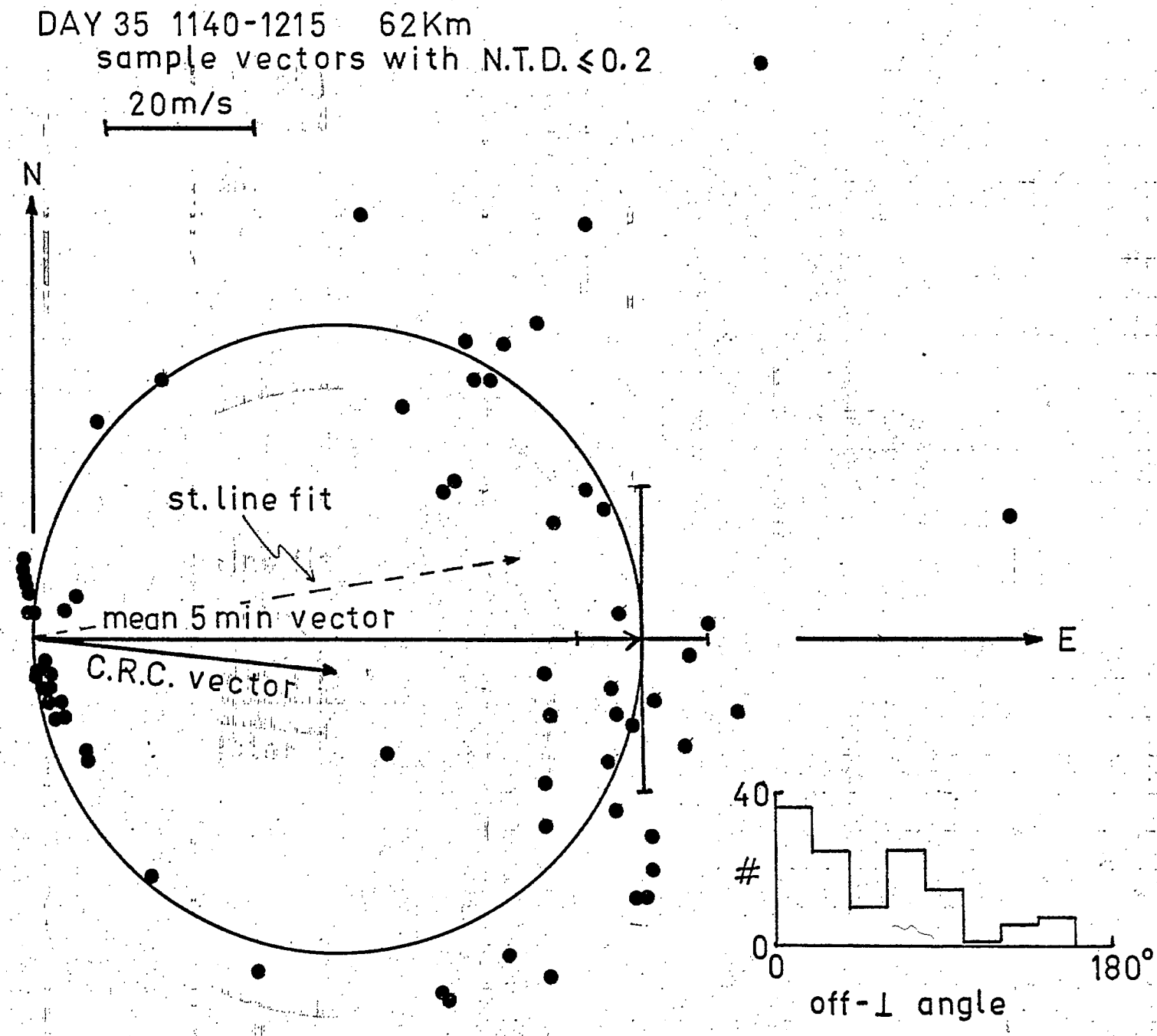
DAY 35 1140-1215 62Km
sample vectors with N.T.D. ≤ 0.2
20m/s
N
E
st. line fit
mean 5 min vector
C.R.C. vector
40
#
0
0
180°
off-⊥ angle

Figure 7.2(a)

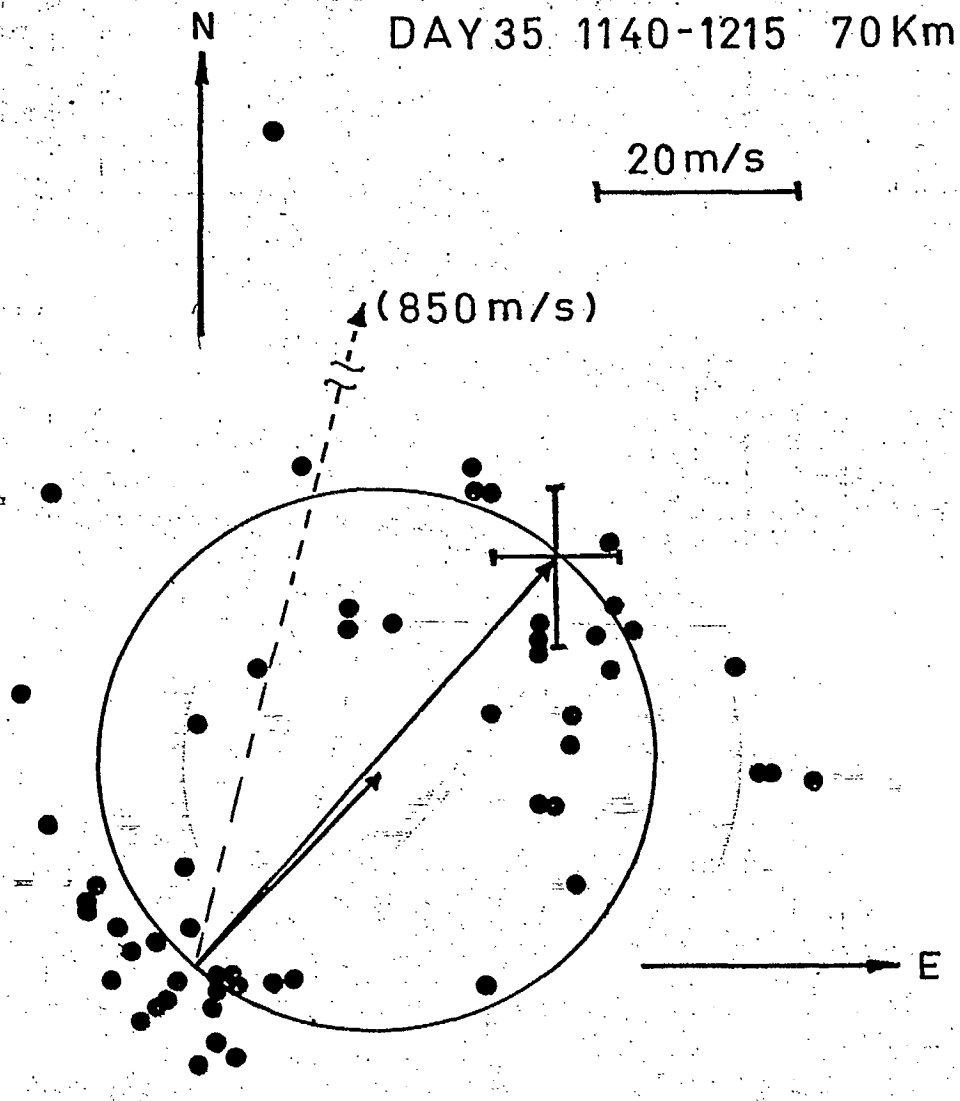

Figure 7.2(b)

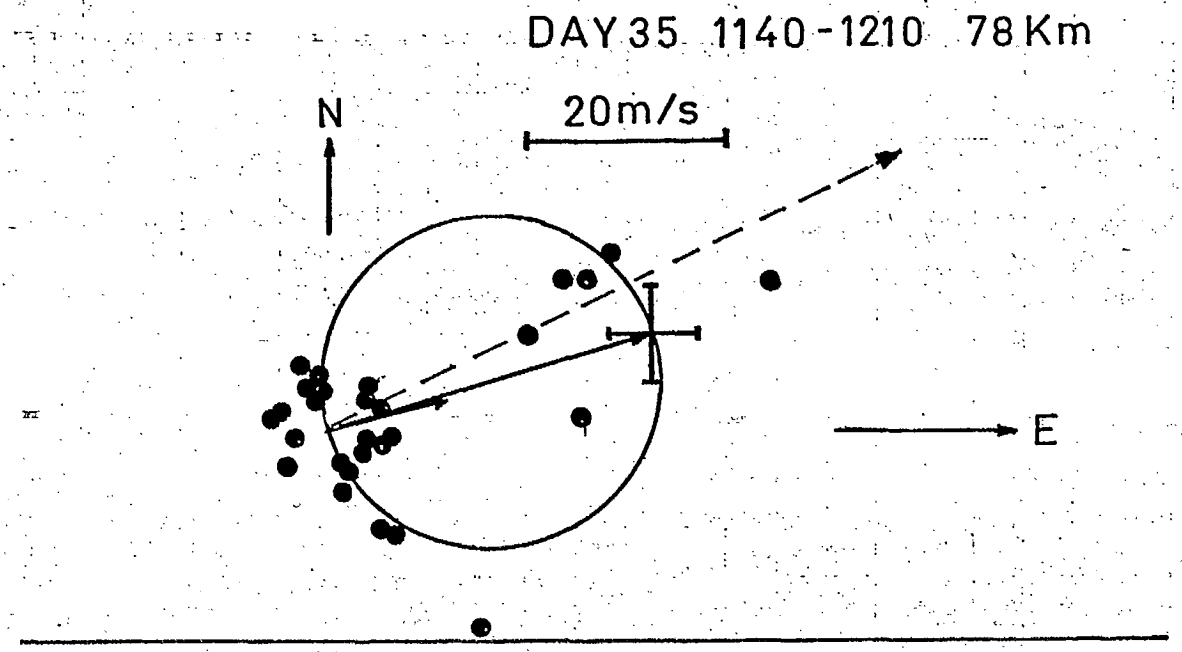

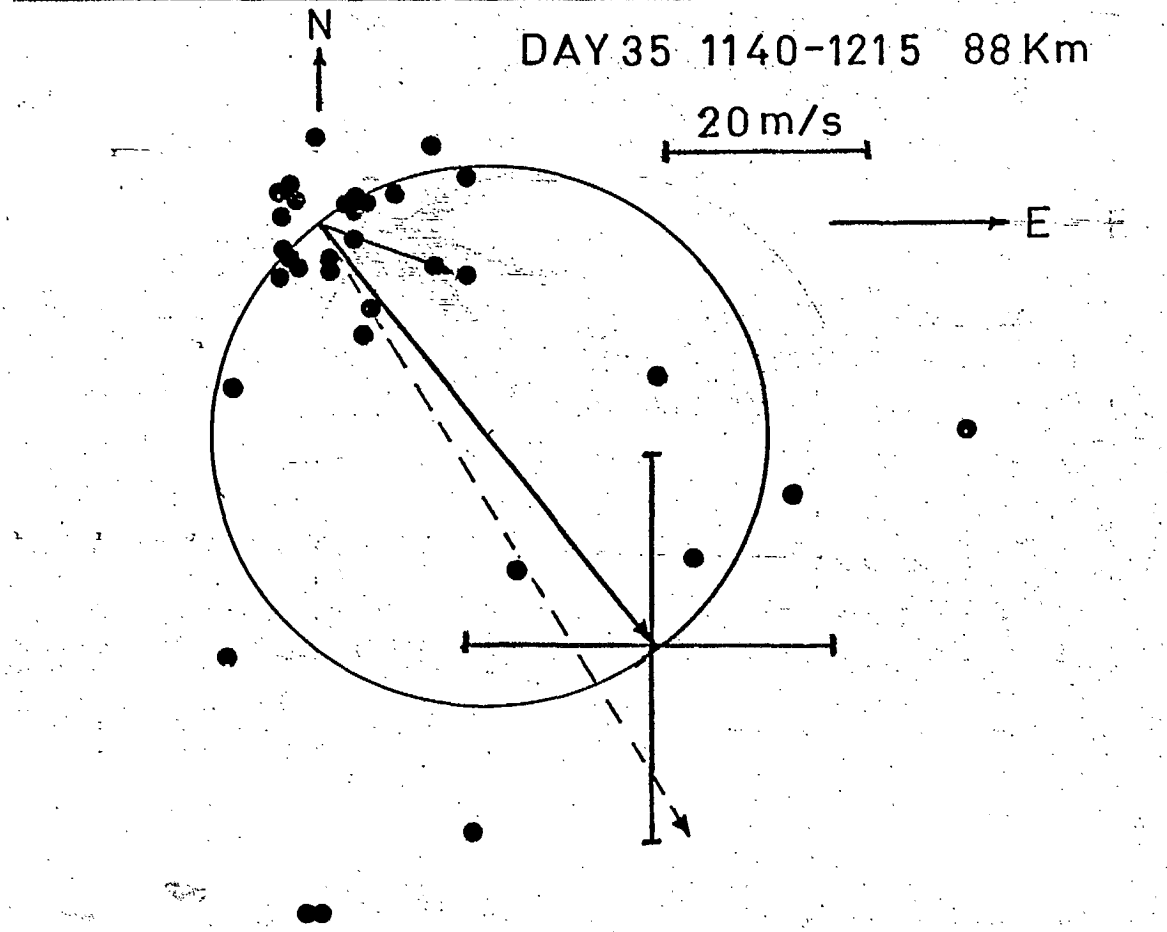

Figure 7.2(c)

Appendix 1. Daily averages of drift values.

The following tables give the daily average drift velocity for unsmoothed C.R.C. data (day 35, 38). Given for the 5 min methods is the number of values (maximum of 8) used in the average after rejection criteria, if any, had been applied; the standard deviation; the standard error in the mean; and the % standard error in the mean, for north and east components. The vector formed with the mean components is at the left-hand side of the table. All magnitudes are in m/s, and angles are in degrees East of North.

The mean cross correlation (titled AVG X-CORREL) sample method rejected sample vectors with N.T.D. > 0.7 in the average to approximate the median vector criteria.

The mean vector method averaged the vectors of all accepted samples over the 40 minute period. No rejection criterion based on N.T.D. was used.

The format of the tables are the same for all of the above mentioned methods.

The mean times sample method has averaged the sample times over the 40 minute period. Given in the table are the number of samples used, the N.T.D. of the final three mean times, the drift vector defined by a least squares fit, to the three times the north and east components, and the values of the mean times.

The C.R.C. values give pattern velocity, not drift, so that they should be divided by 2 for comparison with the other tables, VX is the east, and VY the north, component.

REFERENCES

Andreeva, L.A., B.O. Vugmeister, Yu.D. Ilyichev, E.S. Kazimirovsky, L.A. Katasev, V.D. Kokourov, N.S. Lifshitz, S.V. Pahomov and D.B. Uvarov. 1973. Space Research XIII, 191-196.

Barber, N. 1957. J. Atmos. Terr. Phys., 11, 299-300.

Blamont, J.E. 1966. In "*Les Problemes Meteorologiques de la Stratosphere et de la Mesosphere*", 151-168. Press Universitaires de France.

Briggs, B.H., G.J. Phillips and D.H. Shinn. 1950. Proc. Phys. Soc., 58B, 105-121.

Briggs, B.H. and E.S. Page. 1955. Proc. Phys. Soc. Conf. Ionosphere, 119-122. (Phys. Soc. London).

Deland, R.J. 1973. Tellus, 25, 355.

Felgate, D.G. 1970. J. Atmos. Terr. Phys., 32, 241-245.

Felgate, D.G., A.N. Hunter, S.P. Kingsley and H.G. Müller. 1975. Planet. Space Sci., 23, 389-400.

Fraser, G.J. 1965. J. Atmos. Sci., 22, 217.

Glass, M., J.L. Fellous, M. Massebeuf, A. Spizzichino, I.A. Lysenko, and Yu.D. Portniaghin. 1975. J. Atmos. Terr. Phys., 37, 1077-1088.

Golley, M.C. and D.E. Rossiter. 1970. J. Atmos. Terr. Phys., 32, 1215-1233.

Greenhow, J.S. and E.L. Neufeld. 1961. Quart. J. Roy. Met. Soc., 87, 472.

Gregory, J.B. and A.H. Manson. 1970. J. Atmos. Terr. Phys., 32, 837-852.

Gregory, J.B. and A.H. Manson. 1975a. J. Atmos. Sci., 32, 1667-1675.

Gregory, J.B. and A.H. Manson. 1975b. J. Atmos. Sci., 32, 1676-1681.

Gregory, J.B., A.H. Manson, D.G. Stephenson, J.S. Belrose, M.J. Burke and T.R. Coyne. 1975. Nature, 258, 62-64.

Groves, G.V. 1959. J. Atmos. Terr. Phys., 16, 344-356.

Groves, G.V. 1969. J. Brit. Interplanet. Soc., 22, 285.

Justus, C.G. and A. Woodrum. 1972. Contract No. NAS8-26658, Georgia Tech. Project E-16-612, Final Summary, November, 1972.

Kokourov, V.D., E.S. Kazimirovsky, V.N. Jakharov and E.I. Jovty. 1971. J. Atmos. Terr. Phys., 33, 943-950.

Lloyd, K.H., C.H. Low, B.J. McAvaney, D. Rees and R.G. Roper. 1972. Planet. Space Sci., 20, 761-790.

Lysenko, I.A., Yu.I. Portniaghin, K. Sprenger, K.M. Gresiger and R. Schminder. 1972. J. Atmos. Terr. Phys., 34, 1435-1444.

Manson, A.H., J.B. Gregory and D.G. Stephenson. 1974. J. Atmos. Sci., 31, 2207-2215.

Mitra, S.N. 1949. Proc. Instn. Elect. Engrs, Part III, 96, 441.

Müller, H.G. 1968. J. Atmos. Terr. Phys., 30, 701-706.

Newell, R.E., J.R. Mahoney and R.W. Lenhard. 1966. Quart. J. Roy. Met. Soc., 92, 41-54.

Pütter, P. St. Von. 1955. Phys. Soc. Conf. Phys. of Ionosphere, 191-201. Phys. Soc., London.

Ratcliffe, J.A. 1954. J. Atmos. Terr. Phys., 5, 173-181.

Rossiter, D.E. 1970. Austr. J. Phys., 23, 103-117.

Sprenger, K. and R. Schminder. 1968. J. Atmos. Terr. Phys., 30, 693-700.

Sprenger, K. and R. Schminder. 1969. J. Atmos. Terr. Phys., 31, 1085-1098.

Sprenger, K., I.A. Lysenko, K.M. Gresiger and A.D. Orljanski. 1971. Fiz. Atm. Okeans., 7, 455.

Sprenger, K. and I.A. Lysenko. 1972. Phil. Trans. Roy. Soc. Lond., A271, 473-484.

Stubbs, T.J. 1973. J. Atmos. Terr. Phys., 35, 909-919.

Stubbs, T.J. 1975. Ph.D. Thesis, University of Adelaide.

Stubbs, T.J. and R.A. Vincent. 1973. Austr. J. Phys., 26, 645-660.

Appendix 1

LIST OF TABULATIONS

Sheets 1-12	Median vector, method of zero N.T.D. (Method #2), weighted least squares fit, average cross-correlation, mean vector, and mean times; each for days 35 and 38.
Sheets 13-14	Listing of C.R.C. winds, days 35 and 38. Average values from the 40-minute sequence. (NOTE: Velocities are for pattern: winds are half the magnitude shown).

DAY=35 5 MIN METHOD= 1

Median Vector

H(KM)	#	N-COMP	S.D.	S.E.	%ERR	E-COMP	S.D.	S.E.	%ERR	MAG	DIR
58.	3	10.22	18.18	12.85	126.	115.63	42.10	29.77	26.	116.1	84.9
60.	8	10.68	23.34	8.82	83.	95.22	39.57	14.96	16.	95.8	83.6
62.	8	-0.83	18.90	7.14	860.	82.76	11.39	4.31	5.	82.8	90.6
64.	8	-0.66	16.73	6.32	951.	85.16	16.29	6.16	7.	85.2	90.4
66.	8	13.20	15.76	5.96	45.	73.31	12.29	4.64	6.	74.5	79.8
68.	8	44.88	18.23	6.89	15.	34.80	21.78	8.23	24.	56.8	37.8
70.	8	41.83	6.32	2.39	6.	35.82	6.12	2.31	6.	55.1	40.6
72.	8	32.44	7.08	2.68	8.	36.36	3.43	1.30	4.	48.7	48.3
74.	8	21.15	4.91	1.86	9.	36.81	4.23	1.60	4.	42.5	60.1
76.	8	11.43	7.55	2.85	25.	29.63	8.21	3.10	10.	31.8	68.9
78.	8	9.52	6.66	2.52	26.	25.09	13.02	4.92	20.	26.8	69.2
80.	7	11.86	9.83	4.01	34.	24.12	14.83	6.06	25.	26.9	63.8
82.	4	0.31	4.57	2.64	863.	2.20	3.26	1.88	86.	2.2	82.1
84.	5	-10.11	11.58	5.79	57.	27.59	25.22	12.61	46.	29.4	110.1
86.	8	-30.86	20.52	7.76	25.	38.12	11.65	4.40	12.	49.0	129.0
88.	8	-45.84	21.58	8.15	18.	35.26	10.06	3.80	11.	57.8	142.4
90.	8	-39.69	19.89	7.52	19.	29.43	9.28	3.51	12.	49.4	143.4
92.	6	-43.44	26.05	11.65	27.	22.07	14.26	6.38	29.	48.7	153.1
94.	5	-31.64	22.61	11.31	36.	32.19	18.57	9.29	29.	45.1	134.5
96.	5	-37.14	25.16	12.58	34.	-34.58	33.94	16.97	49.	50.7	223.0
98.	5	-51.26	18.00	9.00	18.	-48.13	30.68	15.34	32.	70.3	223.2

Sheet 1

DAY=35 5 MIN METHOD= 4

METH#2

H(KM)	#	N-COMP	S.D.	S.E.	%ERR	E-COMP	S.D.	S.E.	%ERR	MAG	DIR
58.	8	-41.09	136.24	51.49	125.	201.99	325.77	123.13	61.	206.1	101.5
60.	8	15.24	24.43	9.23	61.	107.54	64.18	24.26	23.	108.6	81.9
62.	8	-0.87	18.83	7.12	817.	82.69	11.50	4.35	5.	82.7	90.6
64.	8	-1.11	17.55	6.63	600.	85.91	15.45	5.84	7.	85.9	90.7
66.	8	13.16	15.76	5.96	45.	73.34	12.27	4.64	6.	74.5	79.8
68.	8	53.59	19.91	7.52	14.	37.97	19.86	7.51	20.	65.7	35.3
70.	8	43.89	8.63	3.26	7.	36.10	7.69	2.90	8.	56.8	39.4
72.	8	32.33	5.60	2.12	7.	36.58	2.95	1.11	3.	48.8	48.5
74.	8	21.33	5.10	1.93	9.	36.96	4.38	1.65	4.	42.7	60.0
76.	8	14.80	6.84	2.58	17.	33.50	4.95	1.87	6.	36.6	66.2
78.	6	12.65	6.82	3.05	24.	32.52	5.26	2.35	7.	34.9	68.7
80.	6	24.18	25.71	11.50	48.	37.56	11.26	5.04	13.	44.7	57.2
82.	5	9.20	9.70	4.85	53.	22.07	22.82	11.41	52.	23.9	67.4
84.	7	-17.18	16.43	6.71	39.	72.51	76.92	31.40	43.	74.5	103.3
86.	8	-42.78	20.44	7.73	18.	43.72	10.70	4.04	9.	61.2	134.4
88.	8	-52.84	18.75	7.09	13.	34.20	16.51	6.24	18.	62.9	147.1
90.	8	-46.83	20.44	7.73	16.	32.16	9.66	3.65	11.	56.8	145.5
92.	8	-41.30	22.12	8.36	20.	29.20	11.50	4.35	15.	50.6	144.7
94.	8	-56.60	48.68	18.40	33.	35.71	32.46	12.27	34.	66.9	147.8
96.	8	-11.03	71.58	27.06	245.	-25.37	82.54	31.20	123.	27.7	246.5
98.	8	-166.37	304.62	115.13	69.	-76.15	70.56	26.67	35.	183.0	204.6

Sheet 2

DAY=35 5 MIN METHOD= 3

WLSFIT2

H(KM)	#	N-COMP	S.D.	S.E.	%ERR	E-COMP	S.D.	S.E.	%ERR	MAG	DIR
58.	8	-61.56	150.94	57.05	93.	224.60	343.54	129.84	58.	232.9	105.3
60.	8	10.80	21.86	8.26	76.	82.12	18.63	7.04	9.	82.8	82.5
62.	8	-0.06	17.19	6.50	10855.	80.94	7.67	2.90	4.	80.9	90.0
64.	8	1.63	14.84	5.61	343.	80.08	7.56	2.86	4.	80.1	88.8
66.	8	11.94	14.73	5.57	47.	78.73	8.37	3.16	4.	79.6	81.4
68.	8	51.61	18.57	7.02	14.	36.58	18.79	7.10	19.	63.3	35.3
70.	8	44.95	6.85	2.59	6.	34.31	6.25	2.36	7.	56.5	37.4
72.	8	36.57	7.96	3.01	8.	33.06	3.50	1.32	4.	49.3	42.1
74.	8	25.56	10.36	3.91	15.	35.64	3.55	1.34	4.	43.9	54.4
76.	8	12.07	8.20	3.10	26.	32.87	5.37	2.03	6.	35.0	69.8
78.	8	9.13	8.48	3.20	35.	27.57	11.49	4.34	16.	29.0	71.7
80.	8	9.10	16.16	6.11	67.	19.02	14.70	5.56	29.	21.1	64.4
82.	8	6.70	13.71	5.18	77.	2.87	7.88	2.98	104.	7.3	23.2
84.	8	-2.80	22.77	8.61	307.	22.33	39.81	15.05	67.	22.5	97.2
86.	8	-35.30	14.42	5.45	15.	48.19	12.06	4.56	9.	59.7	126.2
88.	8	-48.80	19.25	7.28	15.	39.31	9.04	3.42	9.	62.7	141.1
90.	8	-42.97	19.82	7.49	17.	34.55	10.78	4.07	12.	55.1	141.2
92.	8	-34.19	31.36	11.85	35.	20.61	21.89	8.27	40.	39.9	148.9
94.	8	-25.15	25.61	9.68	38.	36.63	37.35	14.12	39.	44.4	124.5
96.	8	-25.62	64.71	24.46	95.	-1.90	66.01	24.95	1313.	25.7	184.2
98.	8	-52.94	30.40	11.49	22.	-96.41	92.85	35.09	36.	110.0	241.2

Sheet 3

DAY=35 SAMPLE METHOD= 1

AVG X-CORREL

H(KM)	#	N-COMP	S.D.	S.E.	%ERR	E-COMP	S.D.	S.E.	%ERR	MAG	DIR
58.	6	7.18	16.78	7.50	105.	79.78	16.08	7.19	9.	80.1	84.9
60.	8	12.78	23.82	9.00	70.	79.11	20.79	7.86	10.	80.1	80.8
62.	8	1.77	18.99	7.18	405.	79.93	11.01	4.16	5.	80.0	88.7
64.	8	3.18	16.85	6.37	200.	79.15	9.53	3.60	5.	79.2	87.7
66.	8	10.26	16.33	6.17	60.	76.58	9.04	3.42	4.	77.3	82.4
68.	7	49.16	15.17	6.19	13.	51.65	18.89	7.71	15.	71.3	46.4
70.	8	44.04	7.82	2.95	7.	36.18	7.33	2.77	8.	57.0	39.4
72.	8	33.68	7.91	2.99	9.	37.20	3.44	1.30	3.	50.2	47.8
74.	7	24.26	5.16	2.10	9.	38.63	6.84	2.79	7.	45.6	57.9
76.	7	16.28	4.76	1.94	12.	33.72	5.46	2.23	7.	37.4	64.2
78.	7	11.96	8.71	3.56	30.	26.70	11.79	4.82	18.	29.3	65.9
80.	3	-1.39	8.24	5.83	420.	22.11	15.59	11.03	50.	22.2	93.6
82.	6	4.97	5.69	2.54	51.	13.02	24.84	11.11	85.	13.9	69.1
84.	3	-14.92	2.33	1.64	11.	60.33	20.17	14.26	24.	62.1	103.9
86.	7	-37.40	15.47	6.32	17.	43.24	13.65	5.57	13.	57.2	130.9
88.	8	-43.26	18.19	6.88	16.	39.36	10.77	4.07	10.	58.5	137.7
90.	7	-39.85	24.66	10.07	25.	29.91	11.12	4.54	15.	49.8	143.1
92.	6	-32.73	29.13	13.03	40.	20.73	18.00	8.05	39.	38.7	147.7
94.	4	-44.50	37.52	21.66	49.	25.14	23.99	13.85	55.	51.1	150.5
96.	3	-72.27	14.97	10.59	15.	-18.95	24.30	17.18	91.	74.7	194.7
98.	6	-56.60	7.11	3.18	6.	-54.10	42.77	19.13	35.	78.3	223.7

Sheet 4

DAY=35 SAMPLE METHOD= 2

Mean Vector

H(KM)	#	N-COMP	S.D.	S.E.	%ERR	E-COMP	S.D.	S.E.	%ERR	MAG	DIR
58.	69	11.98	150.38	18.24	152.	-11.59	212.27	25.74	222.	16.7	316.0
60.	99	3.17	37.51	3.79	120.	35.41	39.26	3.97	11.	35.5	84.9
62.	98	0.54	23.67	2.40	445.	33.84	34.57	3.51	10.	33.8	89.1
64.	100	2.24	28.39	2.85	128.	37.08	57.20	5.75	16.	37.1	86.5
66.	95	0.47	21.93	2.26	480.	14.54	28.77	2.97	20.	14.5	88.1
68.	86	5.90	23.89	2.59	44.	7.06	26.95	2.92	41.	9.2	50.1
70.	95	16.27	25.29	2.61	16.	12.32	21.12	2.18	18.	20.4	37.1
72.	94	9.22	18.87	1.96	21.	10.23	16.29	1.69	17.	13.8	48.0
74.	82	3.72	23.40	2.60	70.	6.59	22.51	2.50	38.	7.6	60.5
76.	74	1.64	11.46	1.34	82.	4.91	19.47	2.28	46.	5.2	71.6
78.	78	2.16	14.07	1.60	74.	4.88	15.44	1.76	36.	5.3	66.1
80.	34	-0.52	8.48	1.48	285.	4.16	15.71	2.73	66.	4.2	97.1
82.	71	-3.49	34.48	4.12	118.	13.83	111.04	13.27	96.	14.3	104.2
84.	34	-3.48	11.57	2.01	58.	0.61	14.02	2.44	397.	3.5	170.0
86.	73	0.29	19.47	2.29	794.	2.20	14.93	1.76	80.	2.2	82.5
88.	95	-6.77	21.07	2.17	32.	5.45	17.95	1.85	34.	8.7	141.2
90.	79	-4.28	21.39	2.42	57.	1.21	11.86	1.34	111.	4.5	164.2
92.	62	-5.96	19.57	2.51	42.	1.21	18.21	2.33	193.	6.1	168.5
94.	44	-1.13	17.24	2.63	233.	4.85	35.43	5.40	112.	5.0	103.1
96.	29	9.95	33.07	6.25	63.	-0.16	16.20	3.06	1973.	10.0	359.1
98.	54	-0.74	10.38	1.43	191.	0.86	13.43	1.84	216.	1.1	131.0

DAY=35 SAMPLE METHOD=MEAN TIMES

H(KM)	#	NTD	DRIFT VECTOR MAG	DIR	N-COMP	E-COMP	MEAN TIMES T21	T32	T13
58.	69	0.54	33.30	150.59	-29.01	16.35	0.906	-3.168	0.043
60.	99	0.10	617.96	17.45	589.53	185.30	-0.125	0.079	0.073
62.	98	0.23	60.54	85.06	5.21	60.32	-0.780	-1.029	1.129
64.	100	0.46	70.57	43.03	51.59	48.15	-0.686	0.504	1.329
66.	95	0.38	184.94	281.39	36.53	-181.30	0.180	0.474	-0.292
68.	86	1.00	314.99	344.95	304.18	-81.81	-0.638	-0.185	-0.439
70.	95	0.16	81.81	54.46	47.56	66.57	-0.729	-0.003	1.011
72.	94	1.00	70.97	345.33	68.65	-17.97	-2.211	-0.201	-1.317
74.	82	0.09	88.24	10.67	86.72	16.34	-0.978	0.528	0.293
76.	74	0.50	40.18	90.06	-0.04	40.18	-1.481	-2.164	1.202
78.	78	0.24	34.85	55.36	19.81	28.67	-2.290	-0.644	1.788
80.	34	1.00	92.88	20.43	87.03	32.43	-1.645	-0.332	-0.293
82.	71	0.04	42.99	180.64	-42.98	-0.48	1.867	-1.391	-0.343
84.	34	0.30	41.78	217.87	-32.98	-25.65	1.461	-0.790	-1.897
86.	73	0.53	119.07	105.67	-32.15	114.65	-0.307	-0.846	0.353
88.	95	1.00	284.09	113.11	-111.49	261.30	0.836	0.554	1.056
90.	79	0.47	99.89	154.53	-90.18	42.96	0.372	-1.014	-0.011
92.	62	0.89	127.74	305.70	74.54	-103.75	-0.712	0.103	-0.970
94.	44	0.02	84.05	245.20	-35.26	-76.30	0.669	0.263	-0.965
96.	29	0.23	31.93	38.41	25.02	19.84	-2.035	0.878	2.367
98.	54	0.03	32.66	113.70	-13.13	29.91	0.247	-2.245	2.118

Sheet 6

DAY=38 5 MIN METHOD= 1

Median Vector

H(KM)	#	N-COMP	S.D.	S.E.	%ERR	E-COMP	S.D.	S.E.	%ERR	MAG	DIR
58.	4	21.34	11.13	6.42	30.	27.76	15.98	9.23	33.	35.0	52.4
60.	4	-0.27	30.31	17.50	6553.	2.98	31.32	18.09	606.	3.0	95.1
62.	2	29.55	4.74	4.74	16.	32.35	2.70	2.70	8.	43.8	47.6
64.	3	11.54	16.05	11.35	98.	14.47	19.68	13.91	96.	18.5	51.4
66.	5	33.52	3.03	1.52	5.	49.87	8.57	4.28	9.	60.1	56.1
68.	8	40.73	5.68	2.15	5.	55.63	6.56	2.48	4.	68.9	53.8
70.	8	35.43	15.39	5.82	16.	49.20	9.27	3.50	7.	60.6	54.2
72.	8	41.29	10.66	4.03	10.	47.77	4.25	1.61	3.	63.1	49.2
74.	8	26.26	14.60	5.52	21.	27.01	19.31	7.30	27.	37.7	45.8
76.	7	18.23	15.50	6.33	35.	28.44	19.99	8.16	29.	33.8	57.3
78.	8	28.67	21.17	8.00	28.	33.34	14.84	5.61	17.	44.0	49.3
80.	8	36.77	13.98	5.29	14.	35.63	19.01	7.19	20.	51.2	44.1
82.	8	45.42	12.83	4.85	11.	55.90	14.49	5.48	10.	72.0	50.9
84.	7	23.76	15.96	6.52	27.	80.38	23.02	9.40	12.	83.8	73.5
86.	8	-64.05	50.73	19.17	30.	82.52	17.86	6.75	8.	104.5	127.8
88.	8	-94.92	14.45	5.46	6.	45.13	22.85	8.64	19.	105.1	154.6
90.	8	-87.19	20.38	7.70	9.	22.35	13.90	5.25	24.	90.0	165.6
92.	7	-65.13	26.34	10.75	17.	11.23	10.62	4.34	39.	66.1	170.2
94.	6	-21.83	25.41	11.36	52.	11.65	11.50	5.14	44.	24.7	151.9
96.	5	-20.21	23.13	11.57	57.	13.49	9.78	4.89	36.	24.3	146.3
98.	6	-4.37	6.56	2.93	67.	1.84	4.86	2.17	118.	4.7	157.1

Sheet 7

DAY=38 5 MIN METHOD= 4

METH#2

H(KM)	#	N-COMP	S.D.	S.E.	%ERR	E-COMP	S.D.	S.E.	%ERR	MAG	DIR
58.	8	-32.28	149.66	56.57	175.	-17.31	137.72	52.05	301.	36.6	208.2
60.	8	-72.55	162.30	61.34	85.	43.36	332.53	125.68	290.	84.5	149.1
62.	8	14.53	51.68	19.53	134.	150.84	398.23	150.52	100.	151.5	84.5
64.	8	26.48	25.60	9.68	37.	41.49	14.56	5.50	13.	49.2	57.5
66.	8	27.60	14.40	5.44	20.	42.37	17.50	6.61	16.	50.6	56.9
68.	8	40.73	5.68	2.15	5.	55.62	6.55	2.48	4.	68.9	53.8
70.	8	47.30	17.36	6.56	14.	51.94	5.39	2.04	4.	70.2	47.7
72.	8	41.32	11.20	4.23	10.	47.69	4.19	1.58	3.	63.1	49.1
74.	8	42.26	19.34	7.31	17.	35.95	15.59	5.89	16.	55.5	40.4
76.	6	34.37	21.11	9.44	27.	40.29	8.19	3.66	9.	53.0	49.5
78.	7	36.80	12.93	5.28	14.	41.76	4.86	1.98	5.	55.7	48.6
80.	8	44.96	18.03	6.81	15.	38.87	19.16	7.24	19.	59.4	40.8
82.	8	45.10	12.40	4.69	10.	55.84	14.57	5.51	10.	71.8	51.1
84.	8	25.39	14.89	5.63	22.	75.82	22.12	8.36	11.	80.0	71.5
86.	8	-57.55	31.29	11.83	21.	77.90	12.35	4.67	6.	96.9	126.5
88.	8	-73.64	15.46	5.84	8.	45.21	22.36	8.45	19.	86.4	148.5
90.	8	-81.58	5.34	2.02	2.	29.29	16.38	6.19	21.	86.7	160.3
92.	8	-79.04	7.43	2.81	4.	20.18	9.38	3.55	18.	81.6	165.7
94.	4	-71.78	3.34	1.93	3.	23.29	7.68	4.44	19.	75.5	162.0
96.	3	-34.03	27.59	19.51	57.	16.99	9.61	6.80	40.	38.0	153.5
98.	3	-18.92	22.53	15.93	84.	12.44	8.28	5.86	47.	22.6	146.7

Sheet 8

DAY=38 5 MIN METHOD= 3

WLSFIT2

H(KM)	#	N-COMP	S.D.	S.E.	%ERR	E-COMP	S.D.	S.E.	%ERR	MAG	DIR
58.	8	8.47	23.93	9.05	107.	35.73	53.02	20.04	56.	36.7	76.7
60.	8	0.04	24.50	9.26	20928.	80.72	107.11	40.48	50.	80.7	90.0
62.	8	-7.21	45.52	17.21	239.	-1.56	90.33	34.14	2193.	7.4	192.2
64.	8	-3.98	27.77	10.50	264.	14.61	41.78	15.79	108.	15.1	105.2
66.	8	-1.00	52.40	19.80	1974.	48.72	18.62	7.04	14.	48.7	91.2
68.	8	40.88	3.07	1.16	3.	61.70	6.68	2.53	4.	74.0	56.5
70.	8	40.50	11.77	4.45	11.	56.95	6.80	2.57	5.	69.9	54.6
72.	8	49.39	5.50	2.08	4.	45.05	6.11	2.31	5.	66.9	42.4
74.	8	44.52	10.39	3.93	9.	32.70	18.89	7.14	22.	55.2	36.3
76.	8	26.75	21.18	8.01	30.	30.74	22.30	8.43	27.	40.8	49.0
78.	8	37.71	19.11	7.22	19.	38.37	8.39	3.17	8.	53.8	45.5
80.	8	51.82	10.38	3.92	8.	35.68	15.32	5.79	16.	62.9	34.6
82.	8	45.66	11.60	4.38	10.	55.30	13.56	5.13	9.	71.7	50.5
84.	8	35.69	39.92	15.09	42.	74.63	17.80	6.73	9.	82.7	64.4
86.	8	-57.54	34.95	13.21	23.	78.36	11.59	4.38	6.	97.2	126.3
88.	8	-82.66	6.39	2.42	3.	40.40	16.85	6.37	16.	92.0	154.0
90.	8	-84.39	6.32	2.39	3.	25.70	13.83	5.23	20.	88.2	163.1
92.	8	-62.06	34.39	13.00	21.	9.00	13.09	4.95	55.	62.7	171.8
94.	8	-40.35	32.11	12.14	30.	3.03	17.15	6.48	214.	40.5	175.7
96.	8	-12.35	26.66	10.08	82.	1.88	10.39	3.93	209.	12.5	171.4
98.	8	-9.49	20.57	7.78	82.	-5.70	12.58	4.75	83.	11.1	211.0

Sheet 9

DAY=38 SAMPLE METHOD= 1

AVG X-CORREL

H(KM)	#	N-COMP	S.D.	S.E.	%ERR	E-COMP	S.D.	S.E.	%ERR	MAG	DIR
58.	2	29.43	4.86	4.86	17.	37.35	10.91	10.91	29.	47.6	51.8
60.	2	47.66	18.94	18.94	40.	69.40	46.88	46.88	68.	84.2	55.5
62.	4	23.59	9.71	5.60	24.	41.39	36.40	21.02	51.	47.6	60.3
64.	3	-2.44	48.86	34.55	1416.	64.83	22.92	16.21	25.	64.9	92.2
66.	5	39.72	3.18	1.59	4.	52.65	7.67	3.84	7.	65.9	53.0
68.	8	44.29	1.26	0.48	1.	54.62	7.69	2.91	5.	70.3	51.0
70.	4	44.39	4.33	2.50	6.	51.29	6.94	4.01	8.	67.8	49.1
72.	7	42.19	12.70	5.18	12.	48.95	8.83	3.60	7.	64.6	49.2
74.	7	39.05	11.84	4.83	12.	23.75	23.34	9.53	40.	45.7	31.3
76.	5	32.26	19.26	9.63	30.	39.07	13.95	6.97	18.	50.7	50.5
78.	4	29.75	23.35	13.48	45.	36.51	10.92	6.30	17.	47.1	50.8
80.	7	43.84	11.96	4.88	11.	42.58	12.39	5.06	12.	61.1	44.2
82.	8	43.87	8.60	3.25	7.	57.44	10.83	4.09	7.	72.3	52.6
84.	8	21.86	11.84	4.47	20.	85.65	27.10	10.24	12.	88.4	75.7
86.	8	-47.26	26.49	10.01	21.	72.78	19.51	7.37	10.	86.8	123.0
88.	8	-80.51	5.87	2.22	3.	39.68	20.83	7.87	20.	89.8	153.8
90.	7	-84.62	7.82	3.19	4.	22.33	9.42	3.85	17.	87.5	165.2
92.	4	-80.58	6.17	3.56	4.	19.88	4.28	2.47	12.	83.0	166.1
94.	3	-27.10	30.34	21.46	79.	24.77	4.21	2.98	12.	36.7	137.6
96.	3	-14.82	14.46	10.23	69.	0.88	21.78	15.40	1751.	14.8	176.6
98.	5	-0.69	1.56	0.78	112.	4.92	5.95	2.98	60.	5.0	98.0

Sheet 10

DAY=38 SAMPLE METHOD= 2

Mean Vector

H(KM)	#	N-COMP	S.D.	S.E.	%ERR	E-COMP	S.D.	S.E.	%ERR	MAG	DIR
58.	22	1.42	23.81	5.20	366.	9.25	27.67	6.04	65.	9.4	81.3
60.	23	2.28	15.92	3.39	149.	0.44	10.16	2.17	488.	2.3	11.0
62.	47	1.73	11.91	1.76	102.	0.94	13.05	1.92	204.	2.0	28.6
64.	31	-2.36	11.57	2.11	89.	2.10	15.49	2.83	134.	3.2	138.3
66.	57	5.47	15.00	2.00	37.	7.42	18.33	2.45	33.	9.2	53.6
68.	96	3.94	17.22	1.77	45.	9.19	22.75	2.33	25.	10.0	66.8
70.	47	9.45	21.47	3.16	33.	7.69	23.04	3.40	44.	12.2	39.1
72.	81	7.47	20.25	2.26	30.	7.20	22.73	2.54	35.	10.4	44.0
74.	86	3.03	15.49	1.68	56.	3.81	13.68	1.48	39.	4.9	51.6
76.	56	4.99	13.99	1.89	38.	3.08	11.25	1.52	49.	5.9	31.7
78.	48	8.95	16.76	2.45	27.	6.72	19.72	2.88	43.	11.2	36.9
80.	82	6.99	22.90	2.54	36.	6.43	18.60	2.07	32.	9.5	42.6
82.	97	9.58	19.67	2.01	21.	18.72	29.38	3.00	16.	21.0	62.9
84.	90	-1.44	74.76	7.92	550.	16.38	37.36	3.96	24.	16.4	95.0
86.	92	-12.61	45.36	4.75	38.	8.78	50.42	5.29	60.	15.4	145.1
88.	91	-12.15	27.88	2.94	24.	7.58	37.80	3.98	53.	14.3	148.0
90.	85	-15.80	33.83	3.69	23.	7.35	28.42	3.10	42.	17.4	155.1
92.	42	-11.93	31.01	4.84	41.	0.80	14.18	2.21	277.	12.0	176.2
94.	35	-1.61	16.66	2.86	178.	5.07	9.15	1.57	31.	5.3	107.6
96.	34	0.71	7.86	1.37	192.	-0.19	13.16	2.29	1180.	0.7	344.7
98.	58	-0.36	8.86	1.17	322.	0.77	8.32	1.10	143.	0.9	115.2

DAY=38 SAMPLE METHOD=MEAN TIMES

H(KM)	#	NTD	DRIFT VECTOR MAG	DIR	N-COMP	E-COMP	MEAN TIMES T21	T32	T13
58.	22	0.72	44.94	48.80	29.61	33.81	-0.586	1.015	2.595
60.	23	0.14	36.95	19.95	34.73	12.61	-2.428	0.890	0.955
62.	47	0.97	91.01	322.74	72.44	-55.10	-0.026	1.383	0.077
64.	31	1.00	215.61	9.23	212.82	34.57	-1.641	-1.019	-1.132
66.	57	0.03	93.56	128.24	-57.90	73.48	0.273	-0.885	0.558
68.	96	0.11	62.50	84.91	5.55	62.25	-0.635	-0.871	1.218
70.	47	0.45	65.78	93.01	-3.46	65.69	-0.777	-1.304	0.786
72.	81	0.45	204.72	289.53	68.45	-192.94	-0.128	0.227	-0.471
74.	86	0.15	92.91	54.13	54.44	75.30	-0.809	-0.162	0.724
76.	56	0.68	150.33	109.32	-49.74	141.87	0.284	-0.196	0.755
78.	48	0.59	34.52	28.31	30.39	16.37	-1.207	1.997	2.667
80.	82	0.22	56.42	313.72	38.99	-40.78	-0.411	1.658	-0.644
82.	97	0.23	35.04	57.40	18.88	29.52	-2.215	-0.713	1.821
84.	90	0.37	40.49	209.66	-35.19	-20.04	2.442	-0.237	-0.890
86.	92	0.19	58.57	244.52	-25.20	-52.87	1.169	0.559	-1.183
88.	91	0.01	60.75	201.71	-56.44	-22.47	1.347	-0.634	-0.745
90.	85	0.23	773.68	87.35	35.83	772.85	-0.024	-0.051	0.121
92.	42	0.84	245.23	117.16	-111.94	218.19	0.289	-0.071	0.506
94.	35	0.73	27.81	140.77	-21.54	17.59	3.475	-1.055	3.316
96.	34	0.33	69.58	49.46	45.22	52.88	-0.772	0.241	1.282
98.	58	1.00	152.55	109.61	-51.19	143.70	1.404	0.927	1.864

Sheet 12

ASHTON FADES FROM 35 11 40 ;LENGTH 2048 SEC
MEAN OF 3 SETS OF FADES
ALL ERRORS;RHO.GE.0.3

HT	V	PHI	%ERROR	VX	VY	ERRX	ERRY	NO.	AMP	DIF(4-2)	DIF(4-3)
42											
44											
46	317.3	243.4	38.7	-283.8	-142.0	108.1	169.0	10.0	2.4	1.0	5.0
48	277.4	40.8	31.2	246.6	285.8	79.4	139.7	6.0	2.4	.0	3.0
50	227.3	74.1	40.9	218.6	62.3	96.2	32.6	8.0	2.5	.0	3.0
52	31.8	54.7	48.5	26.0	18.4	14.6	17.0	25.0	2.5	1.0	14.0
54	146.2	319.7	18.9	-94.5	111.5	28.1	27.4	18.0	2.4	2.0	6.0
56	57.1	323.8	59.6	-33.7	46.1	25.1	38.0	7.0	2.4	3.0	6.0
58	46.7	59.3	47.8	40.2	23.9	19.4	29.1	106.0	3.2	13.0	52.0
60	82.2	78.5	9.0	80.5	16.4	7.4	7.4	196.0	6.0	15.0	59.0
62	83.6	96.0	6.4	83.1	-8.7	5.3	10.7	198.0	7.9	14.0	70.0
64	58.7	93.3	18.0	58.6	-3.4	10.6	7.2	202.0	8.5	18.0	82.0
66	61.0	89.3	9.9	61.0	.7	6.0	6.4	194.0	7.5	21.0	95.0
68	28.3	28.4	25.4	13.4	24.9	10.3	6.0	165.0	10.7	26.0	89.0
70	55.0	40.9	7.3	36.0	41.6	4.4	3.7	188.0	43.5	22.0	71.0
72	50.3	39.9	8.4	32.3	38.6	3.9	4.4	209.0	110.9	19.0	88.0
74	60.7	48.7	20.7	45.6	40.1	7.5	17.0	170.0	160.6	23.0	86.0
76	27.9	80.0	14.6	27.4	4.8	3.9	7.8	150.0	196.1	24.0	87.0
78	25.3	75.2	16.7	24.5	6.4	4.2	4.4	153.0	198.5	32.0	98.0
80	37.4	59.5	19.5	32.2	19.0	7.0	8.1	127.0	165.6	20.0	71.0
82	11.0	92.2	49.2	11.0	-.4	5.4	5.8	145.0	124.3	32.0	83.0
84	29.7	46.5	37.3	21.5	20.4	6.8	14.4	167.0	119.7	44.0	97.0
86	35.9	126.0	21.8	29.0	-21.1	8.2	6.9	178.0	155.0	33.0	102.0
88	28.3	110.8	34.0	26.5	-10.1	8.2	16.5	183.0	186.8	32.0	95.0
90	25.3	123.7	22.9	21.0	-14.0	6.0	5.3	182.0	182.5	40.0	108.0
92	38.9	79.0	54.0	38.2	7.4	21.0	19.7	156.0	154.1	35.0	101.0
94	11.2	20.2	62.1	3.9	10.5	6.2	7.0	147.0	138.0	38.0	90.0
96	20.8	346.9	99.4	-4.7	20.3	7.4	21.1	140.0	138.4	45.0	92.0
98	8.2	349.6	89.5	-1.5	8.1	7.7	7.4	127.0	124.8	45.0	84.0
								3547.0		598.0	1837.0

Sheet 13

ASHTON FADES FROM 38 12 6 ;LENGTH 2048 SEC
MEAN OF 3 SETS OF FADES
ALL ERRORS;RHO.GE.0.3

HT	V	PHI	%ERROR	VX	VY	ERRX	ERRY	NO.	AMP	DIF(4-2)	DIF(4-3)
42											
44											
46											
48											
50											
52											
54											
56											
58	54.3	119.4	35.3	47.3	-26.7	17.7	23.3	22.0	8.4	5.0	4.0
60	32.2	19.2	53.5	10.6	30.4	14.8	17.5	49.0	7.4	11.0	18.0
62											
64	33.1	43.7	24.6	22.9	23.9	9.3	7.0	19.0	8.6	3.0	8.0
66	53.7	51.0	12.0	41.7	33.8	5.9	7.2	158.0	14.1	23.0	79.0
68	40.6	64.1	26.9	36.6	17.7	11.1	10.3	172.0	18.8	45.0	96.0
70	38.7	41.5	20.3	25.6	29.0	9.6	6.1	170.0	24.2	31.0	115.0
72	44.8	82.6	15.0	44.4	5.7	6.7	6.6	161.0	28.4	29.0	91.0
74	34.0	74.4	14.4	32.8	9.1	5.0	3.6	154.0	30.1	31.0	88.0
76	29.2	44.2	15.6	20.3	20.9	4.0	5.0	171.0	29.4	27.0	102.0
78	33.1	46.0	15.8	23.8	23.0	4.5	5.9	162.0	34.8	29.0	88.0
80	45.2	23.8	20.3	18.2	41.4	9.8	9.1	157.0	41.6	31.0	87.0
82	72.6	69.1	11.5	67.9	25.9	8.4	7.9	192.0	61.2	31.0	103.0
84	63.0	77.9	17.7	61.6	13.2	11.3	8.0	191.0	132.7	36.0	104.0
86	45.5	126.3	32.7	36.7	-26.9	13.1	17.7	179.0	414.3	34.0	92.0
88	74.7	141.2	13.4	46.8	-58.2	9.2	10.5	169.0	938.7	31.0	88.0
90	65.6	174.5	15.0	6.3	-65.3	12.2	9.8	186.0	1353.	35.0	100.0
92	21.4	181.3	38.6	-.5	-21.4	8.3	8.3	159.0	1344.5	38.0	92.0
94	13.6	198.5	40.5	-4.3	-12.9	7.3	5.3	169.0	1046.8	32.0	103.0
96	15.4	82.0	41.6	15.3	2.2	6.4	8.3	123.0	678.2	31.0	80.0
98	16.5	123.2	35.2	13.8	-9.0	5.7	6.0	146.0	431.7	41.0	101.0
								2909.0		574.0	1639.0

Sheet 14